Adaptation in the forest deer mouse: evolution, genetics, and development

Dissertation Advisor: Hopi Hoekstra Evan Prentice Kingsley

Adaptation in the forest deer mouse: evolution, genetics, and development

Abstract

Variation in the shape, size, and number of segments along the vertebral column underlies a vast amount of vertebrate diversity. Although the molecular pathways controlling vertebrate segmentation during normal development are well understood, the genetic and developmental underpinnings responsible for the tremendous variation in size and number of vertebrae are relatively unexplored. The main goal of this dissertation is to explore the genetic and developmental mechanisms influencing naturally occurring variation in the vertebral column. To this end, I focus on intraspecific skeletal variation, with an emphasis on tail length, in the deer mouse, *Peromyscus maniculatus*. In Chapter 1, I employ a phylogeographic framework to show that longer tails have evolved independently in different populations of forest-dwelling mice. Closer investigation of the underlying morphology shows that long-tailed mice have both (1) a greater number of tail vertebrae and (2) individually longer vertebrae, compared to ancestral short-tailed mice. Chapter 2 explores the genetic basis of tail length variation. I use quantitative trait locus mapping to uncover six loci that influence differences in total tail length (3 associated with vertebral length and 3 with vertebrae number). Finally, in Chapter 3 I combine comparative data from quantitative measurements of tissue dynamics during somitogenesis in fixed embryos and *ex vivo* explant culture to show that embryos of forest mice make more segments because they produce more presomitic mesoderm, and not because of any significant difference in the timing of somitogenesis. Together, this work integrates phylogeographic, genetic, and developmental studies to pinpoint the ways that natural selection modifies development to produce the repeated evolution of an evolutionarily important trait, and suggests that there are a limited number of ways that long tails can evolve.

This dissertation is dedicated to the memory of my father, Philip C. Kingsley.

Introduction

If we want to understand why two branches of life look or behave differently—essentially, why organisms are the way they are—we must uncover the paths those organisms took to become what they are. But these paths have multiple scales. At the evolutionary level, the direction of evolutionary change depends entirely on what already exists: evolution is a historically contingent process that is constrained by the past. On another level, evolution has, through selective and neutral processes, shaped patterns of genetic change through time. And on yet another scale, these genetic changes, as molded by evolution, remodel the body of multicellular organisms by modifying the process of development. In the spirit of the integrative nature of evolutionary change, in this dissertation I explore evolutionary, genetic, and developmental aspects of adaptive skeletal variation in the deer mouse, *Peromyscus maniculatus*.

Because all evolutionary variation begins as intraspecific variation, understanding the genetic underpinnings of local adaptation is especially relevant to the study of adaptive traits. There are two main advantages to exploring evolutionarily important traits within a species. The first is conceptual: all evolutionarily important differences among species originated as intraspecific variation, which is a compelling argument for the importance of understanding the origin and fate of polymorphic variation within species. The second is practical: a variety of approaches to uncover the loci underlying phenotypic differences—QTL mapping, for example—can only be applied to differences between interfertile organisms, i.e. those of the same, or very closely related, species. On the other hand, the obvious downside to studying intraspecific variation is that there is not often that much of it. Necessarily, the vast majority of evolutionary change is not present within a species but has accumulated between species. By exploring the genetic and developmental mechanisms underlying variation that has evolved over small time scales, i.e., within a species, we may gain insight into mechanisms producing interspecies variation that has had much more time to evolve.

Intraspecific variation in *P. maniculatus* is a rewarding source for studies of adaptation. Deer mice have been studied for over one hundred years in a natural historical context (e.g. Dice 1941; Blair 1950) and the abundant adaptive phenotypic variation present across the continent-wide range of this species has, in the last ten years, led to a number of fruitful investigations into the genetic basis of adaptive traits, including cryptic pigmentation (Linnen et al. 2009, 2013) and high-altitude adaptation (Storz et al. 2007, 2009; Cheviron et al. 2012)

This dissertation fits into a set of classic natural history observations about two ecotypes within deer mice: the forest and prairie forms. As early as Osgood's (1909) revision of the genus, researchers have classified this species into forest forms and prairie forms: the former having longer tails and larger hind feet (Dice 1940; Blair 1950), which Horner (1954) showed, through an extensive set of observational and manipulative experiments, to be correlated with climbing ability. Though some work has suggested that the forms may be partially reproductively isolated in some locations (Dice 1931; Hooper 1942) and mice from some forest populations show strong habitat preference (Harris 1952; Wecker 1963), more recent work has shown substantial gene flow at microsatellite loci across habitat interfaces (Yang & Kenagy 2011). The fact that differences in foot and tail length persist in the face of strong gene flow suggests that natural selection acts strongly to maintain variation in these traits.

The genetic architecture of adaptive traits is of special interest to evolutionary biologists. Here, I investigate the numbers and effects of loci underlying differences in skeletal morphology, with a special interest in the vertebral column of the tail, with the goal of understanding how underlying genetic architecture and genetic correlations can influence the evolution of complex traits (Klingenberg 2008; Flint & Mackay 2009; Armbruster 2014). The genetic architecture of skeletal variation has been extensively studied in the laboratory mouse (e.g. Cheverud et al 2001; Kenney-Hunt et al. 2006; Christians et al. 2003) in laboratory lines that have been artificially selected for

body size, but the genetic architecture of traits may be different in natural and artificial selection regimes (Mackay 2001; Hansen 2006). The genetics of naturally selected skeletal variation has been studied extensively in sticklebacks (e.g. Shapiro et al. 2009; Miller et al. 2014), but few studies have examined the genetic architecture of adaptive skeletal variation in mammals.

Variation in the vertebral column underlies an enormous amount of vertebrate diversity and, though much attention has been paid to how the identities of vertebrae shift through changes in development (e.g. Burke et al. 1995), less is known about the developmental and evolutionary changes that can generate differences in segment number. Gomez et al. (2008) recently showed that differences in the timing of the segmentation clock correlate with the massive disparity in segment number between snakes and mice, and Kimura et al. (2012) suggest that differences in somite size may influence vertebral number differences in medaka, but evidence regarding the developmental basis of vertebral number evolution is scant. Thus, the adaptive difference in caudal vertebrae number between forest and prairie deer mice examined in this dissertation is a unique opportunity to study the evolutionary, genetic, and developmental bases of differences in vertebral number in a mammal.

Outline of the dissertation

Chapter 1 explores intraspecific convergent evolution of the forest deer mouse in geographically distant populations. I show that long-tailed forest mice are evolving independently in eastern and western regions of the species range, and that, when accounting for non-independence of populations within a species, mice in forests do indeed have longer tails than prairie mice. I go on to investigate the skeletal nature of forest-prairie tail length differences and find that both eastern and western forest populations have longer vertebrae and a greater number of vertebrae in their tails compared to prairie populations. Despite the correlation of number and length of tail vertebrae in

natural populations, I show that number and length are not genetically correlated: a population of recombinant individuals from a forest-prairie intercross shows no correlation of vertebral counts with vertebral length. Together, these results show that independently evolving populations of forest mice have converged on the long-tail phenotype by similar morphological mechanisms—increasing number and length of skeletal elements—despite these mechanisms being genetically unconnected.

In Chapter 2, I investigate the genetic basis of this skeletal variation. Using an F2 forest-prairie intercross population, I explore structures of genetic correlations among bone traits and uncover morphological modules that are genetically coupled. I then employ a quantitative trait locus (QTL) mapping approach to map loci influencing tail length trait variation. Six major-effect loci control tail length variation in this cross. These loci coincide with loci underlying the tail's constituent traits: three of the six overlap vertebral count loci and the other three coincide with loci affecting vertebral length. Additionally, at all six tail-length loci the forest allele has a positive effect on tail length, further supporting the idea that natural selection maintains tail length variation in deer mice. Finally, I identify candidate genes from QTL intervals and discuss the implications of polygenic architecture on tail length evolution.

Chapter 3 examines the developmental mechanisms underlying variation in vertebral number in deer mice. Variation in the number of somites, the earliest developmental precursor to vertebrae, could be due to differences in timing of somitogenesis, differences in rates of posterior growth in the embryo, or both. By observing segmentation in *ex vivo* tail explant cultures, I show that there is no difference in the timing of somite formation in forest and prairie embryos. I present evidence that the segment number difference between forest and prairie deer mice is due to a difference in the rate of posterior outgrowth, specifically in the rate of presomitic mesoderm shortening, and that the disparity in outgrowth is not due to differences in proliferation of the tail bud cells. In light of this

evidence, I discuss future directions for developmental investigations of segment number variation in deer mice, specifically relating to promising QTL candidate genes from the previous chapter.

Chapter 1

Convergent evolution of long-tailed forest deer mice

Evan P. Kingsley[1], Krzysztof Kozak[2], and Hopi E. Hoekstra[1]

[1]Department of Organismic and Evolutionary Biology, Museum of Comparative Zoology, Howard Hughes Medical Institute
Harvard University, 26 Oxford Street, Cambridge, Massachusetts 02138, USA
and Department of Molecular and Cellular Biology
Harvard University, 16 Divinity Avenue, Cambridge, Massachusetts 02138, USA

[2]Department of Zoology, University of Cambridge, Downing Street, Cambridge CB2 3EJ, UK

INTRODUCTION

Convergent evolution occurs when similar phenotypes evolve in different lineages. Convergence has been defined at both ends levels of biological organization: at the smallest, most specific scale, the same phenotypes can be produced by the exact same mutations occurring in different lineages, thereby producing identical genetic and morphological outcomes; i.e. true parallelism. But at a larger scale, convergence is also defined simply as natural selection favoring similar phenotypes in different lineages, with nothing implied about the underlying biological mechanisms. The level at which convergent evolution occurs—whether two lineages fix the same adaptive mutation, different mutations at the same gene, different genes in the same biochemical pathway, or by totally different genetic mechanisms—informs us about the ways that selection and constraint influence evolutionary outcomes (Arendt & Reznick 2008; Manceau et al. 2010; Elmer & Meyer 2011).

Variation among populations of the deer mouse, *Peromyscus maniculatus*, provides a system for understanding the organismal basis of convergent evolution by local adaptation. This species has the widest range of North American mammals (Hall 1981) and populations are adapted to their local environments in many parts of the range. This variation has served for the basis of several studies of the genetics of adaptive traits (e.g. Snyder 1981 and Storz et al. 2007, Dice 1941 and Linnen et al. 2009), and the repetition of similar selective pressures in geographically distant parts of its range suggest the possibility of repeated convergent adaptations. Previous authors have placed deer mouse populations into two roughly-defined categories: forest-dwelling and prairie-dwelling (Osgood 1909, Blair 1950). Mice in these categories are differentiated behaviorally and morphologically: mice found in forests tend to have smaller home ranges (Howard 1949, Blair 1942), bigger ears, longer hind feet, and longer tails (Osgood 1909, Blair 1950, Horner 1954). The range of *P. maniculatus* extends across most of North America, and the ranges of the forest and prairie forms roughly comprise the

northerly and southerly parts of the species range, respectively (Fig. 1); it is thought that *P. maniculatus* populations expanded northward into forests following the Pleistocene glaciation (King 1968; Hall 1981) and thus that the deer mouse ancestor was a prairie form.

It is not known whether the widespread forest populations reflect a single origin of the forest morphology that has spread across the continent, or if the forest phenotype has evolved by convergent evolution, i.e., selection acting independently in different populations to produce local adaptation. Previous work on the phylogenetic relationships among deer mouse subspecies has suggested convergence—allozyme (Avise et al. 1979) and mitochondrial studies (Lansman et al. 1983; Dragoo et al. 2006) have shown there to be a split between eastern and western populations—but no studies or which we are aware have explicitly considered morphological and ecological context in a continent-wide sampling. Additionally, mitochondrial-nuclear discordance is common in this species (e.g., Taylor & Hoffman 2012), which complicates the interpretation of mitochondrial studies when traits of evolutionary interest, in this case skeletal variation, are likely controlled by loci in the nuclear genome. Furthermore, though previous work has compared the morphology of forest and prairie mice from different populations, these studies have not accounted for the fact that populations do not represent statistically independent sources of data due to shared evolutionary history and gene flow between those populations (reviewed by Stone et al. 2011).

Previous work has shown that deer mice use their tails extensively while climbing. Horner (1954) carried out a survey of climbing behavior in *Peromyscus*, and found not only a correlation between tail length and climbing ability, but also provided experimental evidence that within *P. maniculatus*, forest mice are more reliant on their tails for their climbing proficiency than their short-tailed counterparts. Smartt and Lemen (1980) showed that, within populations of two other *Peromyscus* species, tail length correlates with degree of arboreality, and climbing ability was shown to be heritable by Thompson (1990).

Here, we investigate the evolution of the deer mouse tail in two complementary ways. First, we reconstruct phylogeographic relationships among populations of *P. maniculatus* to test hypotheses about the convergent evolution of tail length. We show that forest-dwelling deer mice do not belong to a single phyletic group or genetic cluster and thus that forest forms are convergent. We also show that longer tails are correlated with forest habitation, even when taking account of shared history and gene flow among populations. Then we investigate the morphological basis of tail length differences in two geographically distant convergent populations, implicating similar but quantitatively different mechanisms for the generation of these differences. Finally, we show that, despite correlation in the wild, differences in the constituent traits of tail length between forest and prairie mice can be genetically separated in the lab. Together, these results strongly suggest that natural selection maintains multiple locally adapted forest populations, and sets a stage for further investigations of the genetic and developmental bases of an adaptive skeletal trait.

METHODS

Morphometric measurements from museum specimens

Records of *P. maniculatus* were downloaded from the Mammal Network Information System (MaNIS; www.manisnet.org) and the Arctos database (www.arctos.database.museum/home.cfm). We inspected all specimens available at Harvard's Museum of Comparative Zoology. As nearly all specimens were present in the collection as stretched skins, we considered the original collector's data to be the most reliable source of measurements. Juvenile specimens were excluded based on the characteristic grey pelage.

We excluded all specimens labeled as "juvenile", "subadult" or "young adult" or having any tail abnormalities or injuries. We also deleted any individuals with total length below 106 mm or tail length below 46 mm, which are considered the adult minima (Hall 1981; Zheng et al. 2003).

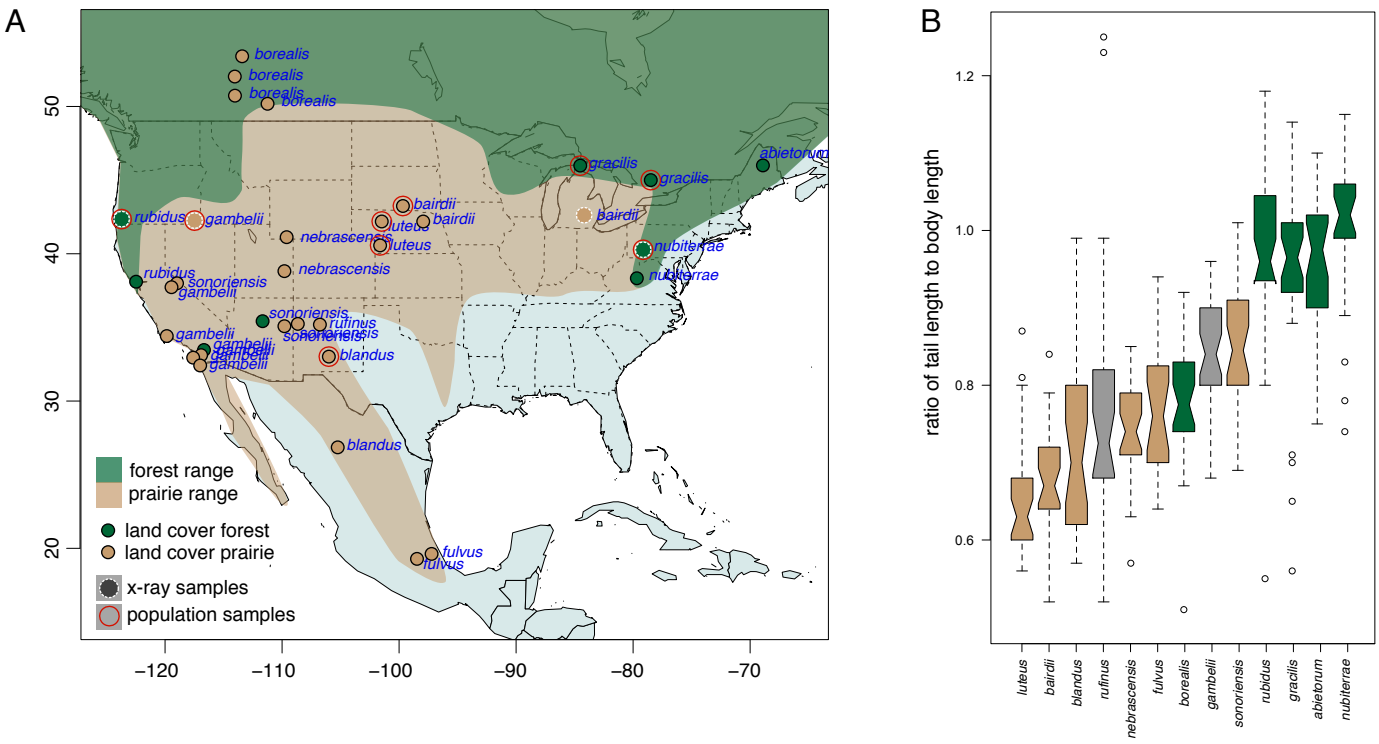

Figure 1. Deer mouse geography and tail length variation. A. Map of North America showing the roughly defined range of *P. maniculatus*. Forest and prairie range limits were obtained from Osgood (1909) and Hall (1981). Dots show locations from which we have samples and the style of the dots show 1) the GIS land cover-defined habitat of the sites and 2) which analyses they were used in. The dashed outline for "x-ray samples" indicates that we used samples from those locations for our comparison of vertebral number and length (see Figure 4). The red circle indicates that the population was used in the intraspecific contrasts analysis for F_{ST} estimates (see Figure 3). **B.** Box-and-whisker plot of tail:body length ratio variation among deer mice subspecies in museum collections. Box color indicates habitat, as described for each subspecies by Hall 1981; tan = prairie, grey = intermediate, green = forest. Note that these do not always match the land cover-defined habitat designations.

Peromyscus maniculatus has highly stable subspecies ranges and subspecific identity can be determined reliably based on appearance and location (Gunn & Greenbaum 1986; Hall 1981; King 1968). We scanned the original distribution maps from Hall (1981) and georeferenced them in ArcGIS v. 9.2 (ESRI 2007). Subspecies were then assigned based on original identification where available and on mapping the coordinates digitally. Subspecies with fewer than three specimens available were excluded.

Morphometric statistics from museum specimens

We calculated two types of dependent variables. Ratios of tail length to body length were used as a simple representation of the relation between the two measurements. We also applied a linear transformation of the data to address potential non-linear scaling of the two lengths (Fox & Weisberg, 2011). We fitted a linear model of tail length *vs.* body length. 30 individuals were randomly selected from each subspecies with over 30 records available in order to reduce bias resulting from large number of records for some common subspecies. We fitted log, square and Box-Cox transformations of the response variable and included quadratic and cubic terms for the predictor. All possible models were compared using ANOVA and the adjusted R^2 values. Due to very low fit of the best model ($R^2 = 0.11$) we decided that simple ratios are an appropriate test statistic. The normality of the ratio distribution was rejected with $p < 0.001$ using the Kolmogorov-Smirnoff test. We therefore used the non-parametric Mann-Whitney U Test to compare the ratios between arboreal and non-arboreal mice. We used the *car* package (Fox & Weisberg 2011) in R (R Development Core Team 2005) for all computation.

Tissue sampling and habitat designation

We extracted DNA (Qiagen DNeasy kit) from of 25-50 mg of liver from 78 individuals that comprise samples from our lab collections, loans from other researchers, and from museum tissue loans (see Appendix for details) and combined this with data from another ongoing study in the Hoekstra Lab for a total of 104 samples. The sampling encompassed the range of *P. maniculatus* and included 33 locations. We assigned animals to habitat types based on their sampling locations: we used ArcGIS (ESRI) to extract land cover, i.e., habitat type, information from the North American Land Change Monitoring System 2010 Land Cover Database (NALCMS, 2010) with a 1 km-radius buffer around each sampling location. We split land cover categories into forest and non-forest/prairie designations for all analyses: we called classes 1-6 and 14 forest (Temperate or sub-polar needleleaf forest, Sub-polar taiga needleleaf forest, Tropical or sub-tropical broadleaf evergreen forest, Tropical or sub-tropical broadleaf deciduous forest, Temperate or sub-polar broadleaf deciduous forest, Mixed Forest, Wetland) and others non-forest/prairie (Tropical or sub-tropical shrubland, Temperate or sub-polar shrubland, Tropical or sub-tropical grassland, Temperate or sub-polar grassland, Cropland, Urban and Built-up).

Array-based capture and sequencing of short-read libraries

To assess genome-wide population structure, we used an array-based capture library and sequenced region-enriched genomic libraries using the Illumina platform (Gnirke et al. 2009). Our MYbaits (MYcroarray; Ann Arbor, MI) capture library sequences have 5114 randomly chosen regions of the *Peromyscus maniculatus* genome averaging 1.5kb in length (5.2Mb of unique, non-repetitive sequence) and are identical to the regions used in Domingues et al. (2012) and Linnen et al. (2013). We extracted genomic DNA using DNeasy kits (Qiagen; Germantown, MD) or the Autogenprep 965 (Autogen; Holliston, MA) and quantified using Quant-it (Life Technologies). 1.5μg of each sample was sonically sheared by Covaris (Woburn, MA) to an average size of 200 bp

and Illumina sequencing libraries were prepared and enriched following Domingues et al. (2012) and Linnen et al. (2013). Briefly, we prepared multiplexed sequencing libraries in five pools of 16 individuals each using a "with-bead" protocol (Fisher et al. 2011) and enriched the libraries following the MYbaits protocol. We pulled down enrichment targets with magnetic beads (Dynabeads, Life Technologies), PCR amplified with universal primers (Gnirke et al. 2009), and generated 150bp paired end reads on a HiSeq2000 (Illumina Inc.; San Diego, CA).

Short-read sequence analysis

To process the capture-enriched sequence data, we used custom Python software available at *github.com/brantp/*. In brief, this software uses Stampy to map merged paired-end reads to the *P. maniculatus* genome scaffolds (Baylor 2012 version) and then combines reads, by individual, into BAM files with Picard (broadinstitute.github.io/picard/). We then used GATK (McKenna et al. 2010; DePristo et al. 2011) to call variants with UnifiedGenotyper in a larger sample of *maniculatus* individuals. We filtered these variants for those present in more than 75% in our 106 individuals and with GQ>20. This filtering produced 12721 variants.

Genetic principal components analysis (PCA)

To assess population structure across the range of *P. maniculatus*, we used SMARTPCA and TWSTATS (Patterson et al. 2008) with the genome-wide SNP data from the enriched short-read libraries described above. We condensed the significant principal components (eigenvectors) by multidimensional scaling in the Python module *scikit-learn* (Pedregosa et al. 2011) into two dimensions for Figure 3A. To visualize genetic relationships inferred by the PCA, we generated a bootstrapped neighbor-joining tree by computing Euclidean distances between individuals in the

significant eigenvectors of the SMARTPCA output. The Python code to produce bootstrapped trees can be found at *github.com/kingsleyevan/phylo_epk*.

Within-species comparative analysis

Samples from different populations within a species are non-independent because of shared ancestry and gene flow (Stone et al. 2011), so we must consider these factors when analyzing phenotypes across populations. We used two measures of genetic similarity to control for this non-independence. First, we pared our data down to populations from which we had three or more individuals and estimated global mean and weighted F_{ST} between populations using the method of Weir and Cockerham (1984) as implemented in VCFtools (Danecek et al. 2011) (see "in population contrasts" in Appendix). Second, we used a measure of genetic similarity ("--relatedness2" in VCFtools: the kinship coefficient of Manichaikul et al. 2010) between all individuals in the dataset for which we have tail and body measurements ("in individual contrasts" in Appendix). For both the population- and individual-level analyses, we used a general linear mixed model approach, as implemented in the R package *MCMCglmm* (Hadfield 2010), to test for an effect of habitat (forest/prairie) on population average tail:body ratio or individual tail:body ratio when including F_{ST} or kinship coefficient as a random effect.

Vertebral morphometrics of wild-caught specimens

We x-ray imaged the skeletons of wild-caught mice from four populations (see Appendix for specimen details) with a Varian x-ray source and digital imaging panel in the Museum of Comparative Zoology Digital Imaging Facility. Then we used ImageJ's segmented line tool to measure the lengths of each individual vertebra, starting from the first vertebra and proceeding posterior to the end of the tail. The boundary between the sacral and caudal segments of the

vertebral column is not always clear, so for consistency's sake we call the first six vertebrae (starting with the first sacral-attached) the sacral vertebrae; the caudal vertebrae are all the vertebrae posterior to the sixth sacral vertebra.

Because tail length scales with body size in our sample, we fitted a linear model with the *lm* function in R (R Development Core Team 2005) to adjust all vertebral length measurements for body size. We regressed total tail length ($R^2 = 0.62$) and the lengths of individual vertebrae ($R^2 =$ 0.14–0.59) on the sum length of the six sacral vertebrae, and used the residuals from the linear fit for all subsequent analyses. We obtain similar results when we regress length measurements on femur length instead of sacral vertebral length (results not shown).

F2 intercross trait correlation analysis

All mice bred in this cross were in the Hoekstra lab colony at Harvard University. We obtained prairie deer mice, *P. m. bairdii*, from the Peromyscus Genetic Stock Center (University of South Carolina), which we crossed with forest deer mice, *P. m. nubiterrae*, from Westmoreland County, Pennsylvania. We mated one male and one female of each subspecies—two mating pairs, one in each direction—and used their offspring to establish 10 F1 sibling mating pairs. We x-ray imaged 96 F2 offspring from these F1 pairs and measured them as described in the "Vertebral morphometrics. . ." section above and we used the *lm* function in R to assess correlations in the resulting measurements. All animals were between 80 and 100 days old when measured.

RESULTS

Non-monophyly of forest forms

We used an array-based capture approach to resequence and call SNPS in >5000 genomic regions in a continent-wide sample of *P. maniculatus* (Fig. 1). With 12721 SNPs from these

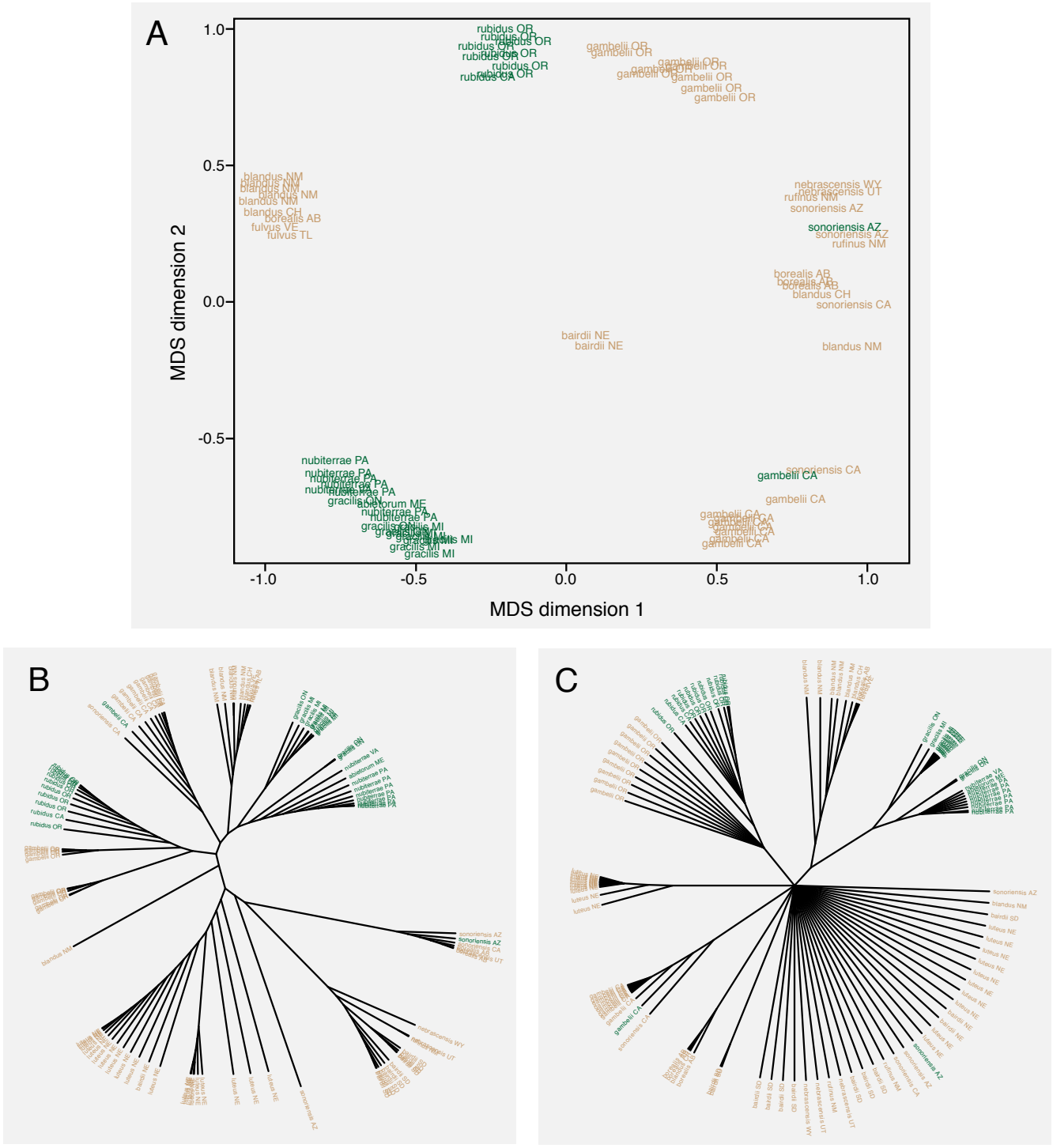

Figure 2. Genetic principal components analysis shows that forest forms are not a single genetic group. A. Multi-dimensional scaling (MDS) of genetic PCA into two dimensions. **B.** Neighbor-joining tree based on Euclidian distances in PCA-space allows visualization of genetic clustering. **C.** Same as B, but with clades collapsed that are not present in >50% of 1000 bootstrap replicates. Note that forest forms from the east and west do not cluster. Color indicates GIS land cover-defined habitat (tan = prairie, green = forest).

resequenced regions, we explored genetic similarity among the sampled individuals by genetic principal components analysis (PCA) (Patterson et al. 2008).

Genetic PCA methods show that individuals from forests (we determined habitat, forest vs. non-forest, using GIS land cover data, as described in Methods, above) do not compose a single, monophyletic group. Instead, we see the mice of the putatively derived forest forms clustering with nearby non-forest forms. To visualize the distances among individuals in the genetic PCA, we generated a neighbor-joining tree from MDS-scaled distances (Fig. 2B). In 1000 bootstrap replicates of this tree (a 50% majority rule tree is shown in Fig. 2C), none produced a tree in which forest mice formed a single group. These results show that forest forms are evolving independently in eastern and western parts of the species range.

Variation in tail length correlates with habitat

To assess whether differences in the length of the tail are significant even when accounting for non-independence of populations created by gene flow and shared ancestry, we included measures of genetic similarity among populations and individuals in a set of generalized linear mixed models. In these models, we ask whether animals in different habitats have significantly different tail:body ratios when including measures of genetic similarity as random effects.

First, we considered whether forest and prairie populations of differ in their mean tail lengths. When taking pairwise F_{ST} (Fig. 3) between populations (Appendix) into account, we find that habitat has a significant effect in our mixed model ($p = 0.002$ for weighted mean F_{ST}, $p < 0.001$ for global mean F_{ST}; fit by Markov Chain Monte Carlo [Hadfield 2010]). Next, we assessed whether individuals from forest and prairie habitats differ in tail length when accounting for genetic similarity. We find a significant effect of habitat on tail:body ratio in our mixed model with kinship coefficient (Manichaikul et al. 2010) as a random effect (MCMC; $p < 0.001$). We show model-

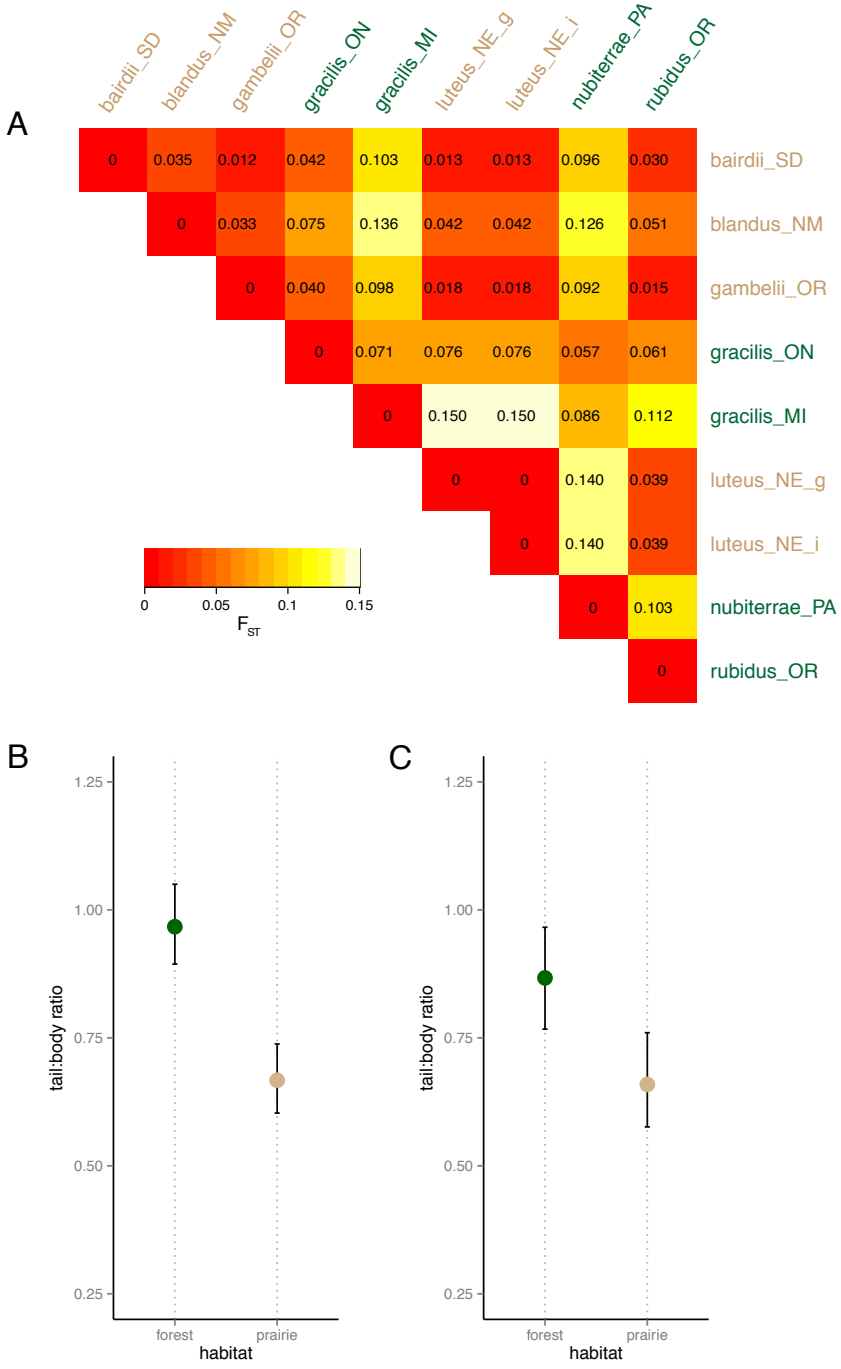

Figure 3. Tail length differs between habitats even when accounting for genetic non-independence. A. Matrix of genome-wide mean F_{ST} between populations used in the within-species comparative analysis (see Appendix for samples used). Larger values indicate more allele-frequency difference between two populations; smaller values indicate more similarity. **B.** Tail:body length ratios for each population predicted by a generalized linear mixed model taking genetic differentiation (F_{ST}) between populations into account. **C.** Tail:body length ratios for prairie and forest individuals predicted by a similar model as in B, but with pairwise genetic relatedness (kinship coefficient [Manichaikul et al. 2010]) between individuals taken into account. Error bars in B and C represent 95% confidence intervals.

predicted population means in Figure 3B and the predicted individual means by habitat in Figure 3C. Together, these results robustly show that, even when taking non-independence of populations into account, deer mice from forested habitats do indeed have longer tails than those from prairie habitats.

Convergence in skeletal morphology

We x-rayed specimens from two pairs of geographically distant forest-prairie populations (see Figure 1 and Appendix) and measured their vertebrae. These four populations were chosen because individuals from the two forest populations (West forest [*rubidus*] and East forest [*nubiterrae*]) are each more closely related to a nearby non-forest population than they are to each other (Figure 2), thereby representing independently evolving forest populations. We measured the total tail length, the lengths of the longest caudal vertebra and the number of caudal vertebrae and found that, in both comparisons, forest mice had 1) significantly longer tails (Wilcoxon test, East: $W = 49$, $p < 0.001$; West: $W = 49$, $p < 0.001$) significantly longer vertebrae (Wilcoxon test, East: $W = 49$, $p < 0.001$; West: $W = 49$, $p < 0.001$) significantly more vertebrae (Wilcoxon test, East: $W = 49$, $p < 0.002$; West: $W = 49$, p-value < 0.003) than their nearby prairie form (Fig. 4). Importantly, forest forms 1) do not have different numbers of trunk vertebrae (all samples had 18 or 19), and 2) we performed all these tests on body-size-corrected data, which means that these forest-prairie differences are specific to the tail. Additionally, when we compared the lengths of the individual caudal vertebrae along the tail we found that not all caudal vertebrae are longer in the forest than in prairie mice. In the eastern population pair, caudal vertebrae 4 through 15 had median lengths in the forest mice than the longest caudal vertebra in prairie mice. The corresponding segment in the western population pair is caudal vertebrae 4 through 16 (Fig. 4B).

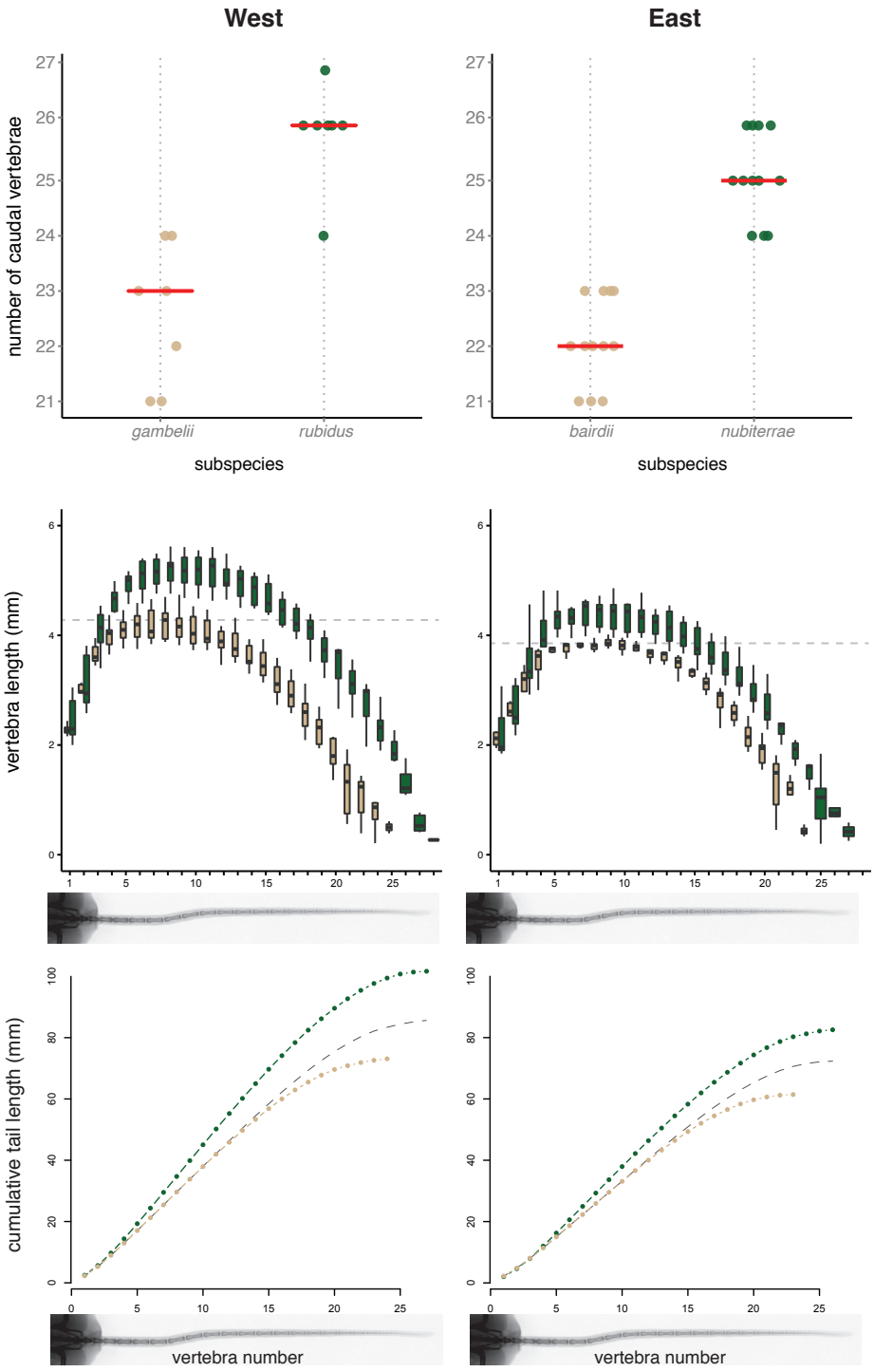

Figure 4. Convergent tail vertebral morphology in eastern and western forest-prairie population pairs. A. Forest mice have more caudal vertebrae than prairie mice in the east and west. Horizontal red lines represent medians. **B.** Forest mice have longer vertebrae than prairie mice in the east and west. Dashed line represents the median length of the longest prairie vertebra; the segment of the forest tail with longer vertebrae is 4–16 and 4–15 for western and eastern populations, respectively. **C.** Summary of tail vertebral differences between forest and prairie mice. Lines represent mean cumulative tail lengths. Dashed line is the cumulative length of the mean prairie tail with three extra vertebrae added, which represents an estimate of the maximum contribution of difference in number of vertebrae to the difference in total length.

We also estimated the relative contributions of differences in vertebral length and vertebral number to the overall difference in tail length. To do this, we simulated the forest and prairie mice having an equal number of vertebrae by inserting three long vertebrae into the center of the prairie tails. These simulated "prairie+3" tails compensated for 42% and 53% of the average difference in overall tail length between the eastern and western forms, respectively (Fig. 4C). These figures represent an upper bound of the contribution of the difference in vertebral number relative to vertebral length in these populations. Finally, a linear model of the form *total length ~ longest vertebra length + number of caudal vertebrae* has an $R^2 = 0.98$, suggesting that differences in length of vertebrae and number of vertebrae are the main factors contributing to differences in total tail length.

Vertebrae length and vertebrae number are genetically separable

In the four populations examined above, both forest populations have both 1) longer caudal vertebrae and 2) more caudal vertebrae. Could these differences be correlated in natural populations because they are under the control of the same genetic loci? To test this hypothesis, we generated 96 F2 recombinant individuals from an intercross between *P. m. nubiterrae* and *P. m. bairdii* and generated x-ray images from each individual. Using these images, we measured the correlation between the length of the longest caudal vertebra and the number of caudal vertebrae. We detect no significant correlation (Fig. 5; $t = 0.87$, $df = 94$, $p = 0.39$) between vertebral length and vertebral number in the tails of our F2 animals (96 individuals allows an 80% probability of detecting a correlation of $r > 0.25$ at $p < 0.05$).

DISCUSSION

The "convergence" in an episode of convergent evolution can occur on many different levels (Arendt & Reznick 2008; Manceau et al. 2010; Elmer & Meyer 2011). Studying instances of a

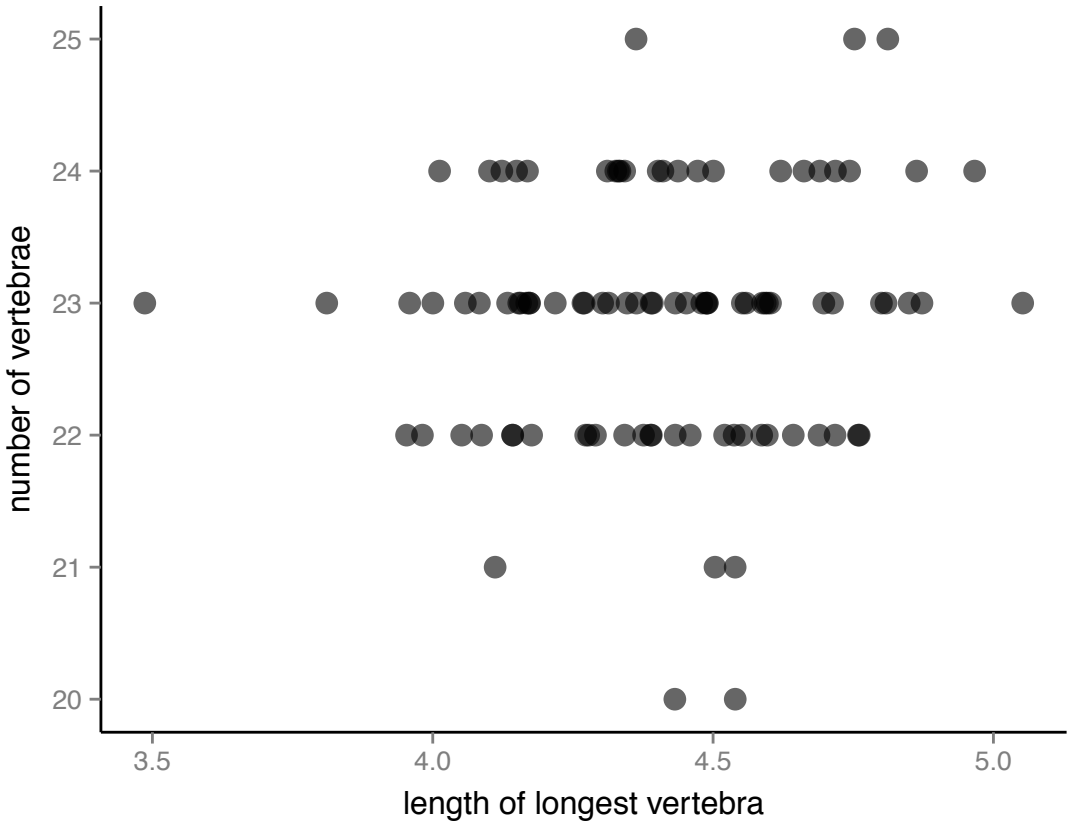

Figure 5. No significant correlation between number and length of caudal vertebrae in a laboratory F2 intercross. Each point is represents the length of the longest caudal vertebra and the number of caudal vertebrae measured from a radiograph of an F2 *nubiterrae* x *bairdii* individual. 96 individuals allows 80% power to detect a correlation of $r > 0.25$.

phenotype's repeated evolution allows us to make inferences not only about the selective conditions under which the phenotype evolves but also about the constraints that limit the production of variation in that phenotype. Repeated evolution of a phenotype usually implies two non-mutually-exclusive explanations: 1) there are intrinsic limits to the phenotypic variation that can be produced, to the extent that similar phenotypes are a frequent outcome of neutral evolution, or 2) similar selection pressures favor similar phenotypic adaptations. In both the neutral and selected cases, the repeated evolution of the phenotype can be due to similar or identical evolution at any level: the same gross phenotypic change could be produced in different evolutionary lineages by identical genetic mutations, similar changes in tissue morphogenesis, similar environmental changes that induce convergent phenotypic change, or anything in between. Only for the case in which selection plays a role, however, are similar phenotypic changes induced by the enhanced survival and/or reproduction of individuals with those phenotypes. It is this case in which we are most interested—understanding the organismal response to repeated bouts of selection allows insight into the process of adaptation that studying a single instance does not.

In his 1950 survey of adaptive variation in *Peromyscus*, W. Frank Blair wrote that the forest form of *P. maniculatus* "ranges through the Appalachians from northern Georgia northward and extends on northward to Labrador." He discussed the two main forms—one grassland and one forest—as two separate groups when he continued: "It ranges across the continent in the Canadian forests…and extends south through the Rocky Mountains and the mountains of the Pacific coast…. The grassland form occupies the grasslands of the interior of the continent and is surrounded on three sides by the long-tailed forest type." Other authors have also described the two forms of *P. maniculatus* as single, separate entities (Osgood 1909) and the work of Dice (1931) and Hooper (1942) suggested that the two forms failed to interbreed, suggesting that forest deer mice might represent an instance of incipient speciation.

Since those studies, several investigations have inferred the relationships among populations of *P. maniculatus* using molecular data. Avise et al. (1979) surveyed biochemical variation in 21 allozymes and showed that there is a broad similarity in allele frequencies in populations spanning most of the range of *P. maniculatus*. They report that "gene flow among widely separated populations of *P. maniculatus* cannot account for the similarity of their allelic contents. Either the populations of *P. maniculatus* have not been separated long enough for greater differentiation to have occurred by chance, and/or some form of natural selection is acting to help maintain similarity in electromorph configuration."

These conclusions are broadly consistent with subsequent studies that used restriction sites in mitochondrial DNA (Lansman et al. 1983) and mitochondrial DNA sequences (Dragoo et al. 2006) to show, though these reports did not explicitly explore forest-prairie dynamics, that well-supported phylogenetic clades are reconstructed that contain forest and prairie subspecies, sometimes with identical mitochondrial haplotypes. Though consistent in the sense that they do not recover monophyletic forest or prairie clades, the mtDNA studies conflict with the allozyme study in two ways: first, the specific topologies of the trees/networks are different, but second, and more importantly, Avise et al. report populations with some of the highest allozyme heterozygosities that had been reported at that time, while Lansman et al. recovered monomorphic mtDNA clades from those same populations.

This cytonuclear discordance was explicitly studied in deer mice populations on the west coast of the United States by Yang and Kenagy (2009) and in the Upper Peninsula of Michigan by Taylor and Hoffman (2012). Both studies found significant disagreement between patterns of genetic differentiation as determined at nuclear microsatellite loci versus mitochondrial sequence, which, together with previous studies of geographically widespread samples (Avise et al. 1979;

Lansman et al. 1983; Dragoo et al. 2006), suggest that relationships based on mtDNA sequence may not be as relevant as patterns of nuclear genomic differentiation for studies of ecological adaptation.

In the present study, we examine the phylogeography of *P. maniculatus* in the context of intraspecific ecological adaptation, and specifically in the framework of the classic forest-prairie dichotomy that has been recognized in this species for over one hundred years. Previous phylogeographic studies that have considered samples from across the range of *P. maniculatus* have only tangentially discussed adaptation, but we explore the phylogeography of the species using > 12000 genome-wide markers and examine correlation between habitat and morphology, making the current study the first to explicitly study the adaptation to forest habitats in *P. maniculatus* in a continent-wide sample. We chose to use a non-tree-based method, genetic principal components analysis (PCA), given the difficulty of constructing bifurcating phylogenetic relationships among intraspecific samples from populations experiencing gene flow.

The results of our genetic PCA are concordant with those of previous studies that found that forest mice are not a single monophyletic group. The pattern of genomic differentiation we see in our PCA data is roughly similar to that recovered by Avise et al. (1979), with a group of populations from eastern North America that are clearly separated from populations in the western half of the continent. But we also see some less expected patterns. Individuals from forest populations of the east, subspecies *nubiterrae* and *gracilis*, have the greatest affinity to the *blandus* populations from New Mexico and Mexico (Fig. 2B-C).

When we assigned habitat values to those populations using GIS land cover data, we found that populations captured in forest habitats have longer tails than those in non-forest habitats, when taking gene flow among populations into account. Thus, we support the interpretation of this pattern made by Lansman et al. (1983): "It is thus very probable that the currently recognized forest-grassland division of *P. maniculatus* does not reflect a fundamental phylogenetic split. Rather, it is

more likely that environmental selection pressures have led to the independent evolutionary appearance of these two morphs in different maniculatus lineages." Our data support at least two, one eastern and one western, independently evolving groups of forest *P. maniculatus*—western North American populations are less differentiated from each other than they are from those in the east, making it difficult to confirm more than a single group of forest mice in the west.

We show that the eastern and western forest forms are convergently evolving at the population level. By this, we mean that similar environments—forests—appear to favor similar phenotypes—long tails—in two phylogenetic groups that are not closely related to each other (in terms of population differentiation within this species). Furthermore, in two forest-prairie population pairs, one eastern and one western, we find that both pairs differ in the two components of the caudal skeleton that could vary to produce differences in tail length, namely the number of tail vertebrae and the length of those vertebrae. This coupling of vertebral length and vertebral number could be explained in two ways: 1) number and length of vertebrae are controlled by identical, or linked, regions of the genome, or 2) multiple genetic variants controlling number and length of vertebrae have independently fixed in eastern and western populations.

To distinguish between these hypotheses, we examined 96 F2 individuals from a laboratory intercross between a forest form, *P. m. nubiterrae*, and a prairie form, *P. m. bairdii*. If differences in the length and number of vertebrae are controlled by variants in the same region(s) of the genome, we expect them to be correlated in the F2 individuals. On the other hand, if the two traits are under control of variants in different genomic regions, recombination during the production of gametes in the F1 parents should decouple these traits in the F2 generation, and we should detect no correlation between these traits. We find the latter: we detect no significant correlation between number and length of vertebrae in the F2 (Fig. 5). This result implies that forest environments have favored separate alleles at loci affecting differences in number and length in eastern and western

populations. It may be advantageous, biomechanically, to have more and longer caudal vertebrae when climbing, or it may be simply that longer tails are favored, and alleles affecting length and number were present in the source population from which the forest mice evolved, and thus alleles affecting both traits increased in frequency from standing genetic variation in these populations.

There is some precedent to variation in number and length of vertebrae being produced by separate genetic mechanisms. Rutledge et al. (1974) performed a selection study in which they applied selection on body length and tail length in replicate mouse strains. The authors found that, in two replicate lines selected for increased tail length, one line had evolved a greater number of vertebrae and the other evolved longer vertebrae. That the number and lengths of vertebrae can be genetically uncoupled may not be surprising, given the timing of processes in development that affect these traits. The process of somitogenesis, which creates segments in the embryo that presage the formation of vertebrae, is completed in the *Mus* embryo by 13.5 days of development (Tam 1981), while the formation of long bones does not begin until much later in embryogenesis and skeletal growth continues well into the early life of the animal. Chapters 2 and 3 of this dissertation investigate the genetic and developmental bases of these morphological differences.

In this study, we aimed to explore the possible convergent evolution of an adaptive phenotype within a species. We confirmed that long-tailed forest-dwelling deer mice are evolving independently in eastern and western parts of its range, and that tail length does indeed differ in forest versus prairie habitats. Furthermore, we showed that longer tails, in both eastern and western forest mice, are due to convergent differences in the number of caudal vertebrae and the lengths of those vertebrae. Finally, we show that, despite the observation that caudal vertebrae number and length evolve in tandem in our natural population samples, the genetic mechanisms producing those differences can be decoupled in a lab intercross. Together, these results put over one hundred years of work on the forest-prairie dichotomy in *P. maniculatus* on more solid population genetic and

phylogeographic footing, along with establishing a framework for studying the genetic basis of local adaptation to forest habitats in this species.

Chapter 2

QTL mapping of skeletal traits in *Peromyscus maniculatus* reveals the genetic basis of arboreal adaptation

Evan P. Kingsley[1], Lorena Benitez[2], and Hopi E. Hoekstra[1]

[1]*Department of Organismic and Evolutionary Biology, Museum of Comparative Zoology, Howard Hughes Medical Institute*
Harvard University, 26 Oxford Street, Cambridge, Massachusetts 02138, USA
and Department of Molecular and Cellular Biology
Harvard University, 16 Divinity Avenue, Cambridge, Massachusetts 02138, USA

[2]*Harvard College, Cambridge, Massachusetts 02138, USA*

INTRODUCTION

Understanding the genetic architecture of complex traits is a key goal of evolutionary biology. The number, effect size, dominance, and pleiotropy of loci underlying complex adaptive traits can all significantly influence the process of evolution, and, furthermore, the architecture itself can evolve (Hansen 2006; Rajon & Plotkin 2013). Recent studies have leveraged powerful approaches like quantitative trait locus mapping and genome-wide association studies to gain insight into the evolution of a variety of complex traits in a variety of organisms from social organization of ants (Purcell et al. 2014) to diet in sticklebacks (Arnegard et al. 2014), to burrow construction in oldfield mice (Weber et al. 2013).

Examining genetic correlations among traits can inform our understanding of how adaptation proceeds in natural populations (Klingenberg 2008; Armbruster et al. 2014). Measurements of two traits that share the same underlying genetic or developmental mechanisms will covary. This morphological integration among traits can constrain evolution: a particular value of one trait may be favored by natural selection, but if its value covaries with that of another trait, then its selective advantage is tied to—and perhaps constrained by—selection on the other trait (Lande 1979, 1980). On the other hand, if the selective advantage of two covarying traits is in the same direction as the covariance, the integration between them can promote, and even accelerate, morphological evolution. This integration reflects a shared genetic basis for variation—pleiotropy—and/or a shared developmental mechanism. With greater integration may come greater constraint: a cost of complexity (Schluter 1996; Orr 2000; but see Wagner et al. 2008). In sum, the covariance structure among traits is a key determinant of evolutionary outcomes.

Variation in the number and size of skeletal elements underlies much of mammalian diversity (Pilbeam 2004; Asher et al. 2011). Previous studies seeking to understand the genetic basis of mammalian skeletal variation has focused on differences between strains of domesticated animal

strains (Morris et al. 1999; Cheverud et al. 2001; Wada et al. 2000), but the patterns of pleiotropy for alleles fixed by natural selection may be different from those fixed by the strong artificial selection in the laboratory (Otto 2004). Crucially, an allele's likelihood of fixation by natural selection may depend on the particular pattern of pleiotropy for that allele (Orr 2000; Welch & Waxman 2003; Otto 2004). It is unclear whether we should expect patterns of trait correlation and pleiotropy to be similar between even closely related taxa. Perhaps they should be similar: much of mammalian development comprises similar mechanisms tweaked by evolution to produce different forms. On the other hand, patterns of pleiotropy are known to be allele-specific. Indeed, mutations in different parts of the same gene—cis-regulatory *versus* protein-coding regions, for example—are expected to have different pleiotropic effects (Stern 2000; Stern and Orgogozo 2008).

In this chapter, we investigate the genetics of adaptive skeletal differences between populations of the deer mouse, *Peromyscus maniculatus*. There exists extensive intraspecific variation in this species, and much of it is proposed to be the result of local adaptation (see Chapter 1). This implies that natural selection has favored different alleles that are now at high frequency in different populations, despite the homogenizing effect of gene flow among populations experiencing divergent selective regimes. Deer mice in forests have longer tails than their prairie counterparts and these differences reliably exist across environmental gradients from forest to prairie (Chapter 1; Blair 1950; Yang & Kenagy 2011) and the longer tail of the forest deer mouse is used extensively when climbing (Horner 1954).

The longer tails of forest deer mice have more vertebrae and longer vertebrae than those of prairie deer mice. Importantly, these differences are specific to the tail: the number and lengths of trunk vertebrae are not significantly different between forms (Chapter 1). Though these traits are correlated in natural populations, we have shown that variation in number and length of caudal vertebrae can be genetically uncoupled. Additionally, these tail-specific differences between forest

and prairie deer mice are accompanied by differences in the size of the hind foot (Blair 1950; Horner 1954), also thought to be an important factor in arboreal locomotion. Here, we explore variation in limb and tail traits, examine how traits covary in an experimental cross, and map loci underlying variation in those traits, all in the context of evolutionary adaptation of complex traits.

METHODS

F2 intercross

To establish our genetic mapping population, we established crosses between prairie (*P. m. bairdii*) and forest (*P. m. nubiterrae*) deer mice. The *bairdii* mice were descendants of mice obtained from the Peromyscus Genetic Stock Center (University of South Carolina), originally from prairie habitat in Washtenaw County, Michigan. The *nubiterrae* were descendants of 18 wild-caught mice that we captured from maple-birch forest in Westmoreland County, Pennsylvania, in 2010. The mapping cross consisted of two families: one cross in each direction (family "0": female *bairdii* x male *nubiterrae*; family "1": female *nubiterrae* x male *bairdii*). Each family began with two mice, one of each subspecies. Because the alleles for most skeletal traits act in a codominant manner in the F1 offspring (Fig. 6B-D), we used an F2 intercross design for QTL mapping (Lynch and Walsh 1998). We established 14 F1 breeding pairs, which produced 495 F2 animals for analysis. When F2s reached 70-120 days old, they were sacrificed, measured for gross morphology (total length, tail length, ear length, hind foot length, and mass), and radiographed in the Museum of Comparative Zoology Digital Imaging Facility (MCZ DIF).

Morphometric statistics

This study is concerned with the bones of the tail and limbs. We and other authors have implicated limb- and tail-length differences in adaptation to forest habitats, and previously showed

that two subspecies of *P. maniculatus*, *nubiterrae* and *bairdii*, differ in a number of skeletal traits (see Chapter 1 of this dissertation and references therein). We measured these traits in four individuals each of *nubiterrae* and *bairdii*, 14 F1 animals, and 495 F2 animals by measuring x-ray radiographs. We used a digital x-ray system (Varian Medical Systems, Inc.; Palo Alto, CA) to obtain radiographs of whole specimens mounted such that plane containing the anterio-posterior and medio-lateral axes was orthogonal to the imaging plane. We measured all traits with Fiji/ImageJ (Schindelin et al. 2012; Rasband 1997–2014) using an included standard to determine scale. Figure 6A describes how we measured each trait. We performed all analyses in R (R Core Team 2008), performed principal components analysis (PCA) using the *psych* (Revelle 2015) package, and used *ggplot2* (Wickham 2009), *reshape2* (Wickham 2007), *scales* (Wickham 2014), and *RColorBrewer* (Neuwirth 2014) packages to display data.

We measured the lengths of 68 bone traits (67 are bone lengths and 1 is a count, caudal vertebra number) (Fig. 6). Most bone length traits were correlated with body size in our cross, so we corrected for body size using linear regression on sacrum length. Sacrum length represents a standard for body size (sacrum length vs. body mass: Pearson's $r = 0.55$, 95% CI: 0.48–0.60; vs. ruler-measured body length: $r = 0.62$, 95% CI: 0.56–0.67) and a section of the vertebral column that is anterior to the caudal vertebrae and that does not significantly differ between subspecies (Wilcoxon test, $W = 38$, $p = 0.1$). We corrected for body size by regressing raw trait measures against the sum length of the six sacral vertebrae, then adding the residuals from that regression to the trait mean to put the corrected measurements in the ranges of the raw measurements.

In previous work (see Chapter 1) we found that *nubiterrae* tails have 1) a larger number of caudal vertebrae and 2) longer caudal vertebrae than the tails of *bairdii*. To summarize these differences, we used three summary statistics to describe these differences: 1) the number of caudal vertebrae (all vertebrae caudal to the six sacral vertebrae), *vert_count*; 2) the longest vertebra in the

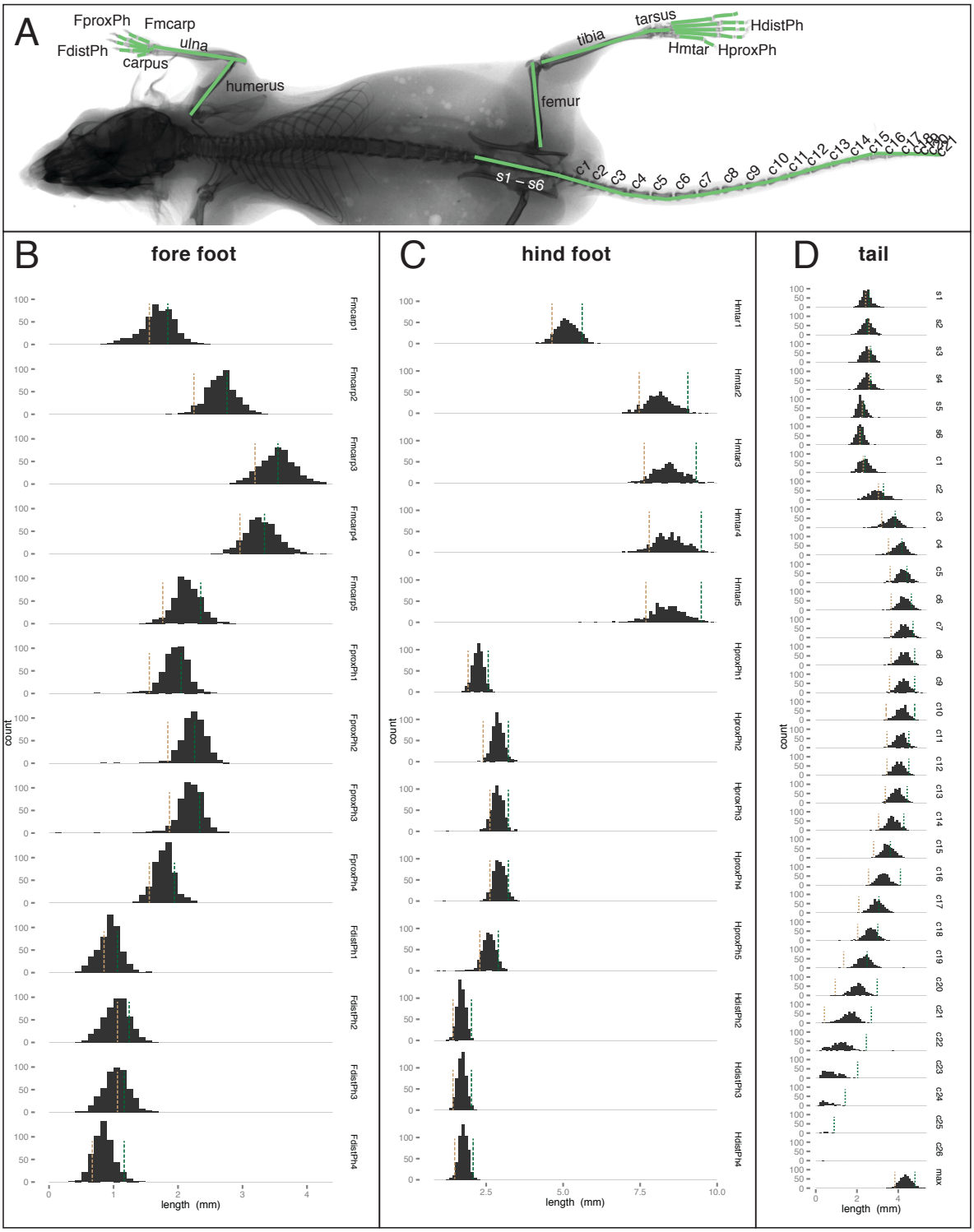

Figure 6. Trait distributions in QTL mapping cross. A. Radiograph showing traits analyzed in the F2 QTL mapping cross. **B.** Histograms showing distributions of forefoot length traits in the F2. **C.** Hindfoot length traits in the F2. **D.** Vertebral length traits in the F2; "max" is the longest vertebra in the tail. Dashed vertical lines represent parental means for each trait; green lines represent *nubiterrae* values and tan lines represent *bairdii* values.

tail, *maxvert*; and 3) the total length of the tail, *tail_total*. A model in which the former two measurements are the explanatory variables (*tail_total* = *vert_count* + *maxvert* + ε) explains $r^2 = 0.89$ of the variance in the total length of the tail, suggesting that differences in the length and number of vertebrae are the main constituent traits describing total tail length.

To explore which skeletal traits are influenced by the same genetic variation, we used correlation coefficients (Pearson's *r*) to explore the basic correlation structure among traits in the F2 animals. We followed that with a PCA with a varimax rotation (as implemented in the "principal" function in the *psych* package in R). Before PCA, we scaled the standard deviations for each trait to 1 and centered the means of each trait to 0. Based on scree analysis, we retained the first four principal components for F2 tail traits and F2 limb traits (see scree plots, Fig. 8B,D). The first four components represent 82% of the variance in tail traits and 63% of the variance in limb traits.

Genotyping

We genotyped parent, F1, and F2 animals with the double digest restriction-site associated DNA sequencing (ddRADseq) method as described in Peterson et al. (2012). Briefly, we extracted genomic DNA from alcohol-preserved liver tissue with the AutoGenprep 965 (AutoGen; Holliston, MA) in the Bauer Core Facility in the Harvard FAS Center for Systems Biology. We digested genomic DNA with EcoRI and MspI (New England Biolabs; Ipswich, MA) and ligated end-specific adapters, P1 and P2; the former includes individual barcodes, the latter is biotin labeled. Next, we combined samples into 48-individual pools and size-selected each pool to 216-276 bp on a Pippin Prep (Sage Science; Beverly, MA), after which we used streptavidin beads (Dynabeads M-270; Life Technologies; Carlsbad, CA) to eliminate fragments without P2 adapters. We PCR-amplified these pools (10 cycles) with an indexed primer. We quantified the mass of these pools using a TapeStation instrument (Agilent; Santa Clara, CA) in the Bauer Core Facility (masses of pools ranged from 0.7 to

5.0 nM) and combined them in equimolar ratios. We sequenced these pools in 150 bp paired-end rapid runs on an Illumina HiSeq 2500 in the Bauer Core Facility.

To process the ddRADseq data, we used custom Python software described in Peterson et al. (2012) and at github.com/brantp/. In brief, this software uses Stampy to map merged paired-end reads to the *P. maniculatus* genome scaffolds (Baylor 2013 version) and then combines reads, by individual, into BAM files with Picard (broadinstitute.github.io/picard/). We then used GATK (McKenna et al. 2010; DePristo et al. 2011) to call variants with UnifiedGenotyper. From 4.3e8 raw reads, this analysis produced 1.1e7 called variants. We hard filtered these variants for those that were fixed in the parents of the cross, those with QD > 5, GQ > 30, and those present in more than half the F2 individuals in our sample (using HTSeq; Anders et al. 2014). This filtering produced 4527 variants, which we used to construct the *maniculatus* genetic map.

Genetic map construction and quantitative trait locus (QTL) mapping

We used R/qtl to construct a linkage map for the F2 intercross between *P. m. bairdii* and *P. m. nubiterrae*. We generated an R/qtl input file with 4527 variants using custom Python software (github.com/brantp/rtd/vcf_to_rqtl.py) and followed the guidelines for generating linkage maps provided by Broman and Sen (2009). We removed individuals with fewer than 1000 genotypes and also those that were more than 90% identical. We filtered redundant markers (if a pair of markers had identical patterns of segregation, we removed one) and removed markers that had unexpected genotype frequencies ($p < 1e\text{-}5$). Using the remaining markers, we generated linkage groups using a maximum recombination fraction of 0.35 and a minimum LOD score threshold of 10. This produced 24 linkage groups (*n* of *P. maniculatus* is 24 [Bradshaw & George 1969]). We ordered markers within linkage groups by permuting orders over 8-marker windows and minimizing the inferred number of crossovers, then permuting over 4-marker windows to maximize likelihood

scores (on the Harvard Research Computing Odyssey Cluster, looped as described by Broman and Sen (2009)). For this and all subsequent map order inference, we used the Carter-Falconer map function with a genotyping error rate of 5e-3. These analyses allowed us to place the scaffolds of the *maniculatus* genome in inferred linkage order; we constrained the order of markers to their physical order, as mapped, within each scaffold. The direction of scaffolds containing few markers was often difficult to determine, especially if the markers are physically close together, so we used the directionality as determined in an interspecific F2 intercross containing a larger number of individuals (A. Bendesky, unpublished). We observed a number of individuals with elevated numbers of crossovers due to a number of obvious genotyping errors that caused the inference of double crossovers. We removed genotypes that consisted of single markers of one state flanked by genotypes of another state. The map uses genotypes from 448 individuals, has 2618 markers with a total length of 1826 centiMorgans (cM), has an average spacing between markers of 0.7 cM, and a maximum spacing of 23.1 cM.

With this linkage map in hand, we used it to map quantitative skeletal traits in the F2 population. For all bone length traits, we performed standard interval mapping with the extended Haley-Knott method ("ehk" in the R/qtl *scanone* function) including *sex*, *age*, *sacrum length* as additive covariates. Because the *count* trait (the number of caudal vertebrae) is noncontinuous count data and is not normally distributed (Shapiro-Wilk test: $W = 0.90$, $p < 1e\text{-}15$), we used the nonparametric method ("np") for QTL mapping. We used permutation tests ($n = 1000$ for autosomes, $n = 26312$ for the X chromosome) to determine significance thresholds for each trait (Churchill & Doerge 1994).

To assess the effect sizes of QTL and the amount of variance they explain, we used multiple-QTL models and drop-one analysis in R/qtl. Using the $p < 0.05$ significance thresholds as determined by permutation test, we fit models for each trait with the genotypes at markers with the

highest LOD scores in each significant QTL as explanatory variables as implemented in *fitqtl*. The models for length traits include *sex, age,* and *sacrum length* as additive covariates.

With 448 individuals, power to detect interactions among QTL is limited, but we used the *scantwo* function in R/qtl to explore possible epistasis among loci. This function produces a matrix of LOD scores for the full model, which includes interactions, and the additive model, which does not. We use differences between the likelihoods of these models to detect interactions (Fig. 12A,B, upper triangles; 0.05 LOD_{int} threshold for *vert_count* = 4.43 and for *maxvert* = 6.62, from permutation tests). We also used the *scantwo* results to assess support for multiple QTL by comparing, for each pair of QTL, the LOD scores of models containing two QTL with those of models containing a single QTL (Fig. 12A,B, lower triangles; 0.05 LOD_{av1} threshold for *vert_count* = 3.58 and for *maxvert* = 3.67, from permutation tests).

We searched within QTL intervals to find genes that could be producing variation in skeletal traits. First, we calculated 1.5-LOD intervals (which corresponds to a ~95% confidence interval [Dupuis & Siegmund 1999]) using the *lodint* function in R/qtl and then obtained annotations for the scaffolds containing markers in the interval (NCBI *Peromyscus maniculatus bairdii* Annotation Release 100). We used the resulting gene names to screen a list of alleles from the Mouse Genome Informatics (MGI) Mammalian Phenotype Browser (www.informatics.jax.org/searches/MP_form.shtml) that are known to affect tail, vertebral, and skeletal traits (Table 2).

RESULTS

Alleles producing skeletal trait variation are codominant and pleiotropic

We measured skeletal traits in an F2 intercross between two subspecies of *Peromyscus maniculatus*: the forest-dwelling *nubiterrae* and the prairie-dwelling *bairdii*. Because the difference in tail

length between subspecies is likely to strongly influence an animal's ability to climb trees (Blair 1950; Horner 1954), we primarily focused on differences in number and length of caudal vertebrae in this cross. We also investigated other skeletal variation that may relate to climbing ability (differences in lengths of bones in the limbs and feet), but how those differences might influence climbing has been less studied, so we focus mainly on the tail.

We phenotyped skeletal traits in parental and F2 animals to assess dominance and segregation patterns of alleles producing variation in those traits. For all traits measured, alleles acted in a codominant fashion: phenotype values in F1 animals were intermediate between the means of the parents. The ranges for most phenotypes in the F2 population encompassed the mean values of the parents, but the presence of few F2 animals with the parental phenotypes suggested that variation in these traits is polygenic in nature (Fig. 6).

Variation in skeletal traits of the limbs and tail are widely correlated in the F2 population. Three general observations emerge from the correlation matrix containing all sacrum-corrected bone length measurements (Fig. 7). First, lengths of bones are most strongly correlated with the lengths of bones in their same morphological group, i.e., within the tail, the hind limb, and the forelimb. Second, there are weak correlations of bone lengths between those of the tail, hind limb, and forelimb. Third, there are groups of traits that covary within these three morphological groups. In the limbs, lengths of bones covary within autopodial segments; e.g., lengths of the metatarsals covary with each other more than with lengths of the proximal phalanges, and vice versa. In the tail, covariance in the lengths of caudal vertebrae appears to divide the caudal vertebral column into three segments possessing high within-segment correlations: proximal: c1–c3, medial: c4–c13, and distal: c14–c23. The most distal vertebrae beyond c23 may also represent a segment, but this is confounded by individuals that do not possess these caudal vertebrae. (This is, presumably, the same

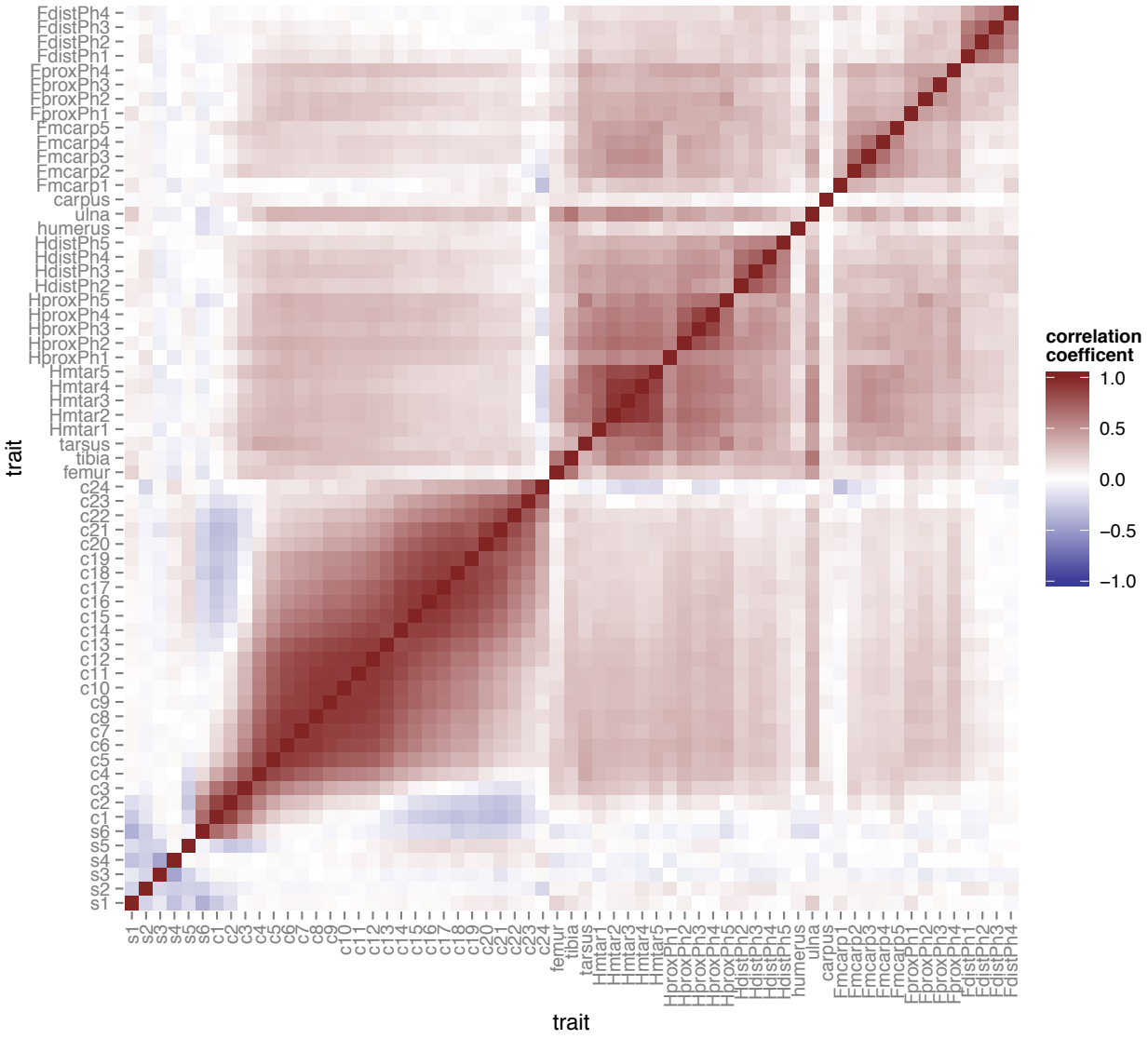

Figure 7. Correlations in F2 bone lengths. Pearson's *r* for all pairs of limb and tail length traits in F2s.

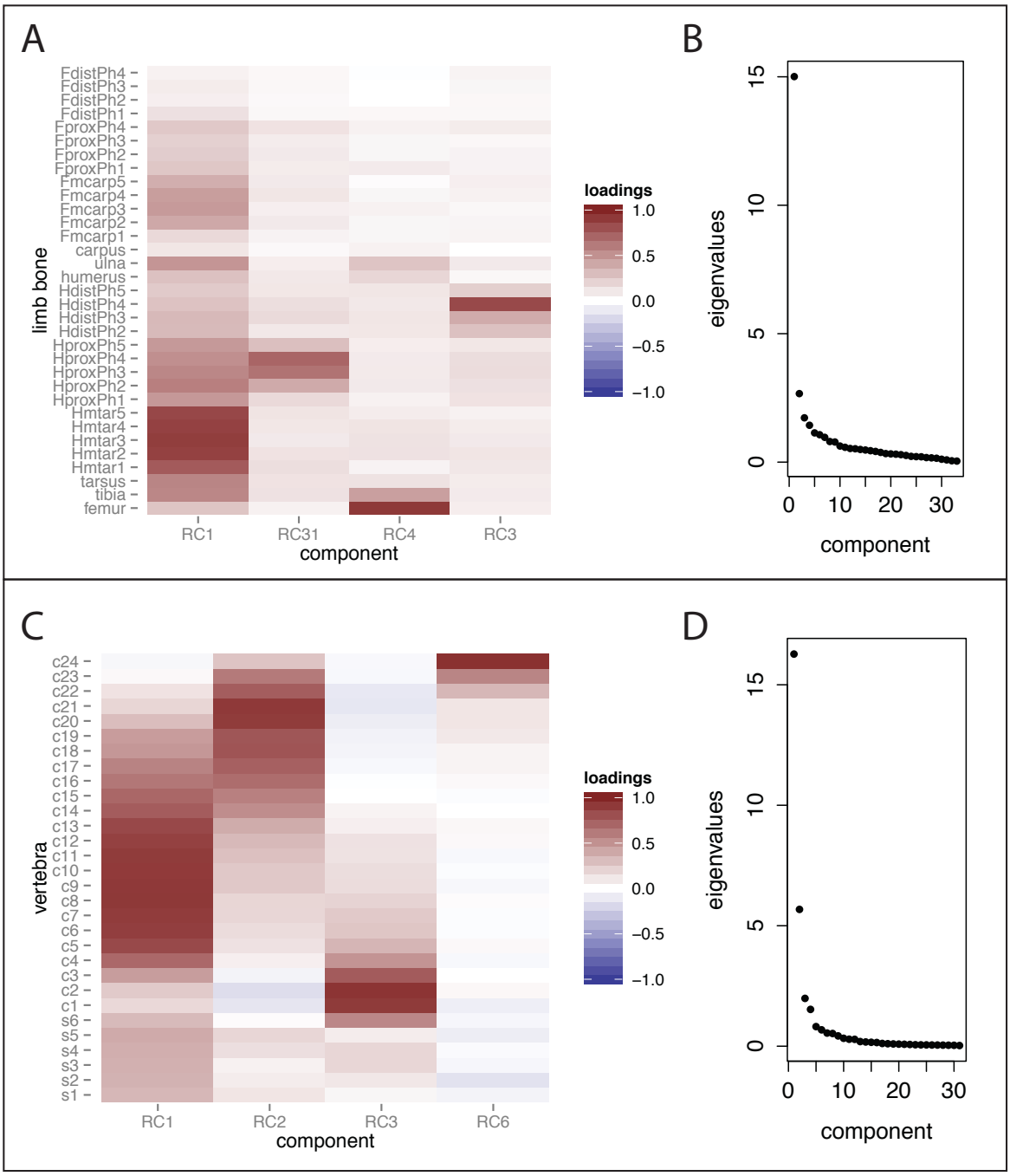

Figure 8. Principal Components Analysis of limb and tail traits. A. Heatmap of F2 limb length trait loadings on four PCA dimensions. **B.** Scree plot for limb PCA. **C.** Heatmap of F2 tail vertebral length loadings on four PCA dimensions. **D.** Scree plot for vertebra PCA.

reason for high correlations between caudal vertebra count and the lengths of the most caudal vertebrae: an individual with a long c23 is more likely to have a c24.)

To further explore the covariance among bone lengths in the tail and limbs, we used PCA to assess how traits clustered by variance in F2 animals. We sought to group traits that share variance by examining their loadings on each rotated component of a PCA. For this analysis, we looked at limb and tail traits separately, and we consider the first four components for each set of traits.

For limb traits in the F2 (Fig. 8A), we see the most proximal autopodial components—the metacarpals and metatarsals—of the fore- and hind foot loading highly on the first component, while the more distal components of the hind foot—the proximal and distal phalanges—each loaded highly on their own component. Lengths of the femur loads on a fourth component. PCA loadings of vertebral lengths in the F2 (Fig. 8C) show a similar pattern to the one described by the correlation matrix: caudal vertebrae can be split into three main segments. Proximal (c1-c3), medial (c4-c15), and distal (c16-c23) lengths each load highly on different components.

Because we are primarily interested in the loci underlying adaptive tail length differences in deer mice, we chose three representative tail traits for subsequent genetic investigation: total tail length (*tail_total*), length of the longest caudal vertebra (*maxvert*), and number of caudal vertebrae (*count*) (Fig. 9). The former two traits correlate strongly with body size (Fig. 9B), so we use body-size-adjusted values (see Methods) for all subsequent analyses of those traits. *Count* and *maxvert* are constituent traits of *tail_total*: both are significantly correlated with *tail_total* (Fig. 9B) and a linear model containing the two constituent traits explains 89% of the variance in *tail_total* in F2s.

QTL mapping identifies major loci underlying tail traits

We identified major-effect loci that effect intraspecific variation in tail length using standard interval mapping in our F2 population (Table 1). For total tail length (*tail_total*), we found six

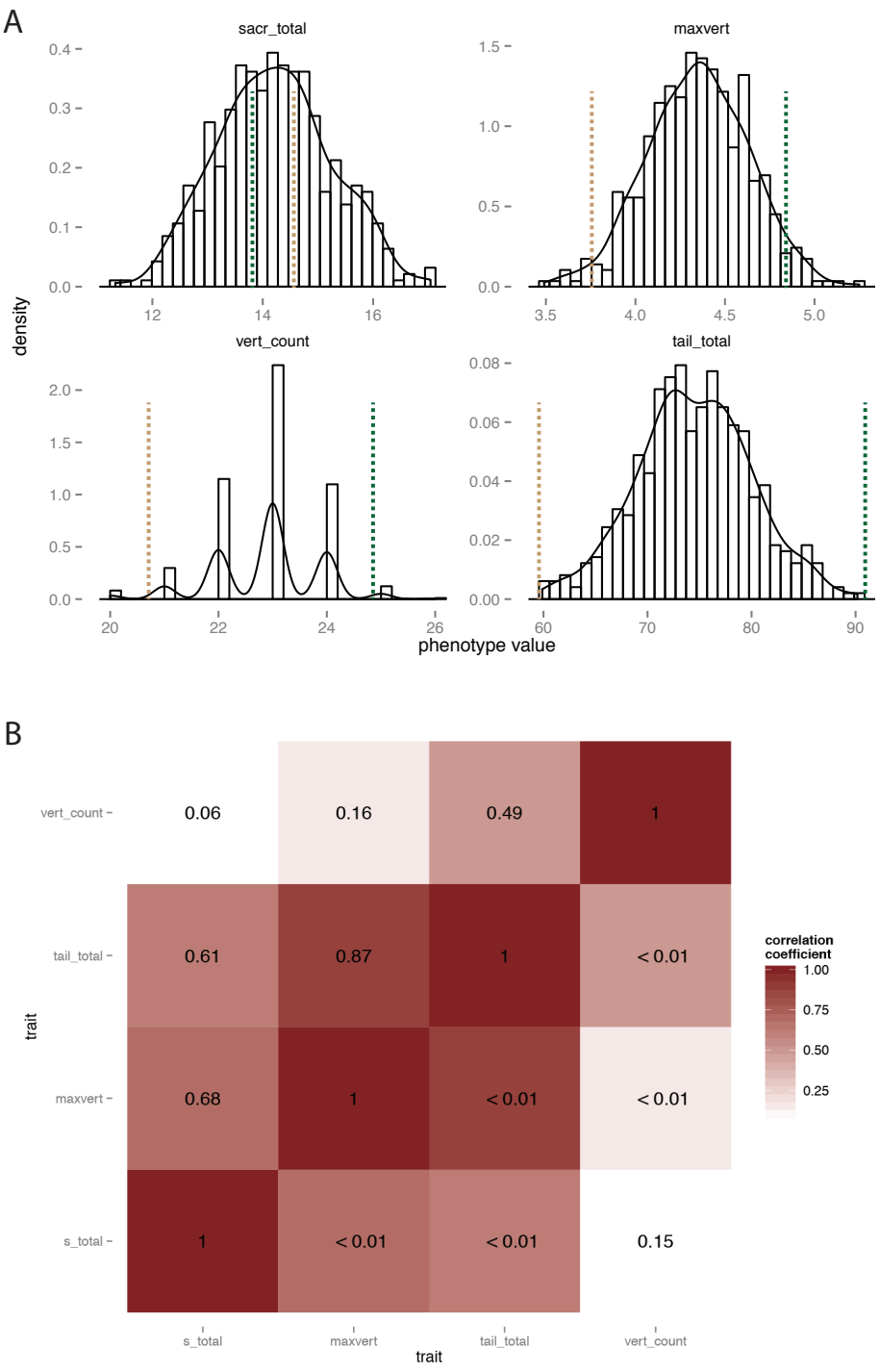

Figure 9. Distributions and correlations in tail summary traits in F2 animals. A. Histograms with density curves for sacrum length (*sacr_total*), length of the longest caudal vertebra (*maxvert*), number of caudal vertebrae (*vert_count*), and total tail length (*tail_total*). Units of *sacr_total*, *maxvert*, and *tail_total* are in millimeters. Dashed lines represent parental means for each trait; green lines represent nubiterrae values and tan lines represent bairdii values. **B.** Correlation matrix for tail traits. Values above the diagonal are Pearson's *r*; p-values indicating significance of *r* estimates are below the diagonal.

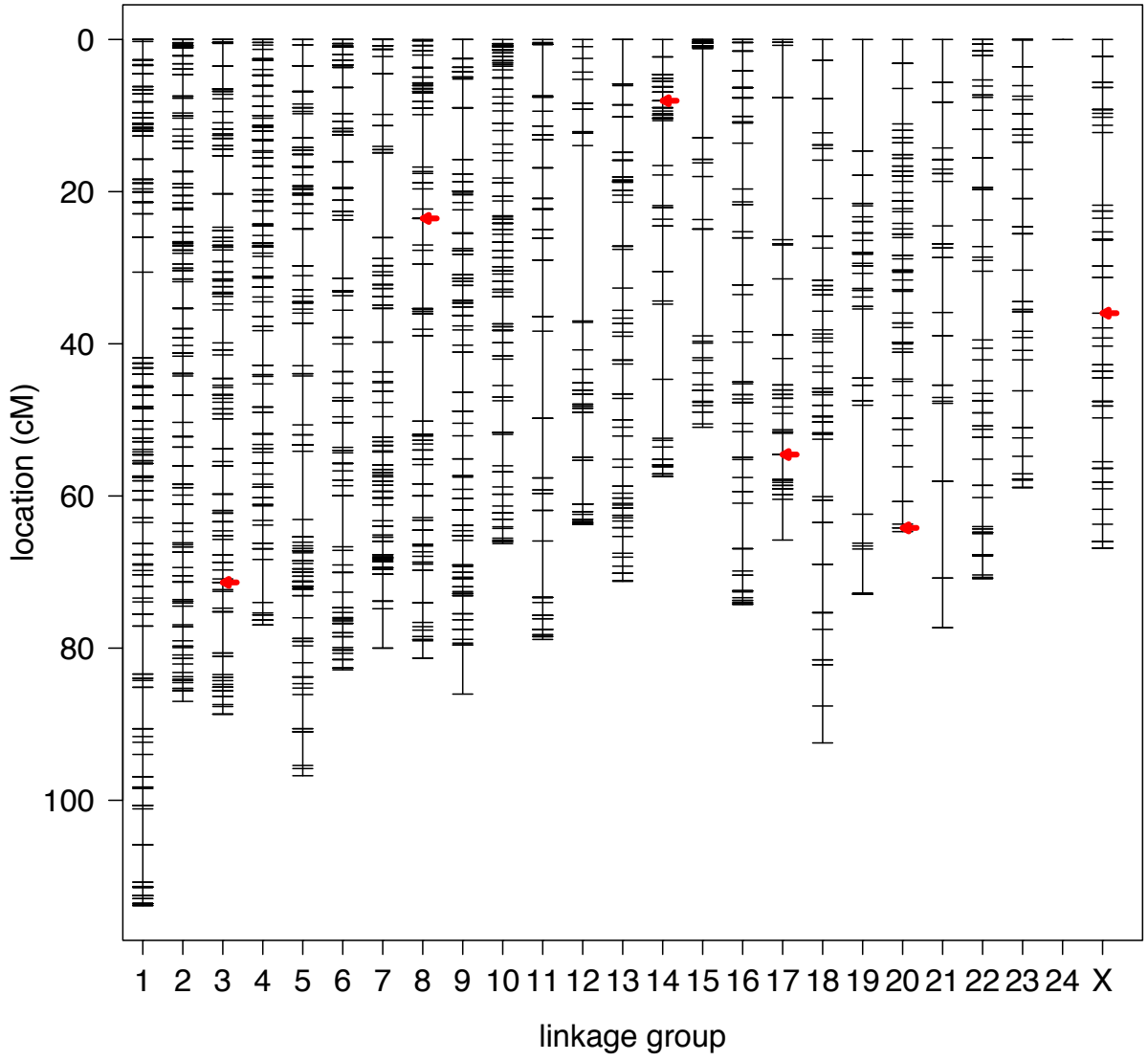

Figure 10. *P. maniculatus* linkage map and locations of tail_total QTL. Red arrows indicate the locations of the peak markers of association with total tail length.

significant QTL that together explain 28% of the variance in F2 tail length (Fig. 10). The peak markers of three of these QTL coincide with the peak markers for the three QTL controlling the number of caudal vertebrae (*vert_count*) (Fig. 11), which together explain 12% of the variance in *vert_count*. The remaining three QTL for *tail_total* coincide with three QTL that influence the length of the longest caudal vertebra (*maxvert*). These three QTL explain 16% of the variance in *maxvert*. (We also find three additional smaller-effect loci for *maxvert*, but they do not coincide with QTL for *tail_total* or *vert_count*, and we do not consider them here.) This architecture of major effect loci is consistent with the lack of correlation between length and number of caudal vertebrae and their role in constituting the total length of the tail.

We assessed the evidence for multiple QTL in two ways: a two-dimensional scan (Fig. 12) and multiple-QTL models (Table 1). Assuming that the six *tail_total* peaks represent the underlying *vert_count* and *maxvert* loci, for each pair of QTL we compared LOD scores of models containing two QTL with those of models containing only a single QTL. The LOD difference between these models was greater than the significance threshold for all pairs of QTL, indicating strong support for all six. We also assessed support for multiple QTL underlying *tail_total*, *vert_count*, and *maxvert* with multiple QTL models for each trait. In these models, we found all QTL to significantly influence the phenotype ($p < 0.05$), lending further support for all six QTL. Finally, we tested for epistasis between pairs of QTL in the two-dimensional scan and in the multiple-QTL models and found no significant interactions.

The effects of alleles affecting tail traits are all in the expected direction, that is, *nubiterrae* alleles produce larger trait values. Additionally, most *nubiterrae* alleles exhibit dominance (Fig. 13), with varying degrees of mean dominance effects ranging from -0.06 to 1.10 (where -1, 0, and 1 indicates complete recessivity, additivity, and complete dominance, respectively)(*d/a;* Falconer & Mackay 1996). In a multiple-QTL model, additive effects of alleles at the three major-effect *maxvert*

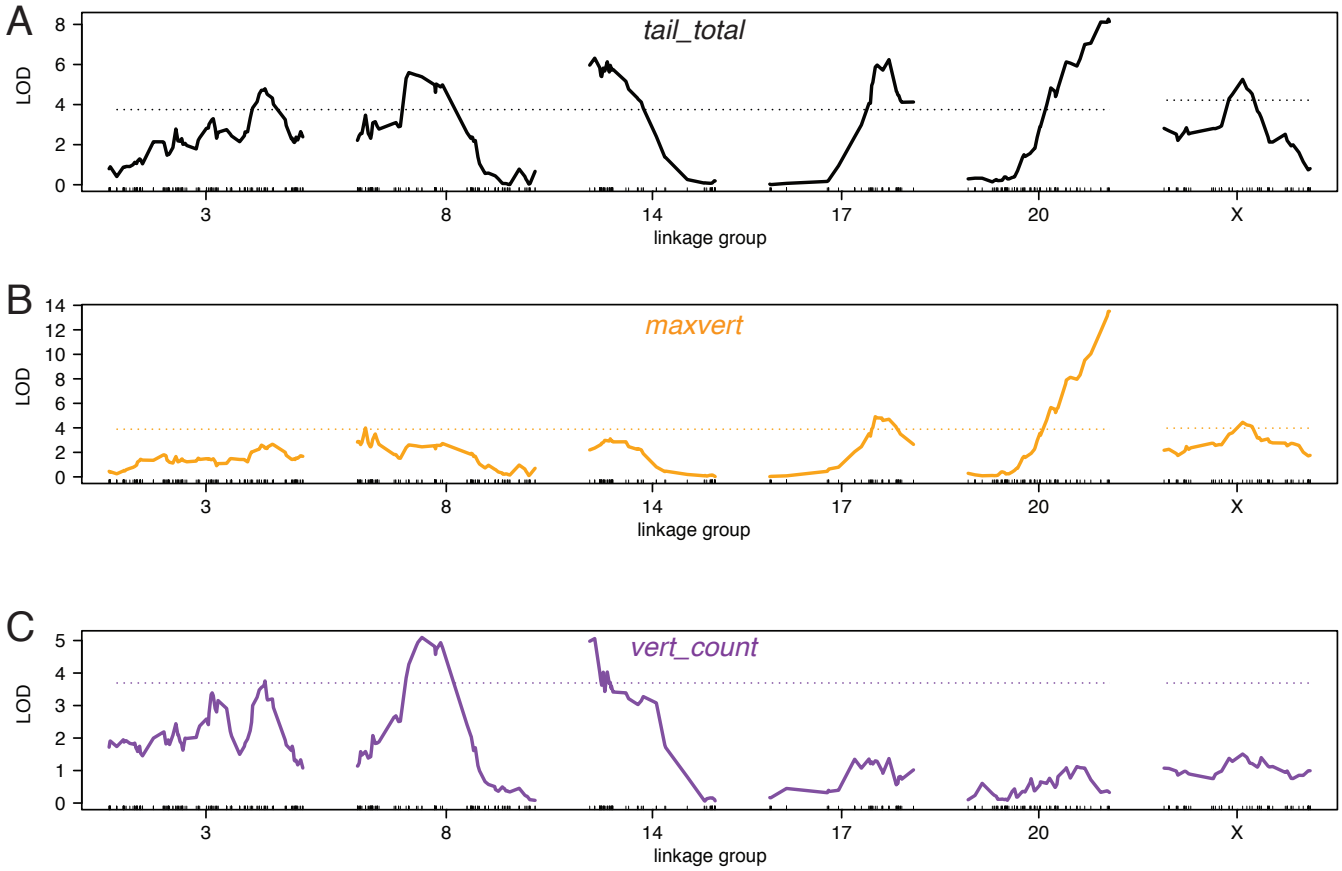

Figure 11. QTL mapping of loci influencing tail length. A. LOD score plot showing significant QTL for total tail length (*tail_total*) on linkage groups 3, 8, 14, 17, 20, and X. **B.** LOD score plot showing significant QTL for length of longest caudal vertebra (*maxvert*) that coincide with those for *tail_total* on linkage groups 17, 20, and X. **C.** LOD score plot showing significant QTL for number of caudal vertebra (*vert_count*) that coincide with those for *tail_total* on linkage groups 3, 8, and 14. Dashed lines on all plots indicate p = 0.05 threshold as determined by permutation test.

Table 1. Tail length QTL

phenotype	linkage group	1.5-LOD interval	peak marker	position (cM)	LOD	p-value in multiple QTL model	mean additive effect	mean dominance (*d*/*a*)
tail_total	3	47.2-80.6	562903406.374669r	71.36	4.79	0.00415	1.08 mm	0.33
	8	19.6-50.2	562903868.1622618r	23.52	5.6	0	0.77 mm	1.06
	14	0-17.8	562903608.62510r	2.29	6.32	0	1.81 mm	0.22
	17	56.1-67.9	562903716.995791r	64.56	6.25	0	1.19 mm	1.13
	20	71.3-84.7	562903388.1057339r	84.2	8.27	0	1.53 mm	0.02
	X	26.3-42.8	562903887.2705603r	35.98	5.26	0.00724	2.3 mm	N/A
maxvert	17	51.9-70.4	562903898.92344r	58.3	4.91	0.00623	0.05 mm	0.6
	20	80.7-84.7	562903278.945341r	84.69	13.52	0	0.1mm	0.1
	X	26.3-48.2	562903887.2705603r	35.98	4.45	0.0397	0.2 mm	N/A
vert_count	3	29.2-80.6	562903406.374669r	71.36	3.76	0.04563	0.26	-0.06
	8	19.6-50.2	562903655.755532r	29.52	5.1	0.00104	0.29	0.05
	14	0-10.3	562903608.62510r	2.29	5.06	0.00104	0.28	0.11

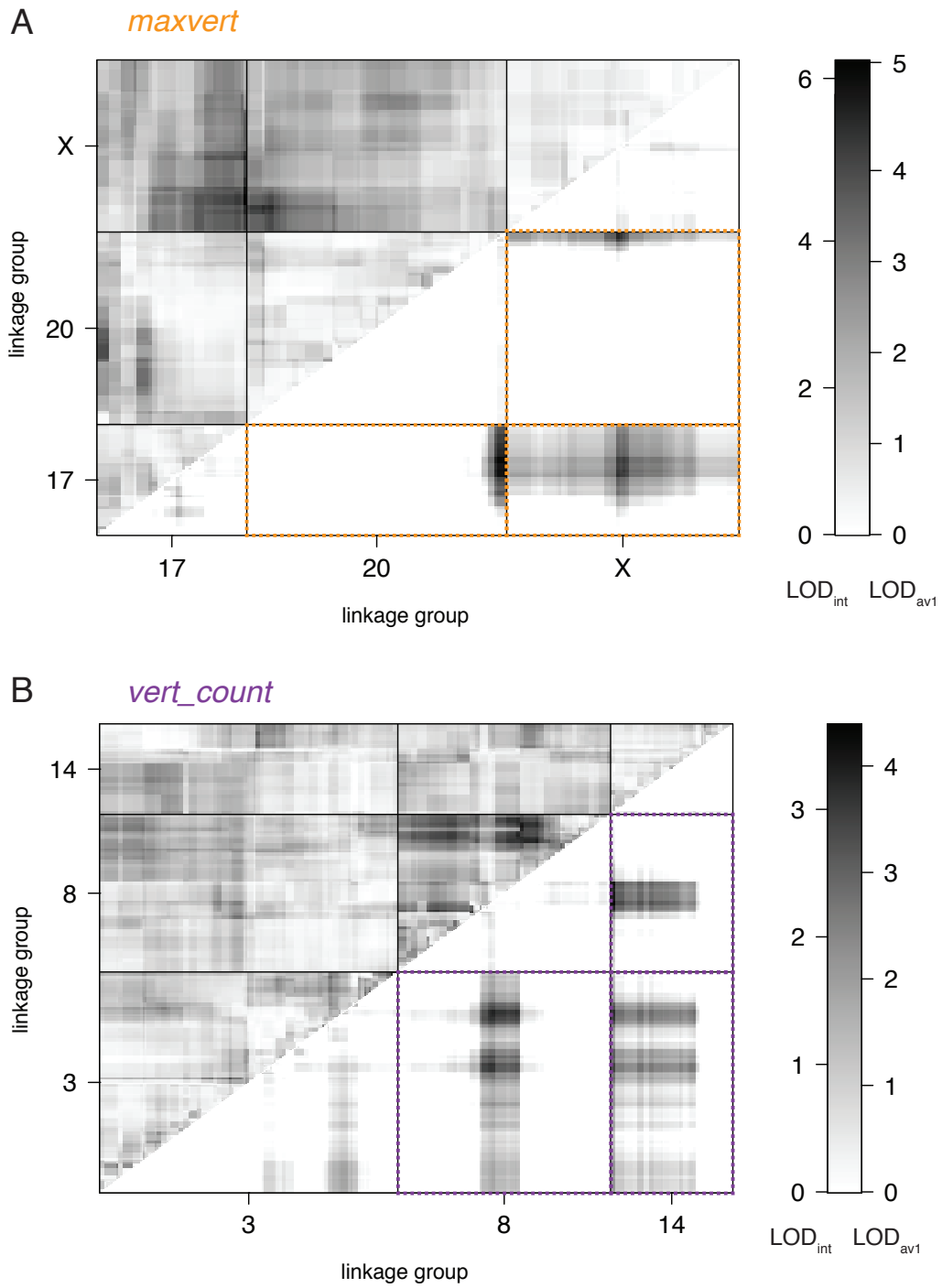

Figure 12. Two-dimensional QTL scans show no significant interactions among loci. Upper triangles show LODint (interaction LOD scores, the difference between LOD for full [including interactions] and additive-only models) and lower triangles show LODav1(the difference between LOD scores an additive two-QTL model and a single-QTL model, i.e. support for two QTL vs. one). **A.** Results of a two-dimensional scan for *maxvert* (p = 0.05 LODint threshold = 6.62; LODav1 threshold = 3.67). **B.** Results of a two-dimensional scan for *vert_count* (p = 0.05 LODint threshold = 4.43; LODav1 threshold = 3.58). There is no support for significant interactions between loci or either trait (LOD thresholds are greater than the maximum value of the scales on the right), but there is significant support for all pairs of QTL across chromosomes for both traits (see quandrants outlined with dashed lines).

QTL range from 0.06 mm to 0.20 mm, with a summed total average effect for the three loci of 0.72 mm. The additive effects of *nubiterrae* alleles at *vert_count* QTL are remarkably close to equal: they range from 0.26 to 0.29; an animal with all *nubiterrae* alleles at the three loci has an average of 1.66 more vertebrae than an animal with *bairdii* alleles.

QTL sign test supports the role of natural selection in maintaining tail length variation

The difference in tail length between forest and prairie deer mice has long been thought to be an adaptive difference, the longer forest tails providing an advantage in arboreal locomotion (Osgood 1909; Blair 1950, Horner 1954). One way to test whether variation in a quantitative trait is adaptive—given a polygenic architecture underlying the trait and having mapped QTL for the trait—is to examine the directions of the allelic effects at QTL for that trait (Orr 1998). For example, in our cross, if natural selection has favored different tail lengths in forest *versus* prairie environments, alleles from *nubiterrae* should produce longer tails while those from *bairdii* should produce shorter tails. On the other hand, if tail lengths differ due only to non-selective evolutionary forces, we would expect that the number alleles affecting tail length in our cross should not be biased in either direction. In the present case, all six QTL for *tail_total* are in the same direction: *nubiterrae* alleles always produce a longer tail (Fig. 8A). Six out of six QTL in the same direction exceeds the null expectation ($p = 0.045$), thus strongly supporting the hypothesis that natural selection is acting on tail length in deer mice.

QTL intervals contain candidate genes for differences in tail length

We searched in the genomic intervals described by each QTL for genes that are known to influence tail and limb traits in the laboratory mouse, and thus would be strong candidate genes to underlie variation in our cross. We used the Mouse Genome Informatics (MGI) Mammalian

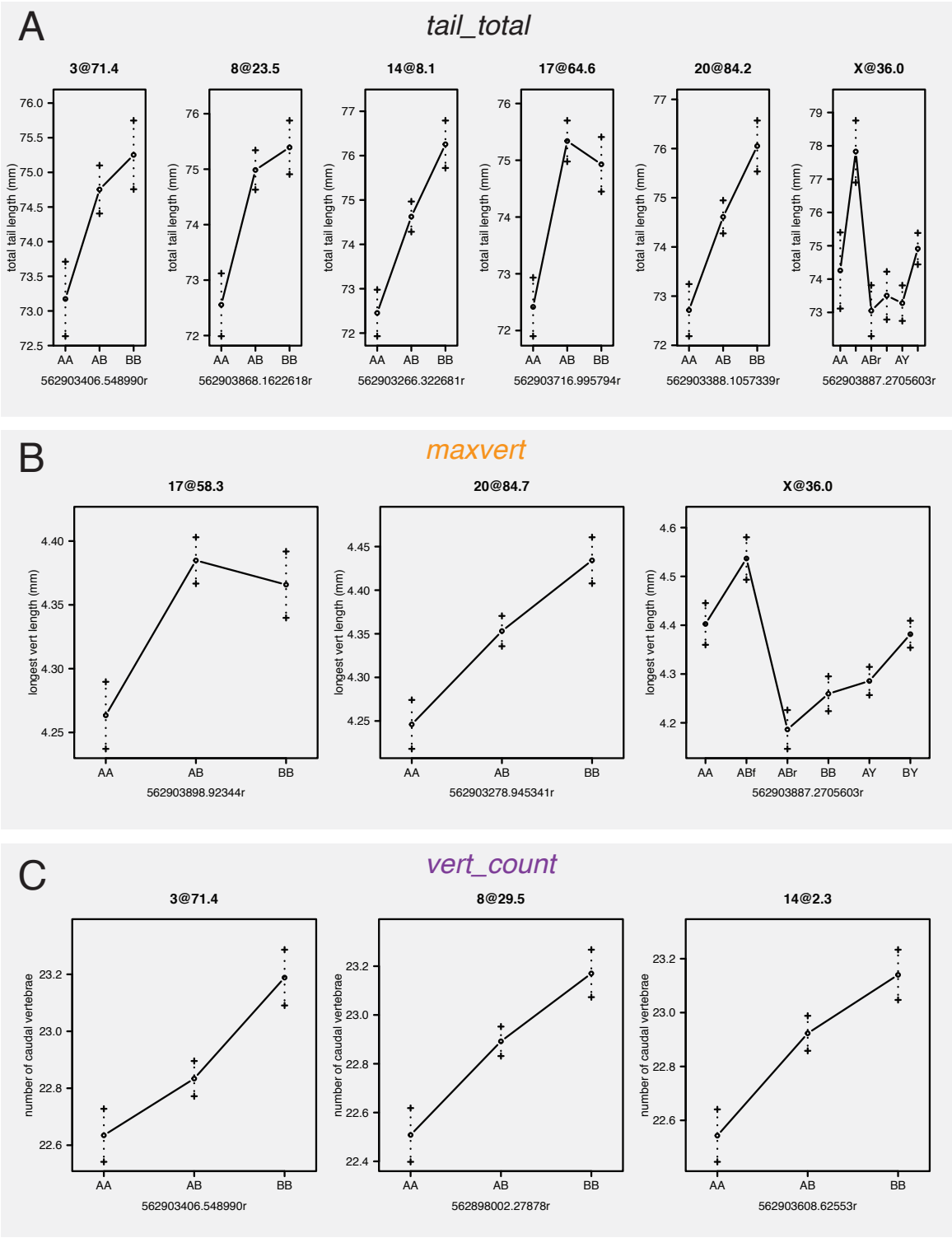

Figure 13. Effects of alleles at tail length QTL. For all plots, dots and bars represent the means and 95% confidence intervals, respectively, of allelic effects. Titles of each plot are in the format "linkage group @ cM position" and the x-axis title is the name of the scaffold and marker position, "scaffold.position".

Phenotype Browser, which catalogs alleles by their phenotypic effects, to find genes in QTL intervals that are known to affect limb and tail traits (Tables 2 & 3). We extracted the gene names of these alleles and searched them for genes in the 1.5-LOD intervals for each QTL. The QTL intervals each contain between 75 and 571 known genes in intervals that range in width from 4.0 to 51.4 cM. A number of biologically interesting candidates exist in these intervals; we consider them in the discussion.

DISCUSSION

The aim of the present work is to describe the major effectors of adaptive skeletal differences in populations of *P. maniculatus*, and to detail how they interact to produce patterns of morphological variation. The variation in question—differences in lengths and numbers of skeletal elements—is of special interest because it very likely represents naturally selected variation in this species. Understanding the genetic basis of adaptive trait evolution means nothing less than understanding the molecular currency of evolution; accordingly, the subject has garnered extensive interest and controversy (Hoekstra & Coyne 2007; Carroll 2008; Rockman 2012). But while finding the specific molecular variation underlying adaptive traits is undoubtedly important, we can learn about key aspects of the variation underlying those traits by investigating at the level of genetic architecture with the goal of apprehending the number, effect size, dominance, and pleiotropic effects of loci that are important for adaptive evolution (Klingenberg 2008; Wagner et al. 2008; Armbruster et al. 2014).

We explore correlations (Fig. 7) between tail and limb skeletal traits and how they cluster by shared variance (by PCA; Fig. 8) in an F2 intercross. Tail and limb bone traits can be grouped into modules, traits that exhibit high covariance within their trait group but little covariance with traits in other groups (Klingenberg 2008). These results show that the codominant alleles underpinning

Table 2. Phenotypes screened from Mouse Genome Informatics database

MGI phenotype
abnormal_limb_mesenchyme_morphology
abnormal_vertebral_body_development
absent_apical_ectodermal_ridge
absent_caudal_vertebrae
absent_tail
decreased_caudal_vertebrae_number
decreased_ventral_ectodermal_ridge_size
elongated_metatarsal_bones
enlarged_tail_bud
increased_caudal_vertebrae_number
increased_tail_bud_apoptosis
long_limbs
long_tail
short_metatarsal_bones
short_tail
small_caudal_vertebrae
small_forelimb_buds
small_hindlimb_buds
small_tail_bud
thick_apical_ectodermal_ridge
thin_apical_ectodermal_ridge
truncated_tail_bud
vestigial_tail

Table 3. Genes in QTL intervals with MGI phenotypes

linkage group	gene symbol	gene name	scaffold	gene start position	MGI phenotype
3	*Hoxd9*	homeobox D9	NW_006501058.1	7994687	decreased caudal vertebrae number
3	*Hoxd11*	homeobox D11	NW_006501058.1	7979423	decreased caudal vertebrae number
3	*Sp5*	Sp5 transcription factor	NW_006501058.1	3532266	decreased caudal vertebrae number, short tail
3	*Sestd1*	SEC14 and spectrin domains 1	NW_006501058.1	10486271	short tail
8	*Hoxa9*	homeobox A9	NW_006501209.1	2521661	decreased caudal vertebrae number
8	*Hoxa11*	homeobox A11	NW_006501209.1	2541296	decreased caudal vertebrae number
14	*Apc*	adenomatous polyposis coli	NW_006501133.1	1222086	short tail
14	*Ndfip1*	Nedd4 family interacting protein 1	NW_006501449.1	63631	short tail

skeletal variation in *P. maniculatus* are pleiotropic, but the sets of traits they affect are genetically separable. This suggests that traits within a group are influenced by alleles at largely overlapping loci. And though traits in different covariance groups likely share some underlying loci—there are weak correlations between caudal vertebra lengths and metatarsal lengths, for example—the bulk of the variance in traits in different groups is likely controlled by alleles at separate, unlinked loci.

Predictions of genetic architectures from examining trait correlations are borne out by our QTL mapping analysis. We find six major effect QTL influencing total tail length (*tail_total*); we further decompose this architecture into three QTL for each of the tail's constituent traits, the number of caudal vertebrae (*vert_count*) and the length of the longest caudal vertebra (*maxvert*). No QTL for *maxvert* overlaps any QTL for *vert_count*. These results show that the genetic variation detectable in our cross for a complex trait, length of the tail, can be broken up into two completely separate major-effect architectures, which has special relevance for evolution of this trait (see below).

Skeletal QTL in deer mice *versus* other taxa

To put these results in a broader context, let us briefly compare our deer mouse skeletal QTL results to those found in a large *Mus* F2 intercross. Kenney-Hunt et al. (2008) investigated pleiotropy of QTL affecting skeletal traits in a cross between two laboratory mouse strains selected for high and low body mass. Relevant to the current study, they measured the lengths of the 3rd caudal vertebra, the 3rd metatarsal, and total tail length (among 67 other skeletal traits) in 1040 F2 mice. Kenney-Hunt et al. found 8 QTL for the length of the 3rd caudal vertebra, 10 QTL for 3rd metatarsal length, and 8 QTL for total tail length. Four tail length QTL overlap metatarsal QTL; one tail QTL overlaps a caudal vertebra length QTL. While our analyses are not easily comparable (we used fewer animals and are primarily concerned with different traits) it is notable that we see no

Table 4. Vertebral QTL in other species

phenotype	species	QTL/ candidate gene	gene name	on native chromosome	homolog on mus chromosome	overlaps deer mouse QTL?	reference
number of vertebrae	*Sus scrofa*	*NR6A1*	nuclear receptor subfamily 6, group A, member 1	1	2		Mikawa et al. 2007
number of vertebrae	*Sus scrofa*	*VRTN*	vertebrae development homolog	7	12		Mikawa et al. 2011
number of vertebrae	*Gasterosteus aculeatus*	*ASPN*	asporin	17	13		Berner et al. 2014
number of vertebrae	*Gasterosteus aculeatus*	*OGN*	osteoglycin	17	13		Berner et al. 2015
number of vertebrae	*Gasterosteus aculeatus*	*COL11A1*	collagen, type XI, alpha 1	21	3		Berner et al. 2016
number of vertebrae	*Oryzias latipes*	*Sfrp2*	secreted frizzled-related protein 2	1	3		Kimura et al. 2012
number of vertebrae	*Oryzias latipes*	*Fgf13*	fibroblast growth factor 13	10	X		Kimura et al. 2013
number of vertebrae	*Oryzias latipes*	*Shisa3*	shisa family member 3	10	5		Kimura et al. 2014
number of vertebrae	*Oryzias latipes*	*Hey1*	hairy/enhancer-of-split related with YRPW motif 1	11	3		Kimura et al. 2015
number of vertebrae	*Oryzias latipes*	*T*	brachyury	11	17		Kimura et al. 2016
number of vertebrae	*Oryzias latipes*	*Hes6*	hairy and enhancer of split 6	17	1		Kimura et al. 2017
number of vertebrae	*Oryzias latipes*	*Snail2*	snail family zinc finger 2	17	16		Kimura et al. 2018
number of vertebrae	*Oryzias latipes*	*Gbx1*	gastrulation brain homeobox 1	17	5		Kimura et al. 2019
number of vertebrae	*Oryzias latipes*	*Wnt3a*	wingless-type MMTV integration site family, member 3A	17	11		Kimura et al. 2020
number of vertebrae	*Oryzias latipes*	*Wnt5b*	wingless-type MMTV integration site family, member 5B	23	6		Kimura et al. 2021
number of vertebrae	*Oryzias latipes*	LOC101165857	prickle-like protein 1	23	15		Kimura et al. 2022
caudal vertebra length	*Mus*	PAPPA2	pappalysin 2	1	1		Christians et al. 2003
tail length	*Mus*	*Skl1*	N/A	1	1		Cheverud et al. 2001
tail length	*Mus*	*Skl2*	N/A	2	2	*vert_count* (LG3)	Cheverud et al. 2002
tail length	*Mus*	*Skl3*	N/A	6	6	*vert_count* (LG3)	Cheverud et al. 2003
tail length	*Mus*	*Skl4*	N/A	10	10		Cheverud et al. 2004
tail length	*Mus*	*Skl5*	N/A	11	11		Cheverud et al. 2005
tail length	*Mus*	*Skl6*	N/A	13	13		Cheverud et al. 2006
tail length	*Mus*	*Skl7*	N/A	16	16	*maxvert* (LG20)	Cheverud et al. 2007

correlation between tail length and metatarsal length in our cross (Fig. 7), suggesting that the pleiotropy of genetic loci underlying these traits in *Mus* are different from those in deer mice. We see half of our tail QTL coincide with vertebral length QTL, while Kenney-Hunt found one out of 8. This difference, however, may be an effect of the two crosses considering different vertebrae in the caudal series: c3, the specific caudal vertebra measured by Kenney-Hunt et al., only differs slightly in length between *nubiterrae* and *bairdii* subspecies (Fig. 6) and is not part of the medial section of the tail that contributes the majority of variability in tail length. In fact, length of c3 exhibits a weak negative correlation with the length of the longest caudal vertebrae. So it is not surprising that there is less overlap in Kenney-Hunt et al.'s QTL for vertebral length and tail length than we see in deer mice.

Other studies of skeletal genetics in mammals provide context for the present work. Morris et al. (1999) report a large-effect QTL on *Mus* chromosome 1 that strongly influences tail length; this QTL affects the length of the 10th caudal vertebra in a replicate cross (Christians et al. 2003). Genes in this QTL are not contained in any of the deer mouse *maxvert* QTL (Table 4). In a replicate population of the SM/J and LG/J lines of *Mus* examined in Kenney-Hunt et al.'s work described above, Cheverud et al. (2001) found 7 QTL for tail length. It is unclear whether these loci affect tail length by influencing number or length of vertebrae, but the reported confidence intervals for three of Cheverud et al.'s tail length QTL overlap QTL from our study: two for *vert_count* and one for *maxvert* (Table 4). It should be noted that, because these studies mapped many QTL and the genome is finite, it is possible that overlapping intervals is entirely due to chance.

The number of caudal vertebrae is an especially interesting trait. The only other mammal in which QTL underlying differences in number of vertebrae have been described is domesticated swine, *Sus scrofa* (vertebra number correlates with body size, a valuable livestock trait). Two QTL have been found to influence the number of thoracic and lumbar vertebrae in swine (Wada et al.

2000) and one gene in each QTL has been implicated (Mikawa et al. 2007; Mikawa et al. 2011). Neither of these genes lies in the intervals for any of our *vert_count* QTL (Table 4). The only other studies of vertebral number are on fish: QTL have been mapped in trout (Nichols et al. 2004), medaka (Kimura et al. 2012), and in two different threespine stickleback crosses (Miller et al. 2014; Berner et al. 2014). The studies detect one vertebral number QTL in trout; two and three QTL in sticklebacks in Berner et al. and Miller et al., respectively, with all five on different chromosomes; and five QTL in medaka. Differences in vertebra number in sticklebacks are perhaps most relevant to the present study for two reasons. First, differences in vertebra number have been proposed to confer differences in locomotion (Swain 1992), making it likely that these differences are favored by natural selection. Second, both stickleback studies found QTL that specifically affect the number of caudal vertebrae, as the QTL in the present study do. For these caudal-specific loci, Berner et al. and Miller et al. find little or no correlation between caudal vertebra number and body size, suggesting that these QTL are not byproducts of selection for body size differences.

Differences in power to detect QTL among all the studies described herein prohibit directly comparing genetic architectures, but we draw three conclusions from the collective results of our study and the ones described above. First, variation in vertebral traits is often polygenic, with alleles of relatively small effect underlying much of the described phenotypic variation in these traits. This is true for all studies described above except for one in domesticated *Mus* (Morris et al. 1999; Christians et al. 2003; Christians et al. 2006). Second, multiple studies find QTL that underlie region-specific differences in vertebral number and size in several species. Variability in (and presumably, constraint on the evolution of) numbers of vertebrae differs among sections of the vertebral column and among taxa. Mammals almost exclusively have seven cervical vertebrae but taxa differ widely in the numbers of vertebrae in other vertebral regions, especially in the caudal region (Hickman 1979; Pilbeam 2004; Galis et al. 2006; Asher et al. 2011). Vertebral number in non-mammalian vertebrates

is much more variable than in mammals—compare, for example, a zebrafish to an eel—so it is notable that in laboratory mice, swine, sticklebacks, and now deer mice, alleles affecting vertebrae in a region-specific manner are common, thus implicating changes in region-specific developmental processes. In what is the other side of the pleiotropy-as-constraint idea presented earlier in this chapter, it has been proposed that alleles with more anatomically specific effects, i.e., those with less pleiotropy, have an evolutionary advantage (Stern 2000; Stern & Orgogozo 2008) and that modularity in gene effects may provide a solution to the selective problem of pleiotropy (Welch & Waxman 2003). Third, and finally, the fact that very few of the QTL influencing tail length traits contain overlapping gene sets among species suggests that there are many ways to evolve differences in the lengths and numbers of vertebrae. This is a contrast to some other well-studied examples of adaptation in deer mice, in which relevant evolutionary variants appear at the same loci as in other taxa, e.g., cryptic pigmentation (Hoekstra 2006) and high-altitude adaptation (Storz et al. 2009, 2012)

Candidate genes

We looked for genes that are known to affect any of 23 limb and tail phenotypes (Table 2) within the 1.5-LOD confidence intervals for each QTL and found several plausible candidates for differences in vertebral number (Table 3). Two genes, *Sp5* and *Ndfip1*, on linkage groups 3 and 14, respectively, exhibit cyclical gene expression in the segmentation clock, the mechanism by which the precursors to vertebrae are formed in the vertebrate embryo (Dequeant et al. 2006). Differences in segmentation clock timing contribute to differences in vertebral number between snakes and other vertebrates (Gomez et al. 2008). Perhaps most intriguing, though, is that two QTL intervals, those on linkage groups 3 and 8, contain the *Hoxd* and *Hoxa* gene clusters, respectively. In addition to the well-known role of *Hox* genes in positioning of landmarks along the embryonic anterior-posterior axis, timing of *Hox* gene expression also regulates the length of the embryonic axis by controlling

the ingression of cells into the presomitic mesoderm (Iimura & Pourquié 2006; Young et al. 2009; Denans et al. 2015), thus making them very strong candidates.

Evolutionary implications

We find strong evidence hat natural selection acts on alleles underlying tail length differences in *P. maniculatus*. Previous work supports the idea that longer tails are favored in forest habitats: other authors have described longer tails in forest-dwelling deer mice (Blair 1950), how deer mice use their tails while climbing (Horner 1954), and how morphological differences between forest and prairie mice persist despite little population genetic structure among those populations (Yang & Kenagy 2011). We have shown a robust correlation between forest habitat and longer tail:body-length ratio in this species (Chapter 1). In the current work we provide the first genetic evidence, via the QTL sign test, supporting natural selection's role in favoring long tails in forests. The fact that the *nubiterrae* alleles at all six tail-length QTL produce longer tails is strong evidence that natural selection is acting on tail length in the expected direction (Orr 1998).

Putting our laboratory QTL mapping results in the context of natural patterns of variation can inform our understanding of trait evolution. Interestingly, in natural populations we have noted a correlation between the lengths and numbers of caudal vertebrae, which we do not see in our F2 animals. This suggests that natural selection maintains the correlation between number and length of caudal vertebrae in the wild, despite the lack of underlying genetic correlation. While this is not particularly surprising—and in a sense represents the null hypothesis of trait evolution: that trait evolution is not constrained by pleiotropy—the fact that we see the same correlation has evolved in independent populations (Chapter 1) suggests that selection may favor not only longer tails, but the combination of longer and more numerous caudal vertebrae. As noted in Chapter 1, the response to selection on long tails does not have to include length and number of vertebrae. Rutledge et al.

(1974) imposed artificial selection for longer tails in two replicate lines of laboratory mouse and obtained different results in each line: one with more vertebrae and one with longer vertebrae.

On the other hand, it is likely that pleiotropy maintains other patterns of naturally occurring skeletal variation in deer mice. The differences in vertebral lengths between forest and prairie populations are evident mainly in a particular segment range in the tail, c4 to c16 or c17 (Chapter 1). In our F2 animals, we find that the vertebrae in this same segment range covary, suggesting that the specific pattern of caudal vertebrae length differences seen among natural populations could be due to the pleiotropy of the alleles producing these differences.

Despite the lack of genetic correlation in number and length of caudal vertebrae in our cross, we have previously shown that different forest populations in the eastern and western parts of the deer mouse's range have independently evolved longer and more numerous caudal vertebrae. The present study represents the first step in understanding the nature of this convergent evolution. Future work will endeavor to answer whether these different lineages evolve similar traits by selection of 1) the exact same alleles, 2) different alleles at the same loci, 3) different loci altogether, or in the case of variation with a polygenic basis, as in this study, 4) a combination of the three.

Chapter 3

Developmental basis of segment number variation in *Peromyscus maniculatus*

Evan P. Kingsley[1], David Zwicker[2], Hopi E. Hoekstra[1]

[1]*Department of Organismic and Evolutionary Biology, Museum of Comparative Zoology, Howard Hughes Medical Institute*
Harvard University, 26 Oxford Street, Cambridge, Massachusetts 02138, USA
and Department of Molecular and Cellular Biology
Harvard University, 16 Divinity Avenue, Cambridge, Massachusetts 02138, USA

[2]*School of Engineering and Applied Sciences, Harvard University, Cambridge, Massachusetts 02138, USA*

INTRODUCTION

Changes in growth and development underlie all morphological diversity in multicellular organisms. Thus, understanding the developmental basis of adaptive changes in morphology is a key goal of modern evolutionary biology. From the floral structures of angiosperms, to the segments of arthropods and annelids, and to the spinal column of vertebrates, a major source of evolutionary change on a large scale is change in the numbers and identities of serially homologous morphological segments. Much work has been done toward understanding the developmental basis of changes in segment identity—e.g., how appendages evolve in crustacea (Averof & Patel 1997; Liubicich et al. 2009) and how *Hox* gene expression reveals transposition of vertebral identities among vertebrates (Burke et al. 1995)—but little is known about how the process of development is modified to produce differences in segment number.

Vertebrates exhibit a wide diversity in total segment number, from nine vertebrae in some frogs (Hedges et al. 2008) to over 300 in snakes (Marx & Rabb 1972). While numbers of vertebrae can vary widely among species, the number of vertebrae within a species is thought to be relatively constant. But intraspecific variation in vertebral number is more common than is often discussed. Variation in vertebral number that could plausibly be evolutionarily important, i.e., genetic variation that is sorted by natural selection, could be common. For example, threespine sticklebacks (*Gasterosteus aculeatus*) from lakes consistently have more vertebrae than those from streams, which may be a locomotor adaptation (Swain 1992; Aguirre et al. 2014). Coastal and inland garter snakes (*Thamnophis elegans*) have different numbers of vertebrae and differ correspondingly in locomotor performance (Arnold 1988; Kelley et al. 1997). And in deer mice, (*Peromyscus maniculatus*) we showed that mice from forested habitats have longer tails—with longer vertebrae, and more vertebrae (Fig. 14)—than mice from prairie habitats (Chapter 1). These mice use their tails extensively while

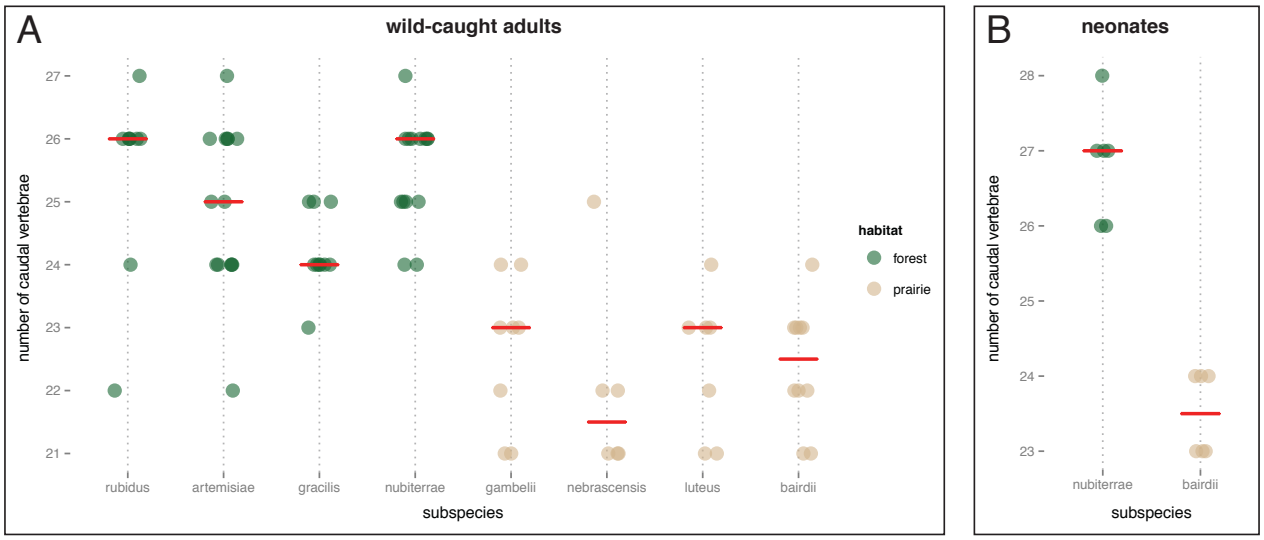

Figure 14. Forest mice have more caudal vertebrae than prairie mice. A. Variation in caudal vertebra counts in eight *P. maniculatus* subspecies. **B.** Forest and prairie mice differ in vertebral number at birth, as measured in Alcian/Alizarin-stained neonates. Newborn (postnatal-day-0) *P. m. nubiterrae* have a significantly larger number of caudal vertebrae than *P. m. bairdii*. Red lines indicate the median.

climbing (Horner 1954) and differences in tail length between forest and prairie mice are likely the result of natural selection (Chapter 2).

The first embryonic precursors to vertebrae are epithelial blocks called somites, which are formed in pairs, sequentially, beginning near the anterior of the embryo and progressing toward the posterior. The somites will go on to form not only the vertebrae and the ribs, but also the dermis and skeletal muscle of the trunk and tail (reviewed in Hirsinger et al. 2000). Somites form lateral to the neural tube from mesodermal strips of tissue called presomitic mesoderm (PSM), which is itself generated during gastrulation by cells ingressing from the epiblast through the regressing primitive streak (in amniotes) and undergoing an epithelial-to-mesenchymal transition (Nakaya & Sheng 2008). The posterior tip of the embryo extends and somite formation follows. Later in development, after the posterior neuropore closes, axial extension occurs mainly from the tailbud in a process often called secondary axis formation (Schoenwolf 1979), during which the PSM that will form the somites of the sacral and caudal regions continues to form by a gastrulation-like ingression from the tailbud mesenchyme (Catala et al. 1995; Knezevic et al. 1998; Cambray & Wilson 2002). This axial extension begins to slow and continues until, effectively, somitogenesis catches up and axial growth ceases (Bellairs 1986).

The rhythmic formation of somites is controlled by oscillating patterns of gene expression known as the segmentation clock (reviewed by Dequéant & Pourquié 2008) consisting of series of oscillations in the cells of the PSM, each of which corresponds to the formation of a somite. Faster oscillations of the segmentation clock would lead to an increase in the number of somites formed (Schröter & Oates 2010; Harima et al. 2013); a more quickly oscillating clock would also produce smaller somites (Fig. 15A). A difference in the speed of segmentation clock oscillation has been implicated in producing greater numbers of somites in snakes compared to mice, zebrafish, and chick (Gomez et al. 2008). Additionally, variation in somite number could be produced by

differences in axial extension: if more PSM is formed then more somites will be formed, even in the absence of any difference in clock oscillation speed (Fig. 15B). Thus, the total number of somites produced in an embryo is a balance of 1) axial extension rates and 2) somite formation rates.

Though the embryological study of the deer mouse lacks the developmental-genetic tools present in the laboratory mouse, vertebral number variation in the deer mouse is a powerful system for understanding the generation of variation in segment number. By applying knowledge gained through the study of segmentation in other vertebrate embryos, including the mouse, chicken, and zebrafish, we can measure tissues in fixed and cultured embryos to test hypotheses about how the developmental processes is modified to produce different numbers of vertebrae.

Here we test hypotheses about the developmental mechanisms underlying adaptive differences in the vertebral numbers of deer mice. We present evidence that the difference in vertebral number between forest and prairie deer mice is due to a difference in the size of the PSM, which affects the eventual number of somites produced. Furthermore, we describe methods we have developed for precisely measuring the parameters of the segmentation process in deer mouse embryos that will allow for exact comparisons of somitogenesis. We end by proposing experiments that will help elucidate the molecular nature of this adaptive segment number variation.

METHODS

Vertebral counts

We compared the number of caudal vertebrae in population samples from eight locations. These individuals were wild-caught by EPK, wild-caught by D.-S. Yang (Yang & Kenagy 2011), or obtained from the Mammalogy collection at the Museum of Comparative Zoology. We designated samples as "forest" or "prairie" based on the subspecies descriptions (Osgood 1909; Hall 1981) and the descriptions of the capture site by the fieldworker. To reliably count vertebrae, we defined the

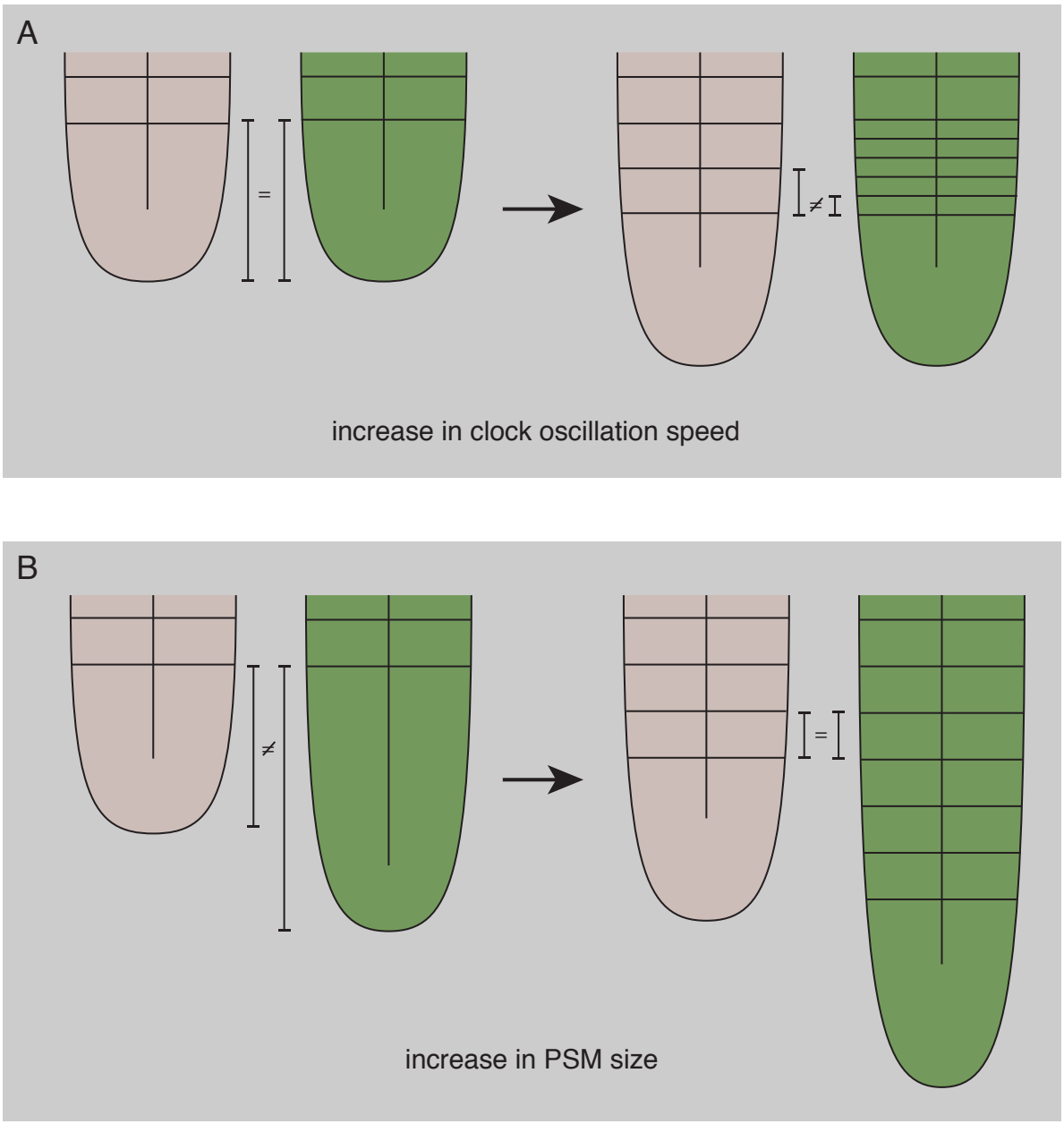

Figure 15. Hypotheses for developmental difference underlying segment number variation. As the embryo finishes segmenting (arrow represents transition from trunk to caudal growth), **A.** a difference in the numbers of segments produced by prairie (tan) and forest (green) deer mouse embryos could be caused by forest embryos making more, smaller somites from the same amount of mesoderm (PSM sizes equal, different somite sizes). **B.** Segment number difference could be caused by differences in PSM size, with the forest form producing more, equivalent-sized somites (PSM sizes different, equal somite sizes. These mechanisms are not mutually exclusive and could be functioning together to produce segment number variation in deer mice.

sacral vertebrae as the first vertebra attached to the ilium and the five vertebrae caudal to that, and the caudal vertebrae as all vertebrae caudal to those six. We excluded individuals that were obviously missing the terminal vertebrae or had broken tails.

We also compared caudal vertebrae counts in laboratory-reared neonatal animals (postnatal-day-0 pups) of forest and prairie subspecies (see below). To count the vertebrae in these animals we performed Alcian/Alizarin bone stains as described previously (Ovchinnikov 2009). For these counts we include all recognizable segments in the tail, which at birth includes non-ossified cartilage condensations.

Embryo measurements

All embryos used in this study were generated in our laboratory colony at Harvard University. The prairie subspecies, *P. m. bairdii*, are descended from mice obtained from the Peromyscus Genetic Stock Center (University of South Carolina); the forest subspecies, *P. m. nubiterrae*, are descendants of 18 mice captured in Westmoreland County, Pennsylvania, in 2010.

We obtained embryos of approximate ages by setting the date of conception as the birth date of a female's last litter. Mice in our *bairdii* colony reliably experience postpartum estrus, which normally allows for accurate embryo timing, but our *nubiterrae* colony is less reliable: only 30% of mating pairs produced a litter 23 days—the standard deer mouse gestation period—after their last litter. The others produced litters after ~28 days (45%) or after an even greater period of time or did not produce litters (25%).

To compare tissue dimensions in fixed embryos, we first sacrificed females and dissected embryos in phosphate buffered saline (PBS), then fixed the embryos in 4% paraformaldehyde for 14-24 hours at 4°C. We stained embryos with DAPI and photographed them with a Zeiss mRc camera on a Zeiss steREO Discovery V.12 dissecting microscope that was scale calibrated. We used

Fiji/ImageJ's (Schindelin et al. 2012; Rasband 1997–2014) linear measurement tool to measure all lengths; we performed analyses in R (R Core Team 2005) and made plots with *ggplot2* (Wickham 2009).

In situ hybridization

We extracted total RNA from ~E12 tail tissue (Qiagen RNeasy kit), reverse transcribed into cDNA (Quanta qScript cDNA synthesis kit), and we cloned fragments of the *Msgn1*, *Uncx*, and *Lfng* into a pCRII vector (Life Technologies TOPO-TA cloning kit) to generate in situ probes. We PCR amplified fragments with the following primers: msgnF2-TCCTTCTCTGGAGTCCTACTCT, msgnR1-CCCCGATGTACTTGATGGTGTA; uncxF1-CCCTTCAAGCTGTCAGACTC, uncxR2-TTCTTTGGCTCGGGTAGAAG; lfngF1-GAGACCTGGATCTCGCGC, lfngR1-CTGGGCCCTTTGGATACCAG. After *in vitro* transcribing digoxigenin-labeled probes (Roche DIG labeling mix; NEB T3/T7 RNA polymerase), we performed *in situ* hybridization in fixed whole-mount embryos as described by Henrique et al. (1995) and photographed embryos as described above.

Proliferation antibody stain

To measure proliferation, we performed immunofluorescent staining for the phosphorylated form of Histone H3 (pHH3), a marker of cell division (Hendzel et al. 1997). We embedded fixed embryos (see above) in cryosectioning medium after grading through sucrose, and then cryosectioned tail tissues at 10 μm (CM3050S; Leica Biosystems). We detected pHH3 on sections using a rabbit antibody to pHH3-Ser10 (Cell Signaling Technologies) with an anti-rabbit-AlexaFluor-488 IgG secondary antibody (Life Technologies), then stained nuclei with Hoechst-332 (Life Technologies). We photographed sections with a Zeiss mRm camera on an Axioplan compound

microscope and processed the resulting images with Fiji/ImageJ (Schindelin et al. 2012; Rasband 1997–2014).

Embryonic tail explant culture and time lapse imaging

To obtain precise measurements of segmentation and axial extension parameters, we cultured posterior embryonic tissues and time-lapse imaged them. We dissected E12.5-E15.5 embryos in DMEM that was prewarmed to 37°C, dissected the portion of the embryo caudal to the hind limb bud, and transferred that explant to an uncoated Mat-Tek glass-bottomed culture dish also containing prewarmed DMEM. We then transferred the dish containing explant to a culture chamber at 37°C with a humidified carbon dioxide (5%) line on a Zeiss Cell Observer (Harvard Center for Biological Imaging). We used Zen 2012 (Zeiss) software to take images every ten minutes over a 12–14 hour period while the explant formed somites and underwent axial extension. We took a Z-stack for each time point and used the "Extended Depth of Focus" function in Zen to collapse the stack into a single image for each time point. From these time-lapse movies, we obtained basic information about the timing of segment formation using Fiji/ImageJ to mark the formation of somite boundaries on individual frames. All explants settled slightly during the first 90-120 minutes; for all time-lapse movies we discarded the first 12 frames.

Automated analysis of explant time-lapse

To more accurately and more reproducibly measure tail explant culture time-lapses, we developed custom Python software that processes the time-lapse images, generates kymographs, and uses the results to measure key segmentation and extension parameters. All code is available at *github.com/david-zwicker* but here we briefly describe how the software functions. First, an edge around the explant is found and a line is drawn inside the resulting bound area at a maximum

distance from the edge. This line represents the center of the tail. From this center line, lines are drawn on either side of the centerline, parallel to the edge line and the center line at a pre-set distance from each (Fig. 19C). One of these lines, the one on the dorsal side, traces a path along the row of newly formed somites and through the presomitic mesoderm to the tip of the tail (results from the ventral line are discarded). A 30-pixel-wide line scan is performed along the dorsal line; from this scan we construct a kymograph (e.g. Fig. 19D). From this kymograph we can estimate axial extension rate (slope of line traced along caudal end of explant), rate of segmentation front progression (slope of line traced along somite formation front), and somite sizes (distance between somite borders).

RESULTS

Forest deer mice have more caudal vertebrae than prairie deer mice

We compared the number of caudal vertebrae in mice from eight geographically widespread populations (Fig. 14A). The median number of caudal vertebrae ranges from 24 to 26 in forest populations, and 21.5 to 23 in prairie populations; comparison of forest *vs.* prairie showed that they differ significantly (n = 5 to 14 per population; Wilcoxon test: $W = 1363$, $p < 1e\text{-}10$). Additionally, among the subspecies we sampled, there is an effect of subspecies among the forest populations (Kruskal-Wallis test: Chi-sq = 10.7, 3 df; $p = 0.01$) but not among prairie populations (Kruskal-Wallis test: Chi-sq = 1.7, 3 df; $p = 0.63$). Together, these data show that 1) in multiple population samples, forest mice have more caudal vertebrae than prairie mice and that 2) populations of forest mice in our sample differ more among themselves than do populations of prairie mice.

To determine whether differences in segment number are produced during embryogenesis, we also compared the number of caudal vertebrae present at birth in two laboratory-reared subspecies (Fig. 14B). The median number of caudal vertebrae at birth in forest mice, *nubiterrae*, is

27, while that of the prairie mouse, *bairdii*, is 23.5 (n = 6 for each subspecies). Wilcoxon test: W = 36, $p < 0.01$). This confirms that the difference in segment number between the adult forms is not due to a difference in growth or ossification during postnatal growth.

Expression of segmentation genes in *P. maniculatus*

We investigated the expression patterns of genes known to participate in the segmentation process in the laboratory mouse by *in situ* hybridization to answer two questions: 1) Are deer mouse expression patterns similar to those in the *Mus* embryo? 2) Does expression of these genes differ in forest and prairie deer mouse embryos?

Uncx is expressed in the posterior half of developing somites in mice and other vertebrates (e.g., Gomez et al. 2008); it is expressed in a qualitatively similar way in deer mouse embryos and we see no difference between forest and prairie forms in the spatial extent of expression (Fig. 16A,B; n = 3). *Msgn1* is expressed in the presomitic mesoderm (PSM) of the mouse embryo, is regulated by Wnt signaling (Wittler et al. 2007), and is the primary known regulator of PSM fate (Chalamalasetty et al. 2014). We see similar expression in deer mice to that in *Mus*: *Msgn1* is expressed in the deer mouse PSM and the size of the expression domain changes through time accordingly with the size of the PSM. The extent of *Msgn1* expression is not qualitatively different between forest and prairie deer mice (Fig. 16C,D; n = 4).

Lfng is a componenet of the Notch signaling pathway and exhibits oscillating expression in PSM of the mouse and other vertebrates (McGrew et al. 1998; Forsberg 1998). This expression pattern consists of a wave that travels from the posterior of the PSM toward the somitogenesis front. When it reaches the front, the broad wave of *Lfng* condenses into the forming somite; this cycle repeats for each somite. The typical pattern in the laboratory mouse is a stripe in the developing somite and dynamic expression in the PSM, which we see in the deer mouse (Fig. 16E).

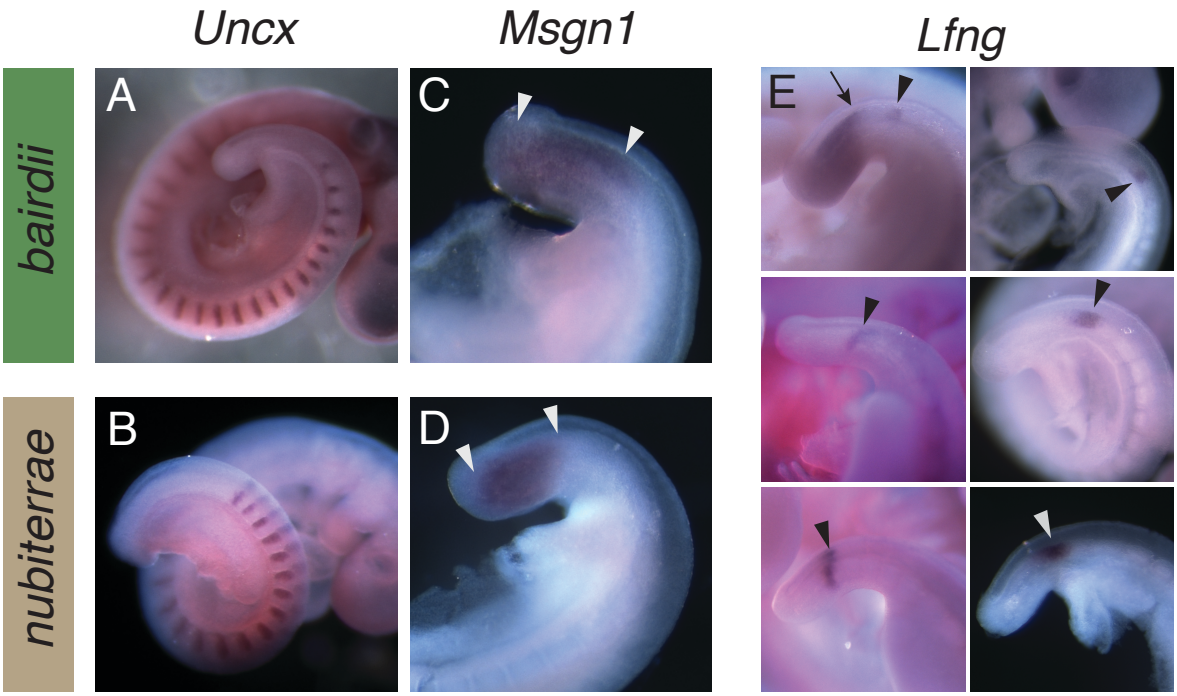

Figure 16. *In situ* hybridization for genes involved in tail axis formation. A,B. *Uncx* is expressed in the posterior half of the somites and does not qualitatively differ in expression pattern between forest and prairie embryos (n = 3). **C,D.** *Msgn1* is expressed similarly in the PSM of prairie and forest embryos (n = 4). Arrowheads indicate the anterior and posterior boundaries of *Msgn1* expression. **E.** *Lfng* is expressed in a dynamic pattern in the PSM of deer mice embryos. Arrowheads show the cycle of *Lfng* expression condensing into the newly forming somite. Arrowhead in the upper-left panel indicates the anterior border of the next *Lfng* cycle in an E11.5 embryo.

Altogether we see no obvious differences in expression of *Uncx*, *Msgn1*, and *Lfng* between the lab mouse and the deer mouse or between forest and prairie deer mouse.

Difference in PSM length correlates with segment number difference

To determine whether differences in segment size or PSM growth could be involved in producing variation in segment number between forest and prairie mice (Fig. 15), we compared linear tissue dimensions in an embryonic time series (Fig. 17). This time series spans the time during which most of the tail segments are formed in the embryo: after the formation of the first post-hindlimb somites. We traced the length of the PSM and the length of the most-recently-formed somite (S1) (Fig. 17A) through time and found that, though the S1 lengths are comparable between forest and prairie embryos, the length of the PSM differs during one phase of posterior growth (Fig. 17A, C). Because differences in the standard staging metric for vertebrate embryos—the number of somites the embryo has formed—may complicate stage matching in this case, we also classified embryos into roughly synchronous bins (arbitrarily, 1–5) based on the development of the limb buds (Fig. 17B, C). Using this staging method, we see a consistent difference in PSM size, though of a smaller effect than when staged by somite number. Regardless, we do not have any *a priori* expectation that staging asynchrony should bias measures of PSM length in either direction. These results show that embryos of forest mice have more PSM than prairie mouse embryos, which suggests a plausible mechanism for producing a segment number difference (Fig. 15).

Next we investigated whether differences in PSM size could be due to proliferation differences in the tailbud (Fig. 18). The tailbud mesenchyme (TBM) is thought to be the major contributor to the paraxial mesoderm of the tail (reviewed by Bénazéraf & Pourquié 2013), so we counted proliferative cells in the TBM of embryos when the difference in PSM size is becoming visible (stages between dotted lines in Figure 17B). Counts of pHH3-positive cells did not

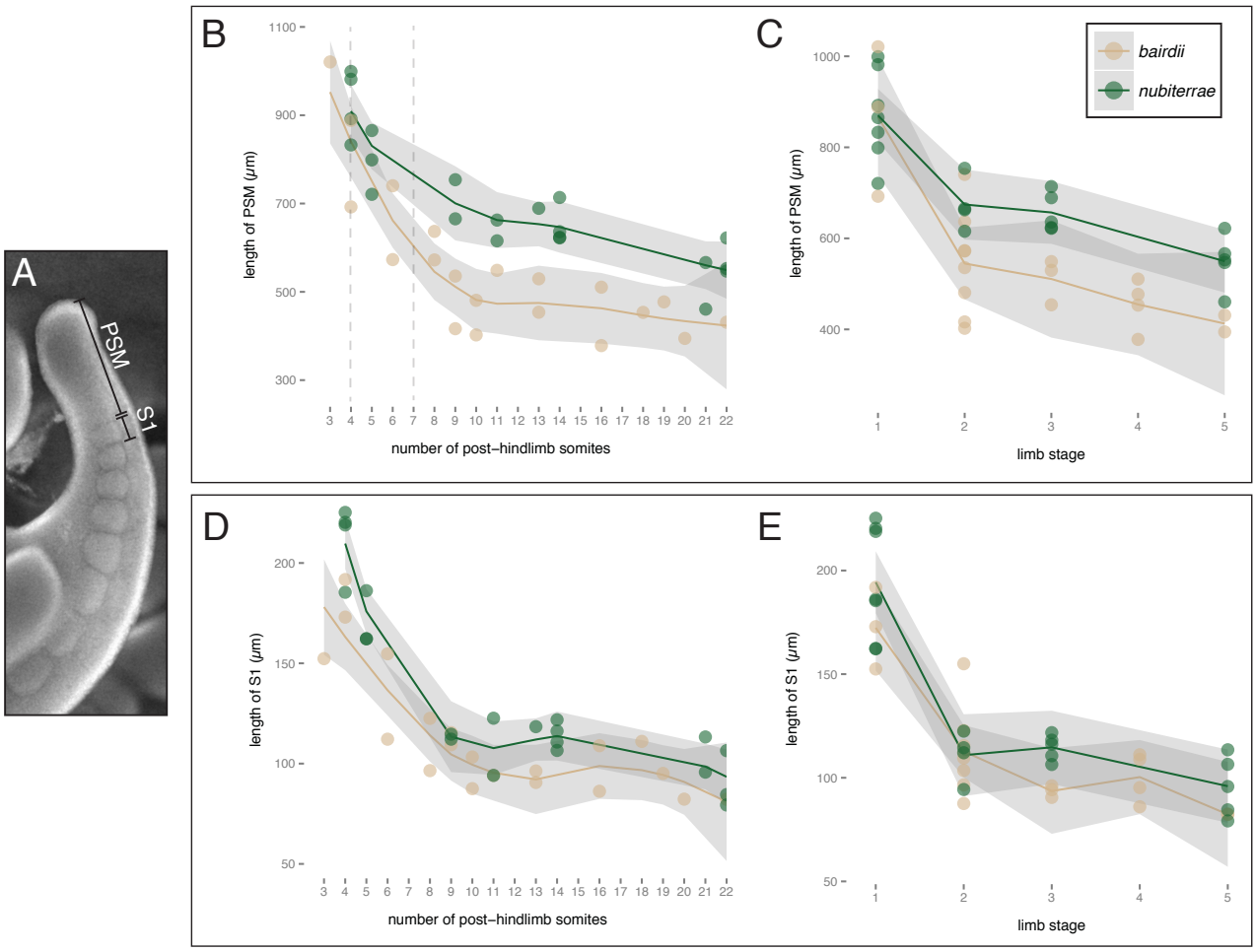

Figure 17. Comparative measures of PSM and somite size through tail development shows a difference in PSM size between forest and prairie embryos. A. Lines indicate measured lengths of presomitic mesoderm (PSM) and of the most recently formed somite (S1). **B,C.** PSM length shortens through time but shortens more slowly in forest mice than in prairie mice. Each point represents the PSM length of a single embryo. Lines are loess smoothed best fit lines and shaded areas represent the 95% confidence intervals of that line. **D,E.** Length of S1 also decreases through time, but does not significantly differ between forest and prairie mice. Each point represents the S1 length of a single embryo; lines and shaded areas indicate the same as in B and C. These patterns are similar whether developmental stage is synchronized by somite number (B,D) or by arbitrary limb stage (C,E).

significantly differ between forest and prairie embryos (n = 6 each) (Fig. 18), suggesting that a difference in TBM proliferation is not a major factor in producing the observed difference in PSM size.

Tailbud explant culture allows timing of somite formation

To further investigate the possibility that differences in the timing of somite formation could be contributing to the difference in segment numbers between forest and prairie embryos, we observed somite formation in tail explant cultures (Fig. 19).

We measured the time it took a somite to form during nine somitogenesis events for each subspecies and found no significant difference between the timing of somite formation (Fig. 19B) (Wilcoxon test: $W = 31.5$; $p = 0.45$). The median rates of somitogenesis were 240 and 280 minutes/somite for forest and prairie embryos, respectively. This, along with the results described above, suggests that differences in timing of somite formation do not play a major role in producing different segment numbers between forest and prairie embryos.

DISCUSSION

The development of vertebrate segments does not appear to have changed significantly since their evolutionary origin: the process of gastrulation, axial extension, somite formation, and somite differentiation appears intact across all amniotes examined so far. But this conservation in mechanism contrasts with the massive variety in segment pattern across vertebrates. Even across mammals, numbers of vertebrae vary widely, especially in the caudal region: humans have a coccyx, usually three vertebrae representing the vestige of a tail, while rats often have more than thirty (Owen 1866). How has the segmentation process changed through evolution to produce such great differences? Here, we investigate polymorphism in vertebral number within a species as a model for

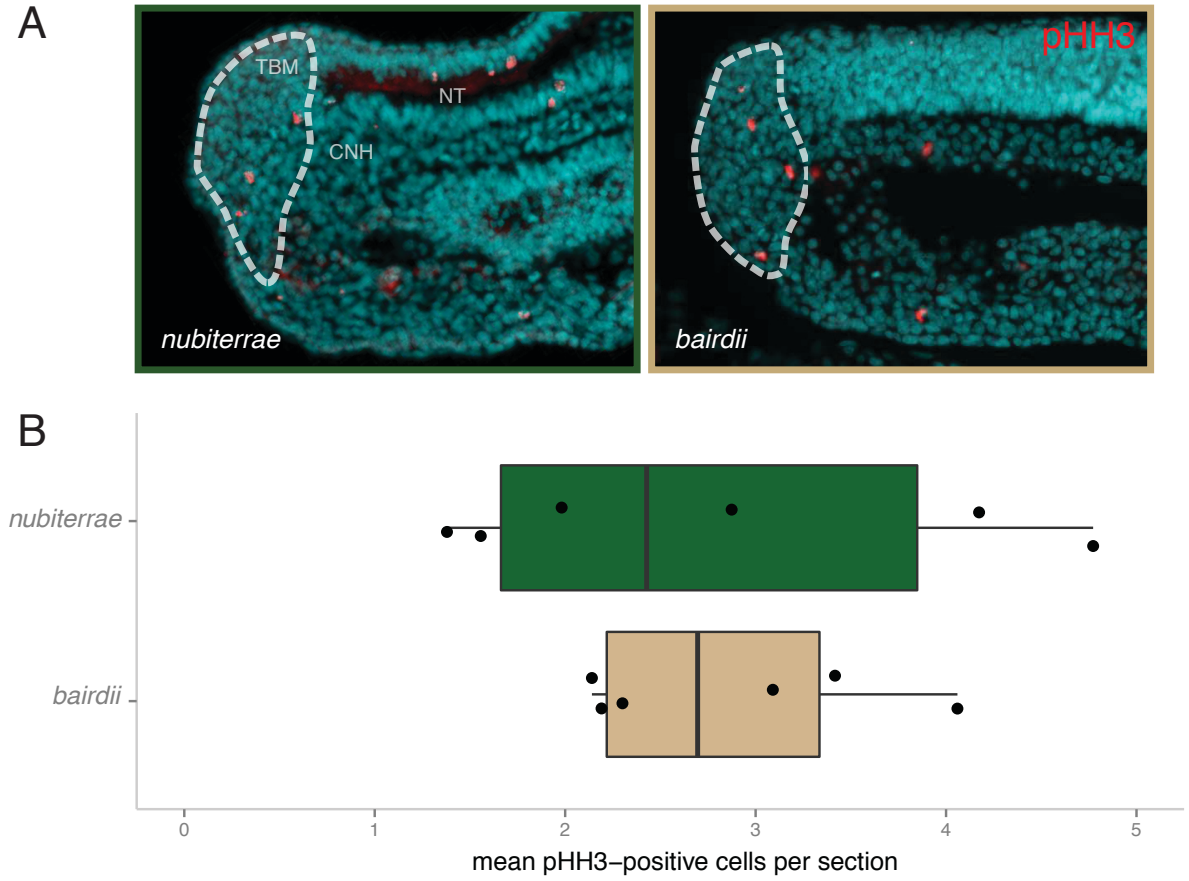

Figure 18. No difference in cell proliferation in tailbud of forest and prairie embryos. A. Immunofluorescence staining for anti-phospho-Histone-H3 (pHH3) in cryosectioned tails of E12.5 embryos. Red is pHH3 and cyan is nuclei (Hoechst). CNH = chordoneural hinge; NT = neural tube; TBM = tail bud mesenchyme. **B.** Counts of pHH3-positive cells do not significantly differ between forest and prairie tail bud. Each point represents the average number of pHH3-positive cells per 10 μm section for one embryo (n = 6; 2–6 sections per embryo).

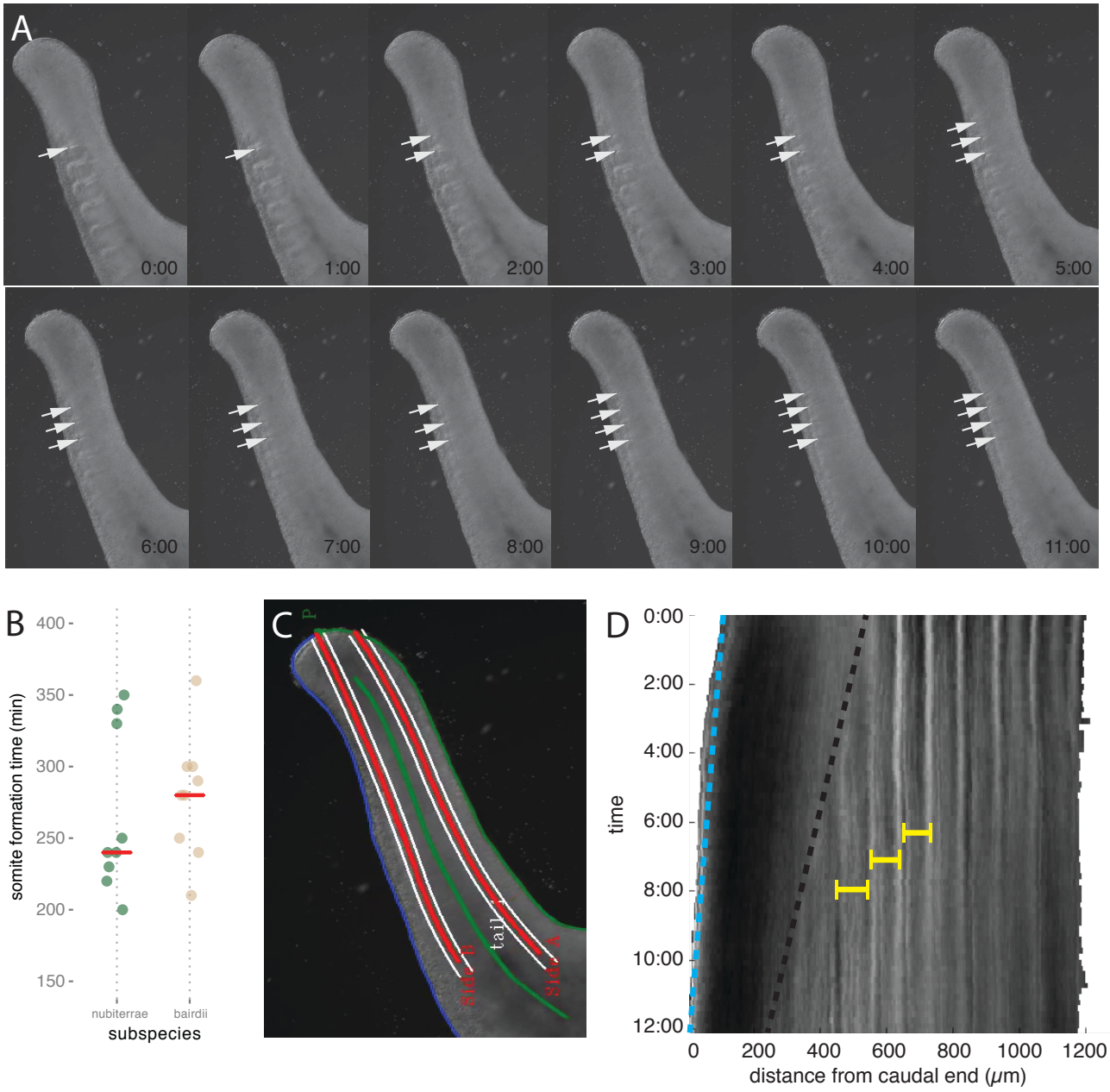

Figure 19. Time lapse imaging of *ex vivo* tail explant culture shows no difference in timing of somite formation. A. Time lapse images of a developing tail explant over 11 hours. Arrows indicate the locations of somite borders as they form. **B.** Forest and prairie embryos do not significantly differ in the timing of somite formation in tail explant culture. **C.** Time lapse frame annotated by custom tail tracking software. Red lines indicate the location of line scans (the width of which are indicated by the flanking white lines, 15 px on each side) used to make kymographs. **D.** Kymograph of tail explant growth showing methods of measuring rate of axial extension (cyan line), rate of somitogenesis front progression (black line), and sizes of somites as they form (yellow segments).

understanding the developmental nature of vertebral number evolution. Though vertebral number variation in the deer mouse is not large in magnitude—an average of 3-4 more vertebrae in forest populations (Fig. 14)—this difference contributes up to half of the disparity in tail length between forest and prairie mice (Chapter 1), and this disparity is very likely to be the result of natural selection related to climbing ability (Chapters 1 & 2). Our main finding in the current chapter is a plausible developmental mechanism producing adaptive segment number variation in the deer mouse. We find that differences in the number of caudal vertebrae correlate with specific modifications of embryonic growth observed between forest- and prairie-derived deer mice.

The total number of vertebrae that can be produced by the embryo is determined relatively early in development (~E13.5 in *Mus* [Tam 1981] and ~E15.5 in *P. maniculatus*) when posterior elongation of the body axis is completed (Gomez & Pourquié 2009). It can be helpful to imagine the cessation of body axis formation as a race between somite formation and axial elongation (Fig. 20 [based on Figure 4 in Bénazéraf & Pourquié 2013]). As the tailbud of the embryo is growing in the posterior direction, the somites are forming at a front moving in the same direction at a roughly constant rate, chasing the axial extension. At some point, the posterior outgrowth slows and the somitogenesis front catches up, signaling the end of axis formation (Bellairs 1986). If axial extension were to slow less quickly, then more PSM would be produced, which would lead to the production of more somites (Fig. 20). This appears to be the primary mechanism producing somite number differences in the deer mouse: as elongation slows and the PSM shortens, the PSM of the prairie embryo shortens faster than that of the forest embryo (Fig. 17A-B). This produces a difference in PSM size, a plausible cause of increased segment number in the forest deer mouse.

But differences in somite number could also be generated by variation in the timing of segmentation clock oscillations. Gomez et al. (2008) showed that, when controlling for total development time and number of cell generations in the PSM, the periodicity of somite formation in

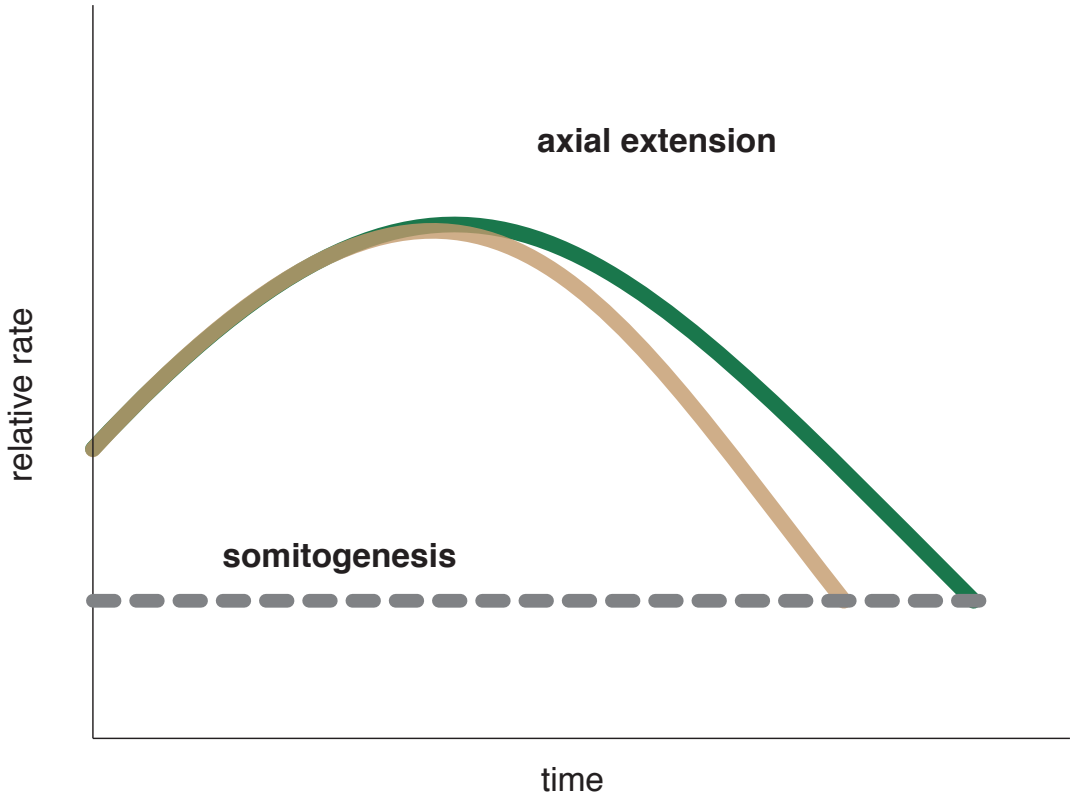

Figure 20. Model for developmental basis of segment number difference between forest and prairie deer mice. The dashed line represents the rate of somite formation, occurring at the same rate in forest and prairie embryos, while the solid lines represent the rates of axial extension (tan=prairie, green=forest). As axial extension begins to slow, the two embryos behave differently: the rate of extension slows less quickly in forest mice, leading to an increase in PSM length at later stages and thus providing more material for somitogenesis.

the corn snake is about four times faster than in mouse. This is proposed to be a major factor in producing many more, smaller somites in the snake embryo. A recent QTL study in medaka (Kimura et al. 2012) found that a difference in number of vertebrae between two strains is correlated with somite size: the strain with smaller somites has more vertebrae and the authors suggest that this may be due to differences in segmentation clock timing. Additionally, several studies have experimentally modified the periodicity of the segmentation clock in mice (Harima et al. 2013) and zebrafish (Schroter & Oates 2010) to produce embryos with different numbers of somites. We, on the other hand, do not see any significant differences in somite size or timing of somite formation (Fig. 17C-D; 19B), suggesting that variation in those factors do not play a major role in producing different numbers of somites in deer mouse embryos.

Our estimates of somite formation time in culture fall in approximately the same range as those for the laboratory mouse. Though the rate we measured (200-350 minutes/somite) is significantly longer than that usually reported for the laboratory mouse (120 minutes), the rate of somite formation varies along the rostro-caudal axis and notably slows at the end of somitogenesis (see Tam 1981; we represent it as constant in Figure 20 for simplicity's sake). Our range of somite formation rate estimates in the caudal region of the deer mouse embryo encompasses the decreased somite formation rate described by Tam (1981) for the caudal part of the laboratory mouse embryo compared to the trunk (2.5*120=300).

Ongoing work will further elucidate the nature of the vertebral number differences between forest and prairie deer mice. First, we can refine our estimates of somite formation rate and accurately measure additional somitogenesis parameters to better understand the dynamic differences between embryos producing different numbers of somites. We developed software for tracking segmentation in explant culture time-lapses, which will allow us to measure precise rates of posterior outgrowth and somitogenesis front migration rates (Fig. 19C-D), as well as somitogenesis

rates. The rates of somite formation that we manually measured have a high variance, and obtaining more precise values could support or refute the claim made here that there is no difference in the timing of segment formation. Interestingly, genes known to exhibit cyclical expression with the segmentation clock are found in QTL intervals for caudal vertebra number (*Sp5* and *Ndfip1* on LG3 and 14, respectively), which would be plausible candidates for future study if a difference in cycle timing were to be detected (Chapter 2; Dequéant et al. 2006). Finally, obtaining estimates of these parameters will also allow for the use of quantitative models of the segmentation process in a similar vein to those previously used to explore the process of somitogenesis (e.g., Soroldoni et al. 2014; reviewed by Oates et al. 2012).

Future work will aim to answer a number of remaining questions about the nature of segment differences in deer mice. Primarily, what are the molecular and tissue-level causes of the difference in PSM size between forest and prairie embryos? One possible way to produce more PSM in forest embryos would be to have an increased rate of cell proliferation in the tail bud mesenchyme (TBM) at the tip of the developing tail, as the posterior wall of the chordoneural hinge and the TBM are the major sources of paraxial mesoderm in the tailbud stage (Bénazéraf & Pourquié 2013). This mechanism is unlikely, however, because we see no significant difference in proliferative cell counts in this region (Fig. 18).

Recent work on *Hox* genes suggests another possible mechanism that could produce variation in axial extension rates and PSM size: differences in the rates of cell ingression into the paraxial mesoderm. Young et al. (2009) showed that premature activation of posterior *Hox* genes, *Hoxa13*, *Hoxb13*, and *Hoxc13*, in the posterior of the mouse embryo cause early termination of axis growth. Denans et al. (2015) showed that expression of posterior *Hox* genes strongly correlates with the slowing of posterior growth in the chick embryo, and that ectopic expression of a subset of

posterior *Hox* genes—including *Hoxd10*, *Hoxd11*, and *Hoxa13*—delays ingression of PSM progenitors.

Intriguingly, the *Hoxa* and *Hoxd* gene clusters lie within two QTL intervals for vertebral count in the cross described in Chapter 2. Because this seems like a remarkable coincidence—that we see a difference in axial extension between forest and prairie, and that some of the only genes known to control the cessation of axial extension appear in two QTL for vertebral count—we will take the liberty of describing some detailed future directions and propose a non-exhaustive set of experiments to test the hypothesis that *Hox* genes are involved in producing segment number variation in *P. maniculatus*.

Work by Iimura & Pourquié (2006) and Denans et al. (2015) shows that modifying timing of posterior *Hox* expression can lead to differences in rates of cell ingression into the PSM. Could differences in the timing of *Hox* gene expression be responsible for differences in segment number in deer mice? We hypothesize that posterior *Hox* genes may be activated at a later developmental stage in forest embryos, thereby allowing more cells to ingress into the PSM and producing more segments. Quantifying the levels (quantitative RT-PCR) and spatial extent (*in situ* hybridization) of posterior *Hoxa* and *Hoxd* gene expression in carefully stage-matched embryos of forest and prairie deer mice would reveal whether the two forms exhibit any difference in timing of posterior *Hox* activation. *Hoxa13* slows mesoderm ingression via Wnt repression and its effect on *T/brachyury* activity (Denans et al. 2015), so investigating levels and extent of *Axin2*, *T/brachyury*, and other Wnt targets may also be fruitful.

If the rate of cell ingression into the PSM differs between forest and prairie embryos, we may be able to test this by injecting cell-tracking dyes into tissue that provides ingressing cells to the PSM (epiblast, chordoneural hinge, and tail bud mesenchyme) in the *ex vivo* tail explant culture method described above. Next, we would compare the distances that cells travel into the PSM in

forest and prairie embryos. If a difference in *Hox* activation were responsible for different cell ingression rates, then we would expect to see cells traveling farther into the PSM of forest embryos than in prairie embryos of comparable stages.

Finally, the sequence and function of Hox proteins is highly conserved among animals (e.g., Lutz 1996), which makes a protein-coding change with a functional effect on a Hox protein unlikely to be the cause of segment number variation in deer mice. But sequencing the coding sequences of posterior *Hoxa* and *Hoxd* genes in forest and prairie mice would be an important step to rule out the possibility of coding changes.

References

Aguirre, W., K. Walker, and S. Gideon. 2014. Tinkering with the axial skeleton: vertebral number variation in ecologically divergent threespine stickleback populations. Biol. J. Linn. Soc. 113:204–219.

Anders, S., P. T. Pyl, and W. Huber. 2014. HTSeq — A Python framework to work with high-throughput sequencing data. Bioinformatics. doi:10.1093/bioinformatics/btu638

Arendt, J., and D. Reznick. 2008. Convergence and parallelism reconsidered: what have we learned about the genetics of adaptation? Trends Ecol. Evol. 23:26–32.

Armbruster, W., C. Pélabon, G. Bolstad, and T. Hansen. 2014. Integrated phenotypes: understanding trait covariation in plants and animals. Phil. Trans. R. Soc. B: Biol. Sci. 369:20130245.

Arnegard, M. E., M. D. McGee, B. Matthews, K. B. Marchinko, G. L. Conte, S. Kabir, N. Bedford, S. Bergek, Y. F. Chan, F. C. Jones, D. M. Kingsley, C. L. Peichel, and D. Schluter. 2014. Genetics of ecological divergence during speciation. Nature 511: 307-311.

Arnold, S. J. 1988. Quantitative genetics and selection in natural populations: microevolution of vertebral numbers in the garter snake *Thamnophis elegans*. Proceedings of the Second International Conference on Quantitative Genetics.

Asher, R., K. Lin, N. Kardjilov, and L. Hautier. 2011. Variability and constraint in the mammalian vertebral column. J. Evol. Biol. 24:1080–1090.

Averof, M., and N. H. Patel. 1997. Crustacean appendage evolution associated with changes in Hox gene expression. Nature 388:682-686.

Avise, J.C., M. H. Smith, and R. K. Selander. 1979. Biochemical polymorphism and systematics in the genus *Peromyscus*. VII. Geographic differentiation in members of the *truei* and *maniculatus* species groups. J. Mammal. 60:177-192.

Bellairs, R. 1986. The tail bud and cessation of segmentation in the chick embryo. In Bellairs et al. eds. Somites in Developing Embryos. Springer USA.

Bénazéraf, B., and O. Pourquié. 2013. Formation and segmentation of the vertebrate body axis. Annu. Rev. Cell Dev. Biol. 29:1–26.

Berner, D., D. Moser, M. Roesti, H. Buescher, and W. Salzburger. 2014. Genetic architecture of skeletal evolution in European lake and stream stickleback. Evolution 68:1792-1805.

Blair, W. F. 1942. Size of home range and notes on the life history of the woodland deer-mouse and eastern chipmunk in northern Michigan. J. Mammal. 23:27-36.

Blair, W. F. 1950. Ecological factors in speciation of *Peromyscus*. Evolution 4:253–275.

Bradshaw, W. N., and W. W. George. 1969. The karyotype in *Peromyscus maniculatus nubiterrae*. J. Mammal. 50:822-824.

Broman, K. W., H. Wu, Ś. Sen, G. A. Churchill. 2003. R/qtl: QTL mapping in experimental crosses. Bioinformatics 19:889-890.

Burke, A. C., C. E. Nelson, B. A. Morgan, and C. J. Tabin. 1995. Hox genes and the evolution of vertebrate axial morphology. Development 121:333–46.

Cambray, N., and V. Wilson. 2002. Axial progenitors with extensive potency are localised to the mouse chordoneural hinge. Development 129:4855–66.

Carroll, S. 2008. Evo-devo and an expanding evolutionary synthesis: a genetic theory of morphological evolution. Cell 134:25-36.

Catala, M., M. A. Teillet, and N. M. Le Douarin. 1995. Organization and development of the tail bud analyzed with the quail-chick chimaera system. Mech. Dev. 51:51–65.

Chalamalasetty, R., R. Garriock, W. Dunty, M. Kennedy, P. Jailwala, H. Si, and T. Yamaguchi. 2014. Mesogenin 1 is a master regulator of paraxial presomitic mesoderm differentiation. Development 141:4285-4297.

Cheverud, J. M., T. T. Vaughn, L. S. Pletscher, A. C. Peripato, E. S. Adams, C. F. Erikson, and K. J. King-Ellison. 2001. Genetic architecture of adiposity in the cross of LG/J and SM/J inbred mice. Mamm. Genome 12:3–12.

Christians, J., A. Hoeflich, P. Keightley, J. Christians, A. Hoeflich, and P. Keightley. 2006. PAPPA2, an enzyme that cleaves an insulin-like growth-factor-binding protein, is a candidate gene for a quantitative trait locus affecting body size in mice. Genetics 173:1547-1553.

Christians, J. K., V. K. Bingham, F. K. Oliver, T. T. Heath, and P. D. Keightley. 2003. Characterization of a QTL affecting skeletal size in mice. Mamm. Genome 14:175–83.

Churchill, G. A., and R. W. Doerge. 1994. Empirical threshold values for quantitative trait mapping. Genetics 138:963-971.

Danecek, P., A. Auton, G. Abecasis, C. A. Albers, E. Banks, M. A. DePristo, R. E. Handsaker, G. Lunter, G. T. Marth, S. T. Sherry, G. McVean, and R. Durbin. 2011. The variant call format and VCFtools. Bioinformatics 27:2156–8.

Denans, N., T. Iimura, and O. Pourquié. 2015. Hox genes control vertebrate body elongation by collinear Wnt repression. eLife 10.7554/eLife.04379.

DePristo, M., E. Banks, R. Poplin, K. Garimella, J. Maguire, C. Hartl, A. Philippakis, G. del Angel, M. A. Rivas, M. Hanna, A. McKenna, T. Fennell, A. Kernytsky, A. Sivachenko, K. Cibulskis, S. Gabriel, D. Altshuler, M. Daly. 2011. A framework for variation discovery and genotyping using next-generation DNA sequencing data. Nat. Genet. 43:491-498.

Dequéant, M. L., and O. Pourquié. 2008. Segmental patterning of the vertebrate embryonic axis. Nat. Rev. Genet. 9:370-382.

Dequeant, M., E. Glynn, K. Gaudenz, M. Wahl, J. Chen, A. Mushegian, and O. Pourquie. 2006. A complex oscillating network of signaling genes underlies the mouse segmentation clock. Science 314:1595–1598.

Dice, L. R. 1931. The occurrence of two subspecies of the same species in the same area. J. Mammal. 12:210-213.

Dice L. R. 1940. Ecologic and genetic variability within species of *Peromyscus*. Am. Nat. 74:212–221.

Dice, L. R. 1941. Variation of the deer-mouse (*Peromyscus maniculatus*) on the sand hills of Nebraska and adjacent areas. Univ. of Mich. Contrib. Lab. Vert. Biol. 15:1-19.

Domingues, V. S., Y.-P. P. Poh, B. K. Peterson, P. S. Pennings, J. D. Jensen, and H. E. Hoekstra. 2012. Evidence of adaptation from ancestral variation in young populations of beach mice. Evolution 66:3209–23.

Dragoo, J., J. Lackey, K. Moore, E. Lessa, J. Cook, and T. Yates. 2006. Phylogeography of the deer mouse (*Peromyscus maniculatus*) provides a predictive framework for research on hantaviruses. J. Gen. Virol. 87:1997–2003.

Dupuis, J., and D. Siegmund. 1999. Statistical methods for mapping quantitative trait loci from a dense set of markers. Genetics 151:373-386.

Elmer, K., and A. Meyer. 2011. Adaptation in the age of ecological genomics: insights from parallelism and convergence. Trends Ecol. Evol. 26:298-306.

Falconer, D. S., and T. F. C. Mackay. 1996. Introduction to Quantitative Genetics. Longman.

Fisher, S., A. Barry, J. Abreu, B. Minie, J. Nolan, T. M. Delorey, G. Young, T. J. Fennell, A. Allen, L. Ambrogio, A. M. Berlin, B. Blumenstiel, K. Cibulskis, D. Friedrich, R. Johnson, F. Juhn, B. Reilly, R. Shammas, J. Stalker, S. M. Sykes, J. Thompson, J. Walsh, A. Zimmer, Z. Zwirko, S. Gabriel, R. Nicol, and C. Nusbaum. 2011. A scalable, fully automated process for construction of sequence-ready human exome targeted capture libraries. Genome Biol. 12:R1.

Flint, J., and Mackay, T. F. 2009. Genetic architecture of quantitative traits in mice, flies, and humans. Genome Res. 19:723-733.

Forsberg, H., F. Crozet, and N. Brown. 1998. Waves of mouse Lunatic fringe expression, in four-hour cycles at two-hour intervals, precede somite boundary formation. Curr. Biol. 8:1027-1030.

Fox, J., and S. Weisberg. 2011. An R Companion to Applied Regression, Second Edition. Sage.

Galis, F., T. Dooren, J. Feuth, J. Metz, A. Witkam, S. Ruinard, M. Steigenga, and L. Wunaendts. 2006. Extreme selection in humans against homeotic transformations of cervical vertebrae. Evolution 60:2643–2654.

Gnirke, A., A. Melnikov, J. Maguire, P. Rogov, E. M. LeProust, W. Brockman, T. Fennell, G. Giannoukos, S. Fisher, C. Russ, S. Gabriel, D. B. Jaffe, E. S. Lander, and C. Nusbaum. 2009. Solution hybrid selection with ultra-long oligonucleotides for massively parallel targeted sequencing. Nat. Biotechnol. 27:182–9.

Gomez, C., E. Ozbudak, J. Wunderlich, D. Baumann, J. Lewis, and O. Pourquié. 2008. Control of segment number in vertebrate embryos. Nature 454:335–9.

Gunn, S. J, and I. F Greenbaum. 1986. Systematic implications of karyotypic and morphologic variation in mainland *Peromyscus* from the Pacific Northwest. J. Mammal. 67:294-304.

Hadfield, J. D. 2010. MCMC methods for multi-response generalized linear mixed models: the MCMCglmm R package. J. Stat. Softw. 33:1-22.

Hall, E. R. 1981. The Mammals of North America. Wiley.

Hansen, T. 2006. The Evolution of Genetic Architecture. Ann. Rev. Ecol. Syst. 37:123–157.

Harima, Y., Y. Takashima, Y. Ueda, T. Ohtsuka, and R. Kageyama. 2013. Accelerating the tempo of the segmentation clock by reducing the number of introns in the Hes7 gene. Cell Rep. 3:1–7.

Harris, V. T. 1952. An experimental study of habitat selection by prairie and forest races of the deermouse, *Peromyscus maniculatus*. Univ. of Mich. Contrib. Lab. Vert. Biol. 56:1-53.

Hedges S. B., Duellman W. E., Heinicke M. P. 2008. New World direct-developing frogs (*Anura*: *Terrarana*): molecular phylogeny, classification, biogeography, and conservation. Zootaxa 1737:1–182.

Hendzel, M., Y. Wei, M. Mancini, A. Hooser, T. Ranalli, B. Brinkley, D. Bazett-Jones, and C. Allis. 1997. Mitosis-specific phosphorylation of histone H3 initiates primarily within pericentromeric heterochromatin during G2 and spreads in an ordered fashion coincident with mitotic chromosome condensation. Chromosoma 106:348–360.

Henrique, D., J. Adam, A. Myat, A. Chitnis, J. Lewis, and D. Ish-Horowicz. 1995. Expression of a Delta homologue in prospective neurons in the chick. Nature 375:787–790.

Hickman, G. C. 1979. The mammalian tail: a review of functions. Mammal Rev. 9:143-157.

Hirsinger, E., C. Jouve, J. Dubrulle, and O. Pourquié. 2000. Somite formation and patterning. Int. Rev. Cytol. 198:1–65.

Hoekstra, H. E., and J. A. Coyne. 2007. The locus of evolution: evo devo and the genetics of adaptation. Evolution 61:995–1016.

Hoekstra, H. E. 2006. Genetics, development and evolution of adaptive pigmentation in vertebrates. Heredity 97:222-234.

Hooper, E. T. 1942. An effect on the *Peromyscus maniculatus* Rassenkreis of land utilization in Michigan. J. Mammal. 23:193–196.

Horner, B. E. 1954. Arboreal Adaptions of *Peromyscus* with Special Reference to Use of the Tail. Univ. of Mich. Contrib. Lab. Vert. Biol. 61:1-84.

Howard, W. E. 1949. Dispersal, amount of inbreeding, and longevity in a local population of prairie deermice on the George Reserve, Southern Michigan. Univ. of Mich. Contrib. Lab. Vert. Biol. 43:1-50.

Iimura, T., and O. Pourquié. 2006. Collinear activation of *Hoxb* genes during gastrulation is linked to mesoderm cell ingression. Nature 442:568–71.

Kelley, K., S. Arnold, and J. Gladstone. 1997. The effects of substrate and vertebral number on locomotion in the garter snake *Thamnophis elegans*. Funct. Ecol. 11:189–198.

Kenney-Hunt, J. P., B. Wang, E. A. Norgard, G. Fawcett, D. Falk, L. S. Pletscher, J. P. Jarvis, C. Roseman, J. Wolf, and J. M. Cheverud. 2008. Pleiotropic patterns of quantitative trait loci for 70 murine skeletal traits. Genetics 178:2275–88.

Kimura, T., M. Shinya, and K. Naruse. 2012. Genetic analysis of vertebral regionalization and number in medaka (*Oryzias latipes*) inbred lines. G3 (Bethesda) 2:1317–23.

King, J. A. 1968. Biology of *Peromyscus*. American Society of Mammalogists.

Klingenberg, C. 2008. Morphological Integration and Developmental Modularity. Annu. Rev. Ecol. Syst. 39:115-132.

Knezevic, V., R. De Santo, and S. Mackem. 1998. Continuing organizer function during chick tail development. Development 125:1791–801.

Lande, R. 1979. Quantitative genetic analysis of multivariate evolution, applied to brain:body size allometry. Evolution 33:402.

Lande, R. 1980. The genetic covariance between characters maintained by pleiotropic mutations. Genetics 94:203–15.

Lansman, R. A., J. C. Avise, C. F. Aquadro, and J. F. Shapira. 1983. Extensive genetic variation in mitochondrial DNA's among geographic populations of the deer mouse, *Peromyscus maniculatus*. Evolution 37:1-16.

Linnen, C. R., E. P. Kingsley, J. D. Jensen, and H. E. Hoekstra. 2009. On the origin and spread of an adaptive allele in deer mice. Science 325:1095–8.

Linnen, C. R., Y-P. Poh, B. K. Peterson, R. D. Barrett, J. G. Larson, J. D. Jensen, and H. E. Hoekstra. 2013. Adaptive evolution of multiple traits through multiple mutations at a single gene. Science 339:1312–6.

Liubicich, D. M., J. M. Serano, A. Pavlopoulos, Z. Kontarakis, M. E. Protas, E. Kwan, S. Chatterjee, K. D. Tran, M. Averof, and N. H. Patel. 2009. Knockdown of Parhyale Ultrabithorax recapitulates evolutionary changes in crustacean appendage morphology. Proc. Natl. Acad. Sci. U.S.A. 106:13892–6.

Lofsvold, D. 1986. Quantitative genetics of morphological differentiation in *Peromyscus*. I. Tests of the homogeneity of genetic covariance structure among species and subspecies. Evolution 40:559–573.

Lunter G., and M. Goodson. 2011. Stampy: A statistical algorithm for sensitive and fast mapping of Illumina sequence reads. Genome Res. 21:936-939.

Lutz, B., H. C. Lu, G. Eichele, D. Miller, and T. C. Kaufman. 1996. Rescue of Drosophila labial null mutant by the chicken ortholog Hoxb-1 demonstrates that the function of Hox genes is phylogenetically conserved. Genes Dev. 10:176–84.

Lynch, M. and B. Walsh. 1998. Genetics and Analysis of Quantitative Traits. Sinauer.

Mackay, T. F. 2001. The genetic architecture of quantitative traits. Ann. Rev. Genet. 35:303-339.

Manceau, M., V. S. Domingues, C. R. Linnen, E. B. Rosenblum, and H. E. Hoekstra. 2010. Convergence in pigmentation at multiple levels: mutations, genes and function. Phil. Trans. R. Soc. Lond. B, Biol. Sci. 365:2439–50.

Manichaikul, A., J. Mychaleckyj, S. Rich, K. Daly, M. Sale, and W.-M. Chen. 2010. Robust relationship inference in genome-wide association studies. Bioinformatics 26:2867–2873.

Marx, H., and G.B. Rabb. 1972. Phyletic analysis of fifty characters of advanced snakes. Fieldiana: Zool. 63:1–321.

McGrew, M., J. K. Dale, S. Fraboulet, and O. Pourquié. 1998. The *lunatic Fringe* gene is a target of the molecular clock linked to somite segmentation in avian embryos. Curr. Biol. 8:979-982.

McKenna A., Hanna M., Banks E., Sivachenko A., Cibulskis K., Kernytsky A., Garimella K., Altshuler D., Gabriel S., Daly M., DePristo M. A. 2010. The Genome Analysis Toolkit: a MapReduce framework for analyzing next-generation DNA sequencing data. Genome Res. 20:1297-303.

Mikawa, S., S. Sato, M. Nii, T. Morozumi, and G. Yoshioka. 2011. Identification of a second gene associated with variation in vertebral number in domestic pigs. BMC Genet. 12:1-13.

Mikawa, S., T. Morozumi, and S. I. Shimanuki. 2007. Fine mapping of a swine quantitative trait locus for number of vertebrae and analysis of an orphan nuclear receptor, germ cell nuclear factor (NR6A1). Genome Res. 17:586-593.

Miller, C., A. Glazer, B. Summers, B. Blackman, A. Norman, M. Shapiro, B. Cole, C. Peichel, D. Schluter, and D. Kingsley. 2014. Modular skeletal evolution in sticklebacks is controlled by additive and clustered quantitative trait loci. Genetics 197:405–420.

Morris, K. H., A. Ishikawa, and P. D. Keightley. 1999. Quantitative trait loci for growth traits in C57BL/6J × DBA/2J mice. Mamm. Genome 10:225-228.

Nakaya, Y., and G. Sheng. 2008. Epithelial to mesenchymal transition during gastrulation: an embryological view. Dev. Growth Differ. 50:755–66.

Neuwirth, E. 2014. RColorBrewer: ColorBrewer Palettes. R package version 1.1-2. http://CRAN.R-project.org/package=RColorBrewer.

Nichols, K. M., P. A. Wheeler, and G. H. Thorgaard. 2004. Quantitative trait loci analyses for meristic traits in *Oncorhynchus mykiss*. Env. Biol. Fishes 69:317-331.

Oates, A. C., L. G. Morelli, and S. Ares. 2012. Patterning embryos with oscillations: structure, function and dynamics of the vertebrate segmentation clock. Development 139:625–39.

Orr, H. A. 2000. Adaptation and the cost of complexity. Evolution 54:13–20.

Orr, H. A. 1998. Testing natural selection vs. genetic drift in phenotypic evolution using quantitative trait locus data. Genetics 149:2099–2104.

Osgood, W. H. 1909. Revision of the Genus *Peromyscus*. North American Fauna.

Otto, S. P. 2004. Two steps forward, one step back: the pleiotropic effects of favoured alleles. Proc. Biol. Sci. 271:705–14.

Ovchinnikov, D. 2009. Alcian blue/Alizarin red staining of cartilage and bone in mouse. Cold Spring Harb. Protoc. doi 10.1101/pdb.prot5170.

Owen, R. 1866. On the Anatomy of Vertebrates. Vol. 2. Longmans, Green and Co.

Pedregosa, F., G. Varoquaux, A. Gramfort, V. Michel, B. Thirion, O. Grisel, M. Blondel, P. Prettenhofer, R. Weiss, V. Dubourg, J. Vanderplas, A. Passos, D. Cournapeau, M. Brucher, M. Perrot, and É. Duchesnay. 2011. Scikit-learn: Machine Learning in Python. J. Machine Learn. Res. 12:2825-2830.

Peterson, B. K., J. N. Weber, E. H. Kay, H. S. Fisher, and H. E. Hoekstra. 2012. Double digest RADseq: an inexpensive method for de novo SNP discovery and genotyping in model and non-model species. PLoS ONE 7:e37135.

Pilbeam, D. 2004. The anthropoid postcranial axial skeleton: Comments on development, variation, and evolution. J. Exp. Zool. 302B:241–267.

Purcell, J., A. Brelsford, Y. Wurm, N. Perrin, and M. Chapuisat. 2014. Convergent genetic architecture underlies social organization in ants. Curr. Biol. 24: 2728-2732.

R Core Team. 2015. R: A language and environment for statistical computing. R Foundation for Statistical Computing, Vienna, Austria. URL http://www.R-project.org/.

Rajon, E., and J. Plotkin. 2013. The evolution of genetic architectures underlying quantitative traits. Proc. Roy. Soc. B: Biol. Sci. 280:1552.

Rasband, W.S. 1997-2014. ImageJ, U. S. National Institutes of Health, Bethesda, Maryland, USA, http://imagej.nih.gov/ij/

Reich, D., A. L. Price, and N. Patterson. 2008. Principal component analysis of genetic data. Nat. Genet. 40:491–2.

Revelle, W. 2015. *psych*: Procedures for Personality and Psychological Research, Northwestern University, Evanston, Illinois, USA, http://CRAN.R-project.org/package=psych Version 1.5.1.

Rockman, M. V. 2012. The QTN program and the alleles that matter for evolution: all that's gold does not glitter. Evolution 66:1–17.

Rutledge, J. J., E. J. Eisen, and J. E. Legates. 1974. Correlated response in skeletal traits and replicate variation in selected lines of mice. Theor. Appl. Genet. 45:26-31.

Schindelin, J., I. Arganda-Carreras, E. Frise, V. Kaynig, M. Longair, T. Pietzsch, S. Preibisch, C. Rueden, S. Saalfeld, B. Schmid, J.-Y. Tinevez, D. White, V. Hartenstein, K. Eliceiri, P. Tomancak, and A. Cardona. 2012. Fiji: an open-source platform for biological-image analysis. Nat. Methods 9:676–682.

Schluter, D. 1996. Adaptive radiation along genetic lines of least resistance. Evolution 50:1766-1774.

Schoenwolf, G. C. 1979. Histological and ultrastructural observations of tail bud formation in the chick embryo. Anat. Rec. 193:131–47.

Schröter, C., and A. C. Oates. 2010. Segment number and axial identity in a segmentation clock period mutant. Curr. Biol. 20:1254–8.

Shapiro, M. D., Summers, B. R., Balabhadra, S., Aldenhoven, J. T., Miller, A. L., Cunningham, C. B., Bell, M. A., and Kingsley, D. M. 2009. The genetic architecture of skeletal convergence and sex determination in ninespine sticklebacks. Curr. Biol. 19:1140-1145.

Smartt, R. A., and C. Lemen. 1980. Intrapopulational morphological variation as a predictor of feeding behavior in deermice. Am. Nat. 116:891-894.

Snyder, L. 1981. Deer mouse hemoglobins: Is there genetic adaptation to high altitude? Bioscience 31:299–304.

Soroldoni, D., D. J. Jörg, L. G. Morelli, D. L. Richmond, J. Schindelin, F. Jülicher, and A. C. Oates. 2014. A Doppler effect in embryonic pattern formation. Science 345:222–5.

Stern, D. L. 2000. Evolutionary developmental biology and the problem of variation. Evolution 54:1079–91.

Stern, D. L., and V. Orgogozo. 2008. The loci of evolution: how predictable is genetic evolution? Evolution 62:2155–2177.

Stone, G. N., S. Nee, and J. Felsenstein. 2011. Controlling for non-independence in comparative analysis of patterns across populations within species. Philos. Trans. R. Soc. Lond. B, Biol. Sci. 366:1410–24.

Storz, J. F., C. Natarajan, Z. A. Cheviron, F. G. Hoffmann, and J. K. Kelly. 2012. Altitudinal variation at duplicated β-globin genes in deer mice: effects of selection, recombination, and gene conversion. Genetics 190:203–16.

Storz, J. F., A. M. Runck, S. J. Sabatino, J. K. Kelly, N. Ferrand, H. Moriyama, R. E. Weber, and A. Fago. 2009. Evolutionary and functional insights into the mechanism underlying high-altitude adaptation of deer mouse hemoglobin. Proc. Natl. Acad. Sci. U.S.A. 106:14450–5.

Storz, J.F., S.J. Sabatino, F.G. Hoffmann, and E.J. Gering. 2007. The molecular basis of high-altitude adaptation in deer mice. PLoS Genet. doi: 10.1371/journal.pgen.0030045.

Swain, D. 1992. The functional basis of natural selection for vertebral traits of larvae in the stickleback *Gasterosteus aculeatus*. Evolution 46:987.

Taylor, Z. S., and S. M. Hoffman. 2012. Microsatellite genetic structure and cytonuclear discordance in naturally fragmented populations of deer mice (*Peromyscus maniculatus*). J. Hered. 103:71–79.

Tam, P. P. 1981. The control of somitogenesis in mouse embryos. J. Embryol. Exp. Morphol. 65 Suppl:103–28.

Thompson, D. B. 1990. Different spatial scales of adaptation in the climbing behavior of *Peromyscus maniculatus*: geographic variation, natural selection, and gene flow. Evolution 44:952–965.

Wada, Y., T. Akita, T. Furukawa, N. Sugai, K. Ishii, Y. Ito, E. Kobayashi, and S. Mikawa. 2000. Quantitative trait loci (QTL) analysis in a Meishan × Göttingen cross population. Anim. Genet. 31:376–384.

Wagner, G. P., J. P. Kenney-Hunt, M. Pavlicev, J. R. Peck, D. Waxman, and J. M. Cheverud. 2008. Pleiotropic scaling of gene effects and the "cost of complexity". Nature 452:470–2.

Weber, J. N., B. K. Peterson, and H. E. Hoekstra. 2013. Discrete genetic modules are responsible for complex burrow evolution in *Peromyscus* mice. Nature 493:402–5.

Wecker, S. C. 1963. The role of early experience in habitat selection by the prairie deer mouse, *Peromyscus maniculatus bairdi*. Ecological Monographs, 307-325.

Weir, B. S., and C. C. Cockerham. 1984. Estimating F-statistics for the analysis of population structure. Evolution 38:1358-1370.

Welch, J. J., and D. Waxman. 2003. Modularity and the cost of complexity. Evolution 57:1723–34.

Wittler, L., E. H. Shin, P. Grote, A. Kispert, A. Beckers, A. Gossler, M. Werber, and B. G. Herrmann. 2007. Expression of Msgn1 in the presomitic mesoderm is controlled by synergism of WNT signalling and Tbx6. EMBO Rep. 8:784–9.

Wickham, H. 2007. Reshaping Data with the *reshape* Package. J. Stat. Softw. 21:1-20. http://www.jstatsoft.org/v21/i12/

Wickham, H. 2009. *ggplot2*: elegant graphics for data analysis. Springer New York.

Wickham, H. 2014. *scales*: Scale functions for graphics. R package version 0.2.4. http://CRAN.R-project.org/package=scales

Yang, D.-S., and G. J. Kenagy. 2011. Population delimitation across contrasting evolutionary clines in deer mice (*Peromyscus maniculatus*). Ecol. Evol. 1:26–36.

Yang, D.-S., and G. J. Kenagy. 2009. Nuclear and mitochondrial DNA reveal contrasting evolutionary processes in populations of deer mice (*Peromyscus maniculatus*). Molec. Ecol. 18:5115–25.

Young, T., J. Rowland, C. Ven, M. Bialecka, A. Novoa, M. Carapuco, J. Nes, W. Graaff, I. Duluc, J.-N. Freund, F. Beck, M. Mallo, and J. Deschamps. 2009. Cdx and Hox genes differentially regulate posterior axial growth in mammalian embryos. Dev. Cell 17:516–26.

Zheng, X., B. S. Arbogast, and G. J. Kenagy. 2003. Historical demography and genetic structure of sister species: deermice (*Peromyscus*) in the North American temperate rain forest. Molec. Ecol. 12:711–724.

Appendix

Samples for Chapter 1 Analyses

capture_ID	state/ province	lat	long	subspp	forest/prairie	in population contrasts	in individual contrasts	x-ray morphology	source
01_SI569775	ME	45.998	-68.907	*abietorum*	1		x		Smithsonian
27_TTU75979	NE	42.19	-98.04	*bairdii*	0		x		Museum of Texas Tech
28_TTU75938	NE	42.19	-98.04	*bairdii*	0		x		Museum of Texas Tech
CRL317	SD	43.22475	-99.67255	*bairdii*	0	bairdii_SD	x		C.R. Linnen/ Hoekstra Lab
CRL318	SD	43.22475	-99.67255	*bairdii*	0	bairdii_SD	x		C.R. Linnen/ Hoekstra Lab
CRL319	SD	43.22475	-99.67255	*bairdii*	0	bairdii_SD	x		C.R. Linnen/ Hoekstra Lab
CRL320	SD	43.22475	-99.67255	*bairdii*	0	bairdii_SD	x		C.R. Linnen/ Hoekstra Lab
CRL321	SD	43.22475	-99.67255	*bairdii*	0	bairdii_SD	x		C.R. Linnen/ Hoekstra Lab
CRL322	SD	43.22475	-99.67255	*bairdii*	0	bairdii_SD	x		C.R. Linnen/ Hoekstra Lab
CRL323	SD	43.22475	-99.67255	*bairdii*	0	bairdii_SD	x		C.R. Linnen/ Hoekstra Lab
CRL324	SD	43.22475	-99.67255	*bairdii*	0	bairdii_SD			C.R. Linnen/ Hoekstra Lab
CRL325	SD	43.22475	-99.67255	*bairdii*	0	bairdii_SD	x		C.R. Linnen/ Hoekstra Lab
CRL326	SD	43.22475	-99.67255	*bairdii*	0	bairdii_SD	x		C.R. Linnen/ Hoekstra Lab
UMMZ93504	MI	Washtenaw Co		*bairdii*	0		x	x	University of Michigan Museum of Zoology
UMMZ93505	MI	Washtenaw Co		*bairdii*	0		x	x	University of Michigan Museum of Zoology
UMMZ116396	MI	Washtenaw Co		*bairdii*	0		x	x	University of Michigan Museum of Zoology
UMMZ116397	MI	Washtenaw Co		*bairdii*	0		x	x	University of Michigan Museum of Zoology
UMMZ116398	MI	Washtenaw Co		*bairdii*	0		x	x	University of Michigan Museum of Zoology
UMMZ126330	MI	Washtenaw Co		*bairdii*	0		x	x	University of Michigan Museum of Zoology
UMMZ163792	MI	Washtenaw Co		*bairdii*	0		x	x	University of Michigan Museum of Zoology
22_NMMNH5380	Chihuahua	27.037	-105.244	*blandus*	0		x		New Mexico Museum of Natural History
23_NMMNH5381	Chihuahua	27.037	-105.244	*blandus*	0		x		New Mexico Museum of Natural History

46_RM1	NM	33.074677	-106.00331	*blandus*	0	blandus_NM	x		R. Mallarino/ Museum of Comparative Zoology
49_RM4	NM	33.074677	-106.00331	*blandus*	0	blandus_NM	x		R. Mallarino/ Museum of Comparative Zoology
50_RM5	NM	33.074677	-106.00331	*blandus*	0	blandus_NM	x		R. Mallarino/ Museum of Comparative Zoology
51_RM6	NM	33.074677	-106.00331	*blandus*	0	blandus_NM	x		R. Mallarino/ Museum of Comparative Zoology
52_RM7	NM	33.074677	-106.00331	*blandus*	0	blandus_NM	x		R. Mallarino/ Museum of Comparative Zoology
53_RM8	NM	33.074677	-106.00331	*blandus*	0	blandus_NM	x		R. Mallarino/ Museum of Comparative Zoology
19_ROM109759	Alberta	50.733	-113.983	*borealis*	0		x		Royal Ontario Museum
24_TTU55496	Alberta	53.406	-113.541	*borealis*	0		x		Museum of Texas Tech
25_TTU71347	Alberta	51.997	-114.043	*borealis*	0		x		Museum of Texas Tech
26_TTU71362	Alberta	50.182	-111.236	*borealis*	0		x		Museum of Texas Tech
30_TTU82708	Tlaxcala	19.281	-98.367	*fulvus*	0		x		Museum of Texas Tech
31_TTU104953	Veracruz	19.57	-97.25	*fulvus*	0		x		Museum of Texas Tech
02_SI569175	CA	32.945	-117.168	*gambelii*	0		x		Smithsonian
03_SI569236	CA	32.945	-117.168	*gambelii*	0		x		Smithsonian
04_SI569270	CA	33.125	-116.675	*gambelii*	0		x		Smithsonian
05_SI569278	CA	33.508	-116.675	*gambelii*	0		x		Smithsonian
06_SI569292	CA	32.552	-117	*gambelii*	0		x		Smithsonian
12_MVZ208126	CA	37.74	-119.396	*gambelii*	1		x		Museum of Vertebrate Zoology
13_MVZ208143	CA	37.741	-119.408	*gambelii*	0		x		Museum of Vertebrate Zoology
14_MVZ216082	CA	34.415	-119.88	*gambelii*	0		x		Museum of Vertebrate Zoology
15_MVZ216101	CA	34.415	-119.88	*gambelii*	0		x		Museum of Vertebrate Zoology
63_DSY10	OR	42.1838	-117.5021	*gambelii*	0	gambelii_OR	x	x	D.-S. Yang/Burke Museum
64_DSY11	OR	42.1838	-117.5021	*gambelii*	0	gambelii_OR	x	x	D.-S. Yang/Burke Museum
65_DSY12	OR	42.1838	-117.5021	*gambelii*	0	gambelii_OR	x	x	D.-S. Yang/Burke Museum
66_DSY13	OR	42.1838	-117.5021	*gambelii*	0	gambelii_OR	x	x	D.-S. Yang/Burke Museum

67_DSY14	OR	42.1838	-117.5021	*gambelii*	0	gambelii_OR	x	x	D.-S. Yang/Burke Museum
68_DSY15	OR	42.1838	-117.5021	*gambelii*	0	gambelii_OR	x	x	D.-S. Yang/Burke Museum
69_DSY16	OR	42.1838	-117.5021	*gambelii*	0	gambelii_OR	x	x	D.-S. Yang/Burke Museum
70_DSY17	OR	42.1838	-117.5021	*gambelii*	0	gambelii_OR	x	x	D.-S. Yang/Burke Museum
71_DSY18	OR	42.1838	-117.5021	*gambelii*	0	gambelii_OR	x	x	D.-S. Yang/Burke Museum
18_ROM98940	Ontario	45	-78.5	*gracilis*	1	gracilis_ON	x		Royal Ontario Museum
20_ROM97094	Ontario	45	-78.5	*gracilis*	1	gracilis_ON	x		Royal Ontario Museum
21_ROM97095	Ontario	45	-78.5	*gracilis*	1	gracilis_ON	x		Royal Ontario Museum
73_EPK21	MI	46.02	-84.43	*gracilis*	1	gracilis_MI	x		Museum of Comparative Zoology
74_EPK22	MI	46.02	-84.43	*gracilis*	1	gracilis_MI	x		Museum of Comparative Zoology
75_EPK23	MI	46.02	-84.43	*gracilis*	1	gracilis_MI	x		Museum of Comparative Zoology
76_EPK24	MI	46.02	-84.43	*gracilis*	1	gracilis_MI	x		Museum of Comparative Zoology
77_EPK25	MI	46.02	-84.43	*gracilis*	1	gracilis_MI	x		Museum of Comparative Zoology
78_EPK26	MI	46.02	-84.43	*gracilis*	1	gracilis_MI	x		Museum of Comparative Zoology
80_EPK28	MI	46.02	-84.43	*gracilis*	1	gracilis_MI	x		Museum of Comparative Zoology
CRL376	NE	42.08135	-101.4692333	*luteus*	0	luteus_NE_g	x		C.R. Linnen/ Hoekstra Lab
CRL377	NE	42.08135	-101.4692333	*luteus*	0	luteus_NE_g	x		C.R. Linnen/ Hoekstra Lab
CRL378	NE	42.08135	-101.4692333	*luteus*	0	luteus_NE_g	x		C.R. Linnen/ Hoekstra Lab
CRL379	NE	42.08135	-101.4692333	*luteus*	0	luteus_NE_g	x		C.R. Linnen/ Hoekstra Lab
CRL380	NE	42.08135	-101.4692333	*luteus*	0	luteus_NE_g	x		C.R. Linnen/ Hoekstra Lab
CRL381	NE	42.08135	-101.4692333	*luteus*	0	luteus_NE_g	x		C.R. Linnen/ Hoekstra Lab
CRL384	NE	42.08135	-101.4692333	*luteus*	0	luteus_NE_g	x		C.R. Linnen/ Hoekstra Lab
CRL385	NE	42.08135	-101.4692333	*luteus*	0	luteus_NE_g	x		C.R. Linnen/ Hoekstra Lab
CRL386	NE	42.08135	-101.4692333	*luteus*	0	luteus_NE_g	x		C.R. Linnen/ Hoekstra Lab
CRL387	NE	42.08135	-101.4692333	*luteus*	0	luteus_NE_g	x		C.R. Linnen/ Hoekstra Lab
CRL461	NE	40.53783333	-101.6206667	*luteus*	0	luteus_NE_i	x		C.R. Linnen/ Hoekstra Lab
CRL462	NE	40.53783333	-101.6206667	*luteus*	0	luteus_NE_i	x		C.R. Linnen/ Hoekstra Lab

CRL463	NE	40.53783333	-101.6206667	*luteus*	0	luteus_NE_i	x		C.R. Linnen/ Hoekstra Lab
CRL464	NE	40.53783333	-101.6206667	*luteus*	0	luteus_NE_i	x		C.R. Linnen/ Hoekstra Lab
CRL465	NE	40.53783333	-101.6206667	*luteus*	0	luteus_NE_i	x		C.R. Linnen/ Hoekstra Lab
CRL466	NE	40.53783333	-101.6206667	*luteus*	0	luteus_NE_i	x		C.R. Linnen/ Hoekstra Lab
CRL467	NE	40.53783333	-101.6206667	*luteus*	0	luteus_NE_i	x		C.R. Linnen/ Hoekstra Lab
CRL468	NE	40.53783333	-101.6206667	*luteus*	0	luteus_NE_i	x		C.R. Linnen/ Hoekstra Lab
CRL475	NE	40.53783333	-101.6206667	*luteus*	0	luteus_NE_i	x		C.R. Linnen/ Hoekstra Lab
CRL476	NE	40.53783333	-101.6206667	*luteus*	0	luteus_NE_i	x		C.R. Linnen/ Hoekstra Lab
29_TTU42218	WY	40.967	-109.604	*nebrascensis*	0		x		Museum of Texas Tech
10_MVZ199465	UT	38.819	-109.773	*nebrascensis*	0		x		Museum of Vertebrate Zoology
11_MVZ199466	UT	38.819	-109.773	*nebrascensis*	0		x		Museum of Vertebrate Zoology
07_SI570138	VA	38.414	-79.58	*nubiterrae*	1		x		Smithsonian
32_ARY-Pm-1	PA	40.145	-79.268	*nubiterrae*	1	nubiterrae_PA	x	x	A.R.Young/Museum of Comparative Zoology
33_ARY-Pm-5	PA	40.145	-79.268	*nubiterrae*	1	nubiterrae_PA	x	x	A.R.Young/Museum of Comparative Zoology
34_ARY-Pm-2	PA	40.145	-79.268	*nubiterrae*	1	nubiterrae_PA	x	x	A.R.Young/Museum of Comparative Zoology
35_ARY-Pm-7	PA	40.145	-79.268	*nubiterrae*	1	nubiterrae_PA	x	x	A.R.Young/Museum of Comparative Zoology
36_ARY-Pm-8	PA	40.145	-79.268	*nubiterrae*	1	nubiterrae_PA	x	x	A.R.Young/Museum of Comparative Zoology
37_ARY-Pm-10	PA	40.145	-79.268	*nubiterrae*	1	nubiterrae_PA	x	x	A.R.Young/Museum of Comparative Zoology
38_ARY-Pm-11	PA	40.145	-79.268	*nubiterrae*	1	nubiterrae_PA	x	x	A.R.Young/Museum of Comparative Zoology
16_MVZ219039	CA	37.994	-122.501	*rubidus*	1		x		Museum of Vertebrate Zoology
17_MVZ219041	CA	37.994	-122.501	*rubidus*	1		x		Museum of Vertebrate Zoology
54_DSY1	OR	42.3451	-124.2056	*rubidus*	1	rubidus_OR	x	x	D.-S. Yang/Burke Museum
55_DSY2	OR	42.3451	-124.2056	*rubidus*	1	rubidus_OR	x	x	D.-S. Yang/Burke Museum
56_DSY3	OR	42.3451	-124.2056	*rubidus*	1	rubidus_OR	x	x	D.-S. Yang/Burke Museum
57_DSY4	OR	42.3451	-124.2056	*rubidus*	1	rubidus_OR	x	x	D.-S. Yang/Burke Museum
58_DSY5	OR	42.3451	-124.2056	*rubidus*	1	rubidus_OR	x	x	D.-S. Yang/Burke Museum
59_DSY6	OR	42.3451	-124.2056	*rubidus*	1	rubidus_OR	x	x	D.-S. Yang/Burke Museum

60_DSY7	OR	42.3451	-124.2056	*rubidus*	1	rubidus_OR	x	x	D.-S. Yang/Burke Museum
61_DSY8	OR	42.3451	-124.2056	*rubidus*	1	rubidus_OR	x	x	D.-S. Yang/Burke Museum
62_DSY9	OR	42.3451	-124.2056	*rubidus*	1	rubidus_OR	x	x	D.-S. Yang/Burke Museum
44_MSB98501	NM	35.24	-108.768	*rufinus*	0				Museum of Southwestern Biology
45_MSB96295	NM	35.24	-106.768	*rufinus*	0				Museum of Southwestern Biology
08_MSB122974	AZ	35.08	-109.8	*sonoriensis*	0				Museum of Southwestern Biology
09_MSB122975	AZ	35.08	-109.8	*sonoriensis*	0				Museum of Southwestern Biology
39_LMT120	AZ	35.34	-111.67	*sonoriensis*	1				L. Turner/Museum of Comparative Zoology
40_LMT264	CA	37.91	-119.11	*sonoriensis*	0				L. Turner/Museum of Comparative Zoology
41_LMT272	CA	37.91	-119.11	*sonoriensis*	0				L. Turner/Museum of Comparative Zoology